Lillian Uthus

Deformation Properties of Unbound Granular Aggregates

Thesis for the degree of philosophiae doctor

Trondheim, May 2007

Norwegian University of
Science and Technology
Faculty of Engineering Science and Technology
Department of Civil and Transport Engineering

NTNU
Innovation and Creativity

Deformation Properties of Unbound Granular Aggregates

Lillian Uthus

Thesis submitted to the Department of Civil and Transport Engineering, Faculty of Engineering Science and Technology, the Norwegian University of Science and Technology, in partial fulfilment of the requirements for
the degree of philsophiae doctor.

May, 2007

The committee for appraisal of this thesis comprised the following members:

Professor, PhD. Guy Doré, Département de génie Civil, Université Laval, Quebéc, Canada.

Senior Researcher, PhD. Maria Arm, Statens Geotekniska Institut, Linköping, Sweden.

Professor, Dr.Ing. Lars Grande, Department of Civil and Transport Engineering, Norwegian University of Science and Technology. (Administrator)

Advisors during this study have been:

Professor, Dr.Ing. Ivar Horvli, Department of Civil and Transport Engineering, Norwegian University of Science and Technology.

Research Manager, Dr.Ing. Inge Hoff, SINTEF Building and Infrastructure.

To my dear family…

PREFACE AND ACKNOWLEDGEMENTS

VI

ABSTRACT

This thesis discusses the resilient and permanent deformation properties of unbound granular aggregates for use in road structures. One of the objectives of the thesis is to identify the influence of the physical properties of the aggregate grains, such as grain size, grain shape, surface texture, mineralogy and mechanical strength through cyclic load triaxial testing. A second objective is to study the effect of water on the deformation properties of materials as well as their frost susceptibility. The third objective is to study the effect of micromechanical properties using a discrete element model (DEM).

Deformation in unbound granular materials under cyclic loading is divided into a resilient (recoverable) part and a plastic part that does not recover. The elastic strain represents the denominator in the resilient modulus and the non-recoverable strain results in permanent deformations over time. As the resilient response is non-linear, the resilient deformations may be interpreted using several models for curve fitting. Two of the simplest models are the k-θ model and Uzans model. The interpretation of the permanent deformation behaviour of unbound aggregates is complicated, as there is a need for a failure criterion to define when the material is at a failure stage. Two methods used for interpretation of the permanent deformations are mentioned in Chapter 3 of this thesis; the Shakedown approach and the "Coulomb approach".

Many factors are known to affect the deformation properties in unbound materials. In this thesis the effect of most of these factors is investigated in the six papers. In Chapter 4 the influence of the different factors is discussed on the basis of the results from the papers and findings in the literature. Cyclic load triaxial testing has been the main method to test the deformation properties of the selected unbound materials. This is so far one of the best methods for laboratory simulation of traffic loading.

Discrete element modelling is performed to gain a better understanding of the deformation properties of unbound aggregates tested in a triaxial apparatus under cyclic loading. This method provides useful information about the contact mechanics between neighbouring particles and the interaction of the grains. In addition, unbound spherical aggregates have been tested in the laboratory using a triaxial apparatus.

The main factors studied in this thesis are the influence of grain shape, grain size distribution, fines content, mineralogy, dry density and water content. Useful information about these key factors has been obtained. However, there is still work to do in order to utilize the conclusions directly in a pavement design system.

The dry density, degree of saturation and stress level seem to be key parameters for determining the deformation behaviour, but mineralogy, fines content and grain size distribution are also of importance. Regarding the practical consequences, the results show that mineralogy, fines content and grain size distribution must be given more attention in the pavement design manuals. More effort should also be placed on the compaction control phase in situ, in order to avoid initial rutting in the road structure.

SAMMENDRAG (IN NORWEGIAN)

Denne avhandlingen diskuterer de resiliente (elastiske) og plastiske egenskapene til ubundne materialer for bruk i vegbygging. Den første målsetningen med avhandlingen er å identifisere betydningen av enkeltkornenes fysiske egenskaper, som kornstørrelse, kornform, overflatetekstur, mineralogi og mekanisk styrke gjennom treaksialforsøk med repetert last. Videre er målet å studere effekten av vann på deformasjonsegenskapene til ubundne materialer i tillegg til telehiv-problematikk. Den tredje målsetningen er å studere effekten av mikromekaniske egenskaper ved å bruke en diskret element modell (DEM).

Deformasjon i ubundne materialer under repetert belastning er delt inn i en resilient (elastisk) del og en plastisk del som over tid fører til permanente deformasjoner. Da den resiliente responsen er ikke-lineær, kan resilientmodulen tolkes ved å bruke ulike modeller for kurvetilpasning. To av de enkleste modellene er k-θ modellen og Uzans modell, som er beskrevet kort i Kapittel 3 i denne avhandlingen. For de permanente deformasjonene er tolkningen mer komplisert, da det er behov for brudd-kriterier for å definere når materialet er i bruddtilstand. To metoder for tolkning av materialoppførsel med tanke på permanente deformasjoner er nevnt i Kapittel 3; Shakedown-tilnærmingen og "Coulomb-tilnærmingen".

Det er mange faktorer som påvirker deformasjonsegenskapene til ubundne materialer. I denne avhandlingen er de fleste av disse faktorene studert gjennom arbeidet med de seks artiklene. I Kapittel 4 er betydningen av de ulike faktorene diskutert på grunnlag av resultatene i artiklene og i litteraturstudiet. Treaksialtesting med repetert belastning har vært hovedmetoden for å teste deformasjonsegenskapene til de utvalgte materialene. Dette er foreløpig en av de beste metodene for laboratoriesimulering av trafikkbelastning.

Modellering med diskrete elementer er utført i denne avhandlingen for å forstå deformasjonsegenskapene til ubundne materialer under repetert belastning bedre. Denne metoden gir oss verdifull kunnskap om kontaktmekanikken mellom to korn og hvordan kornene virker inn på hverandre. I tillegg har prøver med kuler av stein blitt testet i treaksialriggen.

Hovedfaktorene som er studert i denne doktorgradsavhandlingen er betydningen av kornform, kornfordelingskurver, finstoffinnhold, mineralogi, tørrdensitet og vanninnhold. Nyttig informasjon om nøkkelfaktorene er kommet frem i avhandlingen, men det gjenstår ennå en del arbeid for å kunne utnytte konklusjonene for praktisk dimensjonering og materialvalg.

Tørrdensitet, metningsgrad og spenningsnivå er nøkkelparametere for deformasjonsegenskapene, men mineralogi, finstoffinnhold og kornfordeling er også viktig. Når det gjelder den praktiske betydningen av resultatene bør faktorer som mineralogi, finstoffinnhold og kornfordeling få mer oppmerksomhet i retningslinjer og system for dimensjonering av veg. Det bør også settes inn mer innsats for å forbedre komprimeringskontrollen i felt for å unngå initialspor i vegkonstruksjonen.

X

TABLE OF CONTENTS

PAPER OVERVIEW

The following papers are included in the second part of the thesis.

Paper I:
Uthus, L., Hoff, I. and Horvli, I. (2005). Evaluation of grain shape characterization methods for unbound aggregates. Paper Proceedings. 7th International Conference on the Bearing Capacity of Roads, Railways and Airfields, Trondheim, Norway.

Paper II:
Uthus, L., Tutumluer, E., Horvli, I. and Hoff, I. (2007). Influence of grain shape and surface texture on the deformation properties of unbound aggregates in pavements. International Journal of Pavements. Submitted.

Paper III:
Uthus, L., Hermansson, Å., Horvli, I. and Hoff, I. (2006). A study on the influence of water and fines on the deformation properties and frost heave of unbound aggregates. Proceedings of the 13th Intl. Conference on Cold Regions Engineering (CD-ROM), Orono, Maine.

Paper IV:
Uthus, L. (2007). Material Properties of Unbound Granular Aggregates and the Effect on the Deformation Behaviour. International Journal of Pavements. Submitted.

Paper V:
Uthus, L. (2007). Effect of Grading and Moisture on Deformation Properties of Unbound Granular Aggregates. (Will be submitted for the TRB conference 2008).

Paper VI:
Uthus, L., Hopkins, M. and Horvli, I. (2007). Discrete Element Modelling of the Resilient Behaviour of Unbound Granular Aggregates. International Journal of Pavement Engineering. Submitted.

APPENDIX

Extract from draft paper:
Cole, D., Uthus, L. and Hopkins, M (in prep). Normal and Sliding Contact Experiments on Smooth Spherical Grains of Gneiss. (unpublished)

LIST OF SYMBOLS AND ABBREVIATIONS

Symbol: Meaning :

Stress

σ_1	Major principal stress
σ_2	Intermediate principal stress
σ_3	Minor principal stress
σ_a	Reference stress (100 kPa)
σ_m , p	Mean stress
$\sigma_{d,}$ q	Deviatoric stress
τ	Shear stress
σ_d^{dyn}	Applied dynamic deviator stress
σ_θ	Circumferential stress from the rubber membrane
P	Additional confining stress caused by a lateral expansion of a triaxial sample

Strain

ε_1	Major principal strain
ε_2	Intermediate principal strain
ε_3	Minor principal strain
ε_d , ε_q	Deviatoric strain
ε_a^e	Axial resilient strain
ε_θ	Circumferential strain on the rubber membrane
$\dot{\varepsilon}$	Strain rate

Resilient stiffness parameters

E	Young's modulus, E-modulus, Stiffness modulus
ν	Poisson's ratio
M_r, E_r	Resilient modulus
θ	Bulk stress, or the sum of principal stresses ($\theta = \sigma_1 + \sigma_2 + \sigma_3$)
k_1	Material parameter ("modulus number")
k_2	Material parameter ("stress exponent")
$E_{membrane}$	Membrane stiffness

Strength parameters

a	Attraction (in the Mohr - Coloumb model)
Sin (ρ)	Shear mobilisation
Sin (ϕ)	Sinus to the failure angle

Other parameters

C_u	Gradation number
n	Grading coefficient
t	Thickness of membrane
r	Radius of triaxial sample

Abbreviations

KPG	Kvalitet av Pukk- og Grusindustriens produkter
LVDT	Linear Variable Displacement Transducer
CCP	Constant Confining Pressure
NTNU/NTH	Norwegian University of Science and Technology
AASHO	American Association of State Highway Officials
CEN	European Committee for Standardisation
DEM	Discrete Element Method
GARAP	Granular Aggregates in Road and Airfield Pavements
PPP	Public Private Partnership

1. INTRODUCTION

1.1 Title

The title of this thesis is; "Deformation Properties of Unbound Granular Aggregates". Granular aggregates are in this case limited to natural gravel, crushed gravel and crushed rock for use in road pavements. In this thesis traffic loading is simulated by repeated loading in a triaxial apparatus, and the deformation behaviour of unbound granular aggregates is studied. The main focus has been to study the influence of the aggregate properties such as grain shape and texture, mineralogy, grading and fines content.

1.2 Background

A road structure in service is subjected to repeated traffic loading, and the accumulated number of heavy vehicles together with climatic influence cause deterioration over time. Rutting, cracking and unevenness in the longitudinal and transversal direction represents typical damages. The result of improper design is reduced service life and increased maintenance and user costs.

In reality budget limitations are restricting investments or design for long life pavements, in particular on low volume and rural roads. It is a need for utilizing the material strength in each layer properly, and to take the costs into consideration when doing the pavement design.

In order to build roads with a long service life, the potential for deterioration has to be minimized. In cold regions freezing and thawing represents a major contribution to the deterioration processes. Water plays an important role in these processes in interaction with the material properties.

Particle crushing due to traffic loading over time represents one of the deteriorative processes. Traffic load in the pavement structure is transferred by grain-to-grain contacts. Over time these forces may lead to deterioration by crushing and abrasion in the particle contact surfaces. The particles may then rearrange over time to form more dense structures. This reorientation may again cause permanent deformations.

The deformation behaviour of unbound granular aggregates under cyclic loading may be separated into two parts; one elastic or resilient part (recoverable) and one permanent deformation part. These two types of deformation mechanisms are usually treated independently in the scientific interpretations.

The deformation behaviour of unbound aggregates is known to be influenced by many factors. Lekarp (1999) presented a state-of-the-art on both the resilient- and the permanent deformation behaviour. He found that the resilient modulus and the permanent deformation behaviour were mainly influenced by the same factors, for instance; aggregate type and particle shape, grading and fines content, moisture content, density, stress level, stress history and number of load cycles. For the resilient modulus factors like maximum grain size, load duration, frequency and load sequence were mentioned to have some influence. Principal

stress rotation is a factor that has been found to be important for development of permanent deformations.

The purpose of the work in this thesis has been to study the effect of the most important parameters to see how each parameter influence the deformation properties. In Figure 1 the connection between the papers and the focus on different factors are shown.
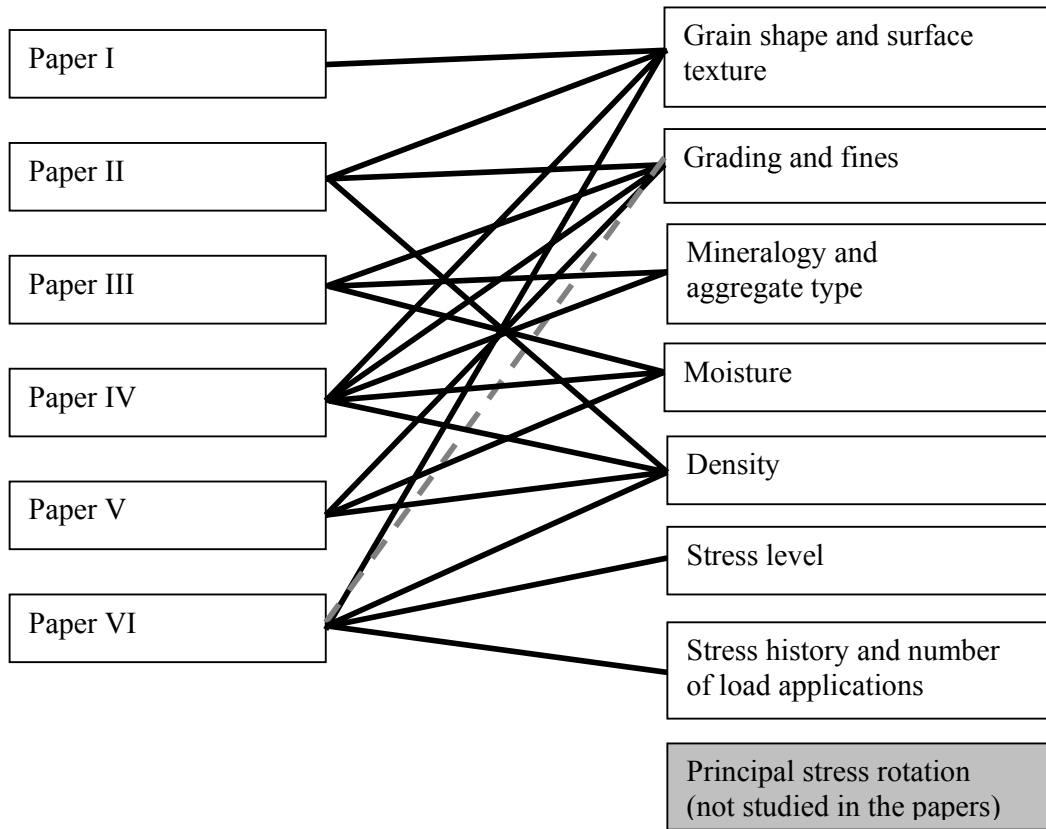
Figure 1. The relation between the six papers in the thesis and the different factors influencing on the deformation properties of unbound granular aggregates

As seen from the figure above most of the factors influencing the deformation properties of unbound granular aggregates are investigated in the individual papers in this thesis. Only the effect of principal stress rotation is left out, because of unsuitable laboratory equipment. This is further explained in Chapter 4.

1.3 Objective

This thesis discusses the resilient and permanent deformation properties of unbound granular aggregates for use in road structures. The first objective of this study is to identify the influence of the physical properties of the aggregate grains, such as grain size, grain shape, surface texture, mineralogy and mechanical strength through cyclic load triaxial testing. By

using the same material throughout the study it is possible to draw conclusions from the results of different papers. The influence of the different properties is discussed in Chapter 4.

A second objective is to study the combinations of different physical properties of the aggregates in a sample and the effect of water on the deformation properties of materials, as well as their frost susceptibility.

The micromechanical grain-to-grain contacts are important elements for the deformation properties of unbound aggregates. A third objective of the thesis is therefore to study the effect of micromechanical properties more in detail by using a discrete element model. The results from the modelling are to a certain extent verified in the laboratory. By using a discrete element model in combination with laboratory testing, the effect of the stress level, contact stiffness, surface friction and grain shape may be studied.

Furthermore, the objectives for each paper define subtopics fitting into these three main objectives.

1.4 Structure of the thesis

The first part of the thesis consists of an introduction, objectives, some theory and an overall discussion and conclusions of the findings from the individual papers. Here the influence of each parameter is discussed and conclusions are drawn.

The second part of this thesis includes six individual papers where the author of this thesis is the main author. In addition an extract of a draft paper, where the main author of this thesis is one of the co-authors, is enclosed as an appendix.

Professor Ivar Horvli at NTNU has been the main supervisor of this thesis, while Research director Inge Hoff at SINTEF has been co-supervisor. The main work in the six papers has been performed by the author of the thesis; including experimental work, evaluation of results and writing of the actual papers.

Paper I: Evaluation of grain shape characterization methods for unbound aggregates.
In this paper the second and third authors are Inge Hoff and Ivar Horvli, respectively. The main author has performed most of the laboratory testing and the writing of the paper. Both co-authors have given advices on the structure of the paper and the analysis of the results.

Paper II: Influence of grain shape and surface texture on the deformation properties of unbound aggregates in pavements.
The co-authors are Erol Tutumluer, Ivar Horvli and Inge Hoff. The triaxial testing and the writing is done by the main author, while the second author, Associate Professor Erol Tutumluer, has contributed with the three dimensional image analysis on the materials using the University of Illinois Aggegate Image Analyzer (UIAIA), and QA of language. The third and fourth authors, Horvli and Hoff, have contributed with advices and discussions.

Paper III: A study on the influence of water and fines on the deformation properties and frost heave of unbound aggregates.
The co-authors are Åke Hermansson, Ivar Horvli and Inge Hoff. The main author has been responsible for the triaxial testing and writing the paper. The second author, Åke Hermansson from VTI in Linköping Sweden, has contributed with frost heave testing of the three materials in the study and also some literature references together with advices and correction of language. The third and fourth authors, Horvli and Hoff, have contributed with advices and in discussions.

Paper IV: Material Properties of Unbound Granular Aggregates and the Effect on the Deformation Behaviour.
The paper is written by the author of this thesis alone. The author has also performed all the planning and main parts of the triaxial testing of the materials and providing other laboratory results.

Paper V: Effect of Grading and Moisture on the Deformation Properties of Unbound Granular Aggregates.
The paper is written by the author of this thesis alone. The author has also performed all the planning and triaxial testing and the Tube Suction testing of the materials and providing other results.

Paper VI: Discrete Element Modelling of the Resilient Behaviour of Unbound Granular Aggregates.
The co-authors are Mark Hopkins and Ivar Horvli. The main author has been responsible for the triaxial testing of the aggregate spheres, the writing and interpretation of results and some of the simulations. The second author, research scientist Mark Hopkins at the Cold Regions Research and Engineering Laboratory in Hanover, NH, USA, has developed the discrete element model and run most of the simulations. He has also written parts of the paper and provided some literature references. The third author, Ivar Horvli, had the basic idea of this paper and started the adaptation of the DEM model for granular materials in cooperation with Mark Hopkins.

Appendix: Normal and Sliding Contact Experiments on Smooth Spherical Grains of Gneiss. (Extract of the draft paper)
In this paper David Cole at Cold Regions Research and Engineering Laboratory (CRREL) in Hanover NH, USA, is the main author, writing the paper and performing all the testing. The author of this thesis is second author of the paper, contributing with the aggregate specimens, providing routine data for the material used and also contributing in discussions on the findings from the experiments. The third author is Mark Hopkins, who has contributed with information from the discrete element modelling of the spheres and also in discussions on the findings of the paper.

2. PAVEMENT DESIGN IN NORWAY

The objective of this chapter is to present some important milestones in the Norwegian modern history of road construction, especially regarding pavement design and the use of unbound granular materials. This should be considered as a background for this thesis.

The Norwegian manual for pavement design, currently denoted Handbook 018 (Statens vegvesen, 2005a), has been developed in several phases. One of the first steps was a table for pavement design for different road classes and subgrades, presented by Nordal (Nordal, 1960). The first version of the design manual existed as a collection of leaflets, and it has over time been under continuous development through numerous revisions.

2.1 Important projects and milestones

In this chapter important projects and milestones affecting the pavement design manual and the development of road construction are described.

The Vormsund Test Road
The Vormsund Test Road (Nordal et al., 1987) was built to study the effect of frost action and its influence on bearing capacity of roads. The project was planned in 1956, and the road construction was carried out in 1957/58. Different types of tests were carried out, and recordings and observations were run for a period of about ten years. The main objective of this project was to obtain information about the design and construction of roads on frost susceptible subgrade, to build roads that could cope with the future traffic.

The Vormsund Test Road has been very important for pavement design in Norway, especially for the knowledge of frost effects on Norwegian materials in subgrades, subbase and base layers. The results were incorporated in the first table for pavement design (Nordal, 1960) where the frost susceptibility criteria were first presented. The first Norwegian pavement design guide was published during the observation period of the Vormsund project.

The Kjellstad Test Road
The Norwegian Road Research Laboratory built the Kjellstad Test Road in 1966. The test section was about 200 m in length, and the purpose was to test the frost insulating properties of different materials. EPS (expanded polystyrene), XPS (extruded polystyrene) and leca (expanded clay) were used as frost insulating materials to study the effects.

The development of this test section has been followed closely with sampling every third year until 1996. The results from this test section form the basis of how frost insulation is used in Norway. This work did not result in any final report and the information presented here is given by Geir Refsdal in NPRA (Refsdal, 2007).

The "Frost in Ground" project
The "Frost in Ground" project was started in 1968, and during the period from1970 to 1976 the work was intensified, financed by the Royal Norwegian Council for Scientific and Industrial Research and the Norwegian Public Roads Administration (NPRA). This work was

presented in a summary report (Utvalg for Frost i Jord, 1976) where the research was presented.

Also the "Frost in Ground" project influenced the development of guidelines and practice of frost protection of roads and other constructions. One of the effects of the project was the tables of annual average temperatures and frost indices for all Norwegian municipalities, first presented as an annex in the 1980 edition of the Norwegian manual for pavement design (Statens vegvesen, 1980).

During the period 1970-1987 totally 26 reports were published through the "Frost in Ground" project. These publications contributed to the increased knowledge in Norway on the effects of frost. Also the effects of permafrost have been thoroughly covered through this work. In 2005 a new committee was actuated to continue the work from the original "Frost in Ground" project by publishing recent work on frost action. The first report from this committee was published in 2005.

The STINA project
The STINA project (Samarbetsprojekt för tillämpning i Norden av AASHO-undersökningen) was a joint project between the Nordic countries to adapt the results from the US AASHO-project to Nordic conditions (Nordiska ministerrådets secretariat, 1976). The project started in 1974 and finished in 1976. The objective was to adapt the results from the AASHO test road, by a detailed study of the effect of the differences in traffic, climate and subgrade types to have a better framework for pavement design.

The STINA project was important for the increased knowledge on the influence of climate, subgrade and different axle loads on deterioration of pavement structures, and many of the findings from this project were later included in the Norwegian pavement design manual.

Development of the water susceptibility criterion for base materials
The work of Christine Hauck (Hauck, 1988) was important for the development of the frost and water susceptibility criteria for base and subbase layers that are used today.

Up to 1990 Nordals frost susceptibility criterion (Nordal, 1960) was used for subgrades and unbound materials in the road structure. Like most other criteria regarding frost susceptibility, Nordals criterion was based on Casagrandes "rule-of-thumb" criterion (Casagrande, 1932), limiting the material less than 0.020 mm to only 3 %. The background of Haucks study was the experience in Norway with the Casagrande frost susceptibility criterion, which in some cases appeared to be too strict.

Hauck (1988) concluded that the water susceptibility of gravel materials could be classified from the amount of material less than 0.075 mm of the fraction passing the 19 mm sieve. This was the basis for the requirements regarding the amount of fines in the pavement structure that was introduced in the 1992 design manual (Statens vegvesen, 1992). Today this is still used, except for an adjustment from 0.075 to 0.063 mm sieve and 19 mm to 20 mm sieve. In addition the materials for use in base and sub base layers should be non-frost susceptible after Nordals criterion.

The BUAB project and the removal of the seasonal load restrictions
On the first of January 1995, the seasonal load restrictions in Norway were removed. This was a result of the findings in the BUAB project (BUAB = Better utilization of the bearing capacity of roads) (Senstad, 1994). This was a project run by the Norwegian Public Roads Administration (NPRA). It was started in 1990 and finished in 1994.

In 1994, about 50 % of the national roads and 80 % of the county roads were affected by seasonal load restrictions. The load restrictions were removed for all these roads without any further strengthening of the road structure. The expected result of this action was that maintenance of the roads by resurfacing had to take place more frequently.

Except for the removal of seasonal load restrictions, the BUAB project also led to some conclusions regarding heavy vehicles. One of the objectives was to encourage the use of heavy vehicles that were more "road friendly", meaning heavy vehicles with dual axles instead of single axles, dual wheels instead of single wheels and other adjustments that decrease the concentrated load from each wheel. Super single wheels are known to have the most deteriorative effect on a pavement structure.

The KPG project
In 1993, partners from the aggregate industry, suppliers and public administrations agreed on a joint project; Quality of aggregate products (KPG). The main objective was to study the properties of crushed materials from quarries for use in roads, railways and airfields and compare this to gravel. At this point the aggregate industry was not satisfied with the requirements regarding aggregates in the pavement design manual. One of the arguments was that the potential of this material was not fully utilized.

Totally 22 publications were written during the KPG project and the project was summarized in a special edition of the Norwegian Journal Våre Veger (Våre Veger, 2000).

Based on experience from practice and some investigations from the KPG project the load distribution index for crushed rock in the Norwegian pavement design manual was increased from 1.25 to 1.35 in 1999, meaning that the layer thicknesses may be decreased for unbound base and subbase layers when using crushed.

The GARAP project
The GARAP project (Granular Aggregates in Road and Airfield Pavements) was started in 2002 and finished in 2006. This project was also financed by partners from the aggregate industry, NPRA, Norwegian National Rail Administration, Avinor and the Norwegian Research Council. The main objective of the GARAP project was to continue the work from the KPG project by improvement of laboratory equipment and analyses for design of roads, airfields and railways.

A final report from the project is yet not available, but some of the sub-topics that may be mentioned are the round-robin test of triaxial equipment in cooperation with several international laboratories, and studies on the effect of compaction methods and sample size on the results from triaxial testing. This PhD study has been a part of the GARAP project.

2.2 Doctoral theses on pavement issues at NTNU/NTH

In this paragraph the dissertations submitted at NTH/NTNU related to materials and pavement design are listed. Each of the theses has been important for the current knowledge of material behaviour and design parameters. As a consequence of their doctoral work, many of these persons have contributed to the development of road design by participating in technical committees and groups having influence on new requirements and developments in the Norwegian pavement design manual.

Per Magne Noss, *Suction in soils*, 1978 (in Norwegian)
Eigil Angen, *Moisture migration in soils*, 1978 (in Norwegian)
Tore Slyngstad, *Filler in bituminous pavements*, 1977 (in Norwegian)
Karl Melby, *Repeated loading on clay*, 1977 (in Norwegian)
Ivar Horvli, *Dynamic testing of clay for pavement design*, 1979 (in Norwegian)
Jostein Myre, *Fatigue in asphalt pavements*, 1988 (in Norwegian)
Helge Mork, *Analysis of load response in road pavements*, 1990 (in Norwegian)
Geir Berntsen, *Reduction of bearing capacity during spring thaw*, 1993 (in Norwegian)
Even K. Sund, *Life-Cycle Cost Analysis of Road Pavements*, 1996
Inge Hoff, *Material Properties of Unbound Aggregates for Pavement Structures*, 1999
Bjørn Ove Lerfald, *Study of Ageing and Degradation of Asphalt Pavements on Low Volume Roads*, 2000
Jostein Aksnes, *A Study of Load Responses towards the Pavement Edge*, 2002
Rabbira Saba Garba, *Permanent Deformation Properties of Asphalt Concrete Mixtures*, 2002

3. DEFORMATION PROPERTIES OF UNBOUND GRANULAR AGGREGATES

3.1 Resilient Modulus

The theory of elasticity traditionally defines the elastic properties of a material by the modulus of elasticity, E, and the Poisson's ratio, ν. Dealing with unbound aggregates in base layers, the elastic modulus E is replaced by the resilient modulus, M_R, to describe the elastic, recoverable behaviour of a material subjected to cyclic loading in a triaxial apparatus. The resilient modulus M_R is known to be nonlinear and stress dependent.

The resilient modulus of a material under constant confining pressure is expressed as:

$$M_R = \frac{\sigma_d^{dyn}}{\varepsilon_a^e}$$

(Equation. 1)

where,

M_R = resilient secant modulus;
σ_d^{dyn} = applied dynamic deviator stress;
ε_a^e = axial resilient strain.

A resilient modulus test is in principle non-destructive, as most of the deformations are recovered. For these type of tests the same sample may be used several times. For high stress levels however, some permanent deformations will occur. In these cases the resilient modulus may sometimes be dependent on how large the permanent deformations are and the effect of changes in the structure of the material. But in most cases when the initial phase of development of permanent deformations is over, the resilient modulus is independent of the permanent deformations.

Lekarp (1999) presented a "state-of-the-art" on the research on the resilient modulus behaviour of unbound granular materials. Most of the research done on the response of unbound granular materials to cyclic loading in a triaxial apparatus has been concentrated on the resilient part of the deformation.

By studying the literature on earlier research Lekarp (1999) found that the resilient behaviour of unbound granular materials was affected by several factors, like; stress, density, moisture content, fines content, grading, aggregate type, number of load applications, stress history, load duration, frequency and load sequence. The influence of most of these factors will be further discussed in Chapter 4.

A lot of effort has been made to develop models that can describe and predict the non-linear resilient behaviour of unbound granular materials. In this chapter two of the oldest and most used models are discussed.

More advanced models exist, taking the anisotropic behaviour or the resilient dilatancy into account (Hoff et al., 1999). However, these models have not been taken into common use.

k-θ model

The k-θ model is a non-linear, stress-dependent power function model first described by Seed et al. (1962). This curve-fitting model is based on the sum of principal stresses or bulk stress. It is a commonly used model to account for the stress dependency of resilient modulus. In its dimensionless form, the model is given as follows:

$$M_R = k_1 \cdot \sigma_a \left(\frac{\theta}{\sigma_a} \right)^{k_2}$$
(Equation. 2)

where,

θ = bulk stress; $\theta = \sigma_1 + \sigma_2 + \sigma_3 = \sigma_1 + 2\sigma_3$
k_1 and k_2 = model parameters from regression analyses of triaxial test results;
σ_a = reference pressure (100 kPa).

The original k-θ model has several shortcomings (Hicks and Monismith, 1971;Uzan, 1985). It considers the all-around bulk stress to represent triaxial stress states and does not account for the confining pressure and deviator (or shear) stress individually. Stress level is only accounted for by the bulk stress in this model. This means that all combinations of principal stresses giving the same sum will have the same effect on the resilient modulus.

The k-θ model is also discussed in Paper II.

Uzans model

Uzan (1985) developed a new non-linear model from the k-θ model, to account for the shortcomings of the earlier models. The effect of shear strain was taken into account in this model, which was one of the serious shortcomings of the k-θ model.

The model was first presented as follows;

$$M_R = k_1 \cdot \sigma_a \left(\frac{\theta}{\sigma_a} \right)^{k_2} \left(\frac{\sigma_d}{\sigma_a} \right)^{k_3}$$
(Equation. 3)

where,
σ_d = deviatoric stress.
k_1, k_2 and k_3 = model parameters from regression analyses of triaxial test results.

This model seems to fit well with results obtained from cyclic load triaxial testing and has been used by many researchers. The model is proved to be superior to the k-θ model (Kolisoja, 1997). The model has also been further developed, as for the three-dimensional case where the deviatoric stress is replaced with the octahedral shear stress.

3.2 Permanent deformation behaviour

Permanent deformations represent the non-recoverable part of the deformations. The plastic strain accumulates as the loading continues until the material is either rearranged into a stronger structure or failure occurs. Rutting is the most common damage caused by permanent deformations in unbound granular layers.

As mentioned earlier, most of the research work done on the deformation behaviour of unbound granular materials is concentrated on the resilient behaviour. Lekarp (1999) summarized the research on permanent deformations in a "state-of-the-art". He found that the development of permanent strain was affected by several factors, like; stress level, principal stress reorientation, number of load applications, moisture content, stress history, density, fines content, grading and aggregate type. The influence of each of these factors will be discussed in Chapter 4.

Lekarp (1999) also stated that there is a need for developing computational models for prediction of permanent strain response in unbound granular materials. The existing models are mostly based on the effect of the number of load applications.

The shakedown approach
The concept of shakedown in materials was originally developed to describe the deformation behaviour of metal in pressure wessels under cyclic loading. Later this concept has been applied to describe the plastic behaviour of unbound granular aggregates under cyclic loading (Sharp et al., 1985). Further details on the theoretical background of the concept are given in Collins et al.(1993).

Werkmeister et al. (2001) studied the permanent deformation behaviour of unbound granular material using the shakedown approach. Here the results from the cyclic load triaxial testing, permanent strain test, is reported as either shakedown range A, B or C. Where A refers to a plastic shakedown range, where the material after a post-compaction period becomes entirely resilient with no further permanent strain. Range B is defined as an intermediate response, or plastic creep, where the high level of plastic strain decreases during the first load cycles to a low, nearly constant level. Range C represents the incremental collapse where the permanent strain only increases with increasing number of load applications.

Werkmeister (2003) suggested criteria for the shakedown ranges A-C, based on the accumulation of vertical permanent strain, strain rate, from 3000 to 5000 load applications. The boundaries between the different ranges were defined as follows;

Range A $\qquad$ $\varepsilon_1^{\,p}{}_{5000} - \varepsilon_1^{\,p}{}_{3000} < 0.045 \cdot 10^{-3}$

Range B $\qquad$ $0.045 \cdot 10^{-3} < \varepsilon_1^{\,p}{}_{5000} - \varepsilon_1^{\,p}{}_{3000} < 0.4 \cdot 10^{-3}$

Range C $\qquad$ $\dot{\varepsilon}_1^{\,p}{}_{5000} - \dot{\varepsilon}_1^{\,p}{}_{3000} > 0.4 \cdot 10^{-3}$

The determination of these range limits was made on the basis of the results from the cyclic load triaxial testing.

The "Coloumb approach"

The Coulomb criterion may be applied to the results from cyclic load triaxial testing for unbound granular materials, keeping in mind that the equilibrium and failure envelopes from repeated load testing would be different from the results from a static triaxial test. Figure 2 shows the principles of the Coulomb criterion in a τ-σ-plot.
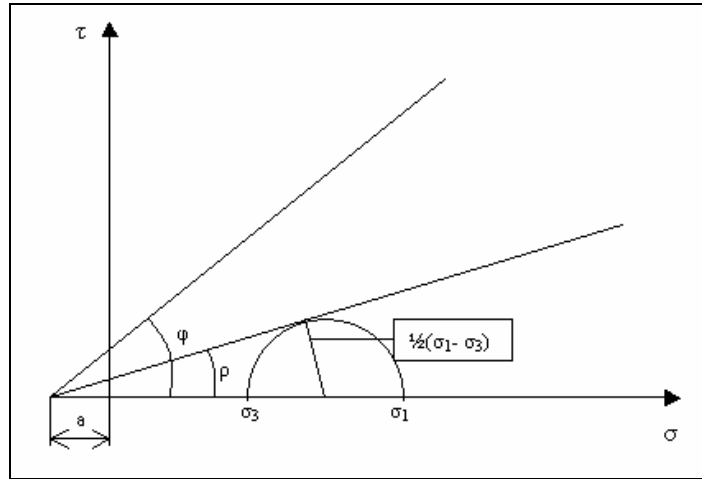

Figure 2. Degree of mobilized shear strength expressed by the mobilized angle of friction and the failure line expressed by the failure angle

The degree of mobilized shear strength is the most important factor for development of permanent deformations. The mobilized shear stress related to the maximum shear stress (failure) shows how far the material is from failure. The mobilized shear strength expressed by the mobilized angle of friction, ρ, is found by the expression;

$$sin\,\rho = \frac{\sigma_1 - \sigma_3}{\sigma_1 + \sigma_3 + 2a}$$
(Equation. 4)

where a is the apparent attraction in the material.

Figure 3 shows the different ranges of material behaviour that may be found by testing a material in a cyclic load triaxial apparatus. However, there is a need for criteria to define the limits between the different ranges of material behaviour; elastic, elasto-plastic and plastic or failure.
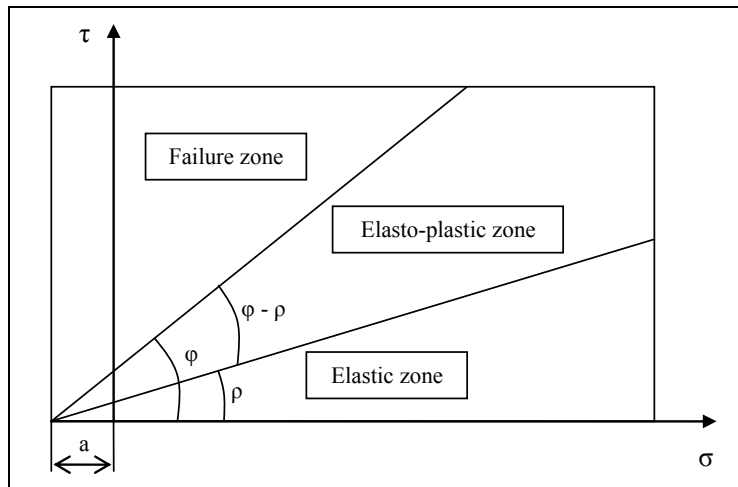
Figure 3. τ-σ - diagram showing the different ranges of material behaviour

Hoff et al.(2003) presented this way of interpreting the permanent deformation behaviour of an unbound granular material when testing the material in a cyclic load triaxial apparatus.

The strain rate $\dot{\varepsilon}$ is a measure of the speed of the permanent deformation. Here, the term is used for development of permanent deformation per cycle. The strain rate is normally highest for the first few pulses of loading and decreases gradually by time. Figure 4 shows the accumulation of permanent axial strain as a function of the number of cycles for one sequence in a multistage loading procedure (Uthus et al., 2007d).
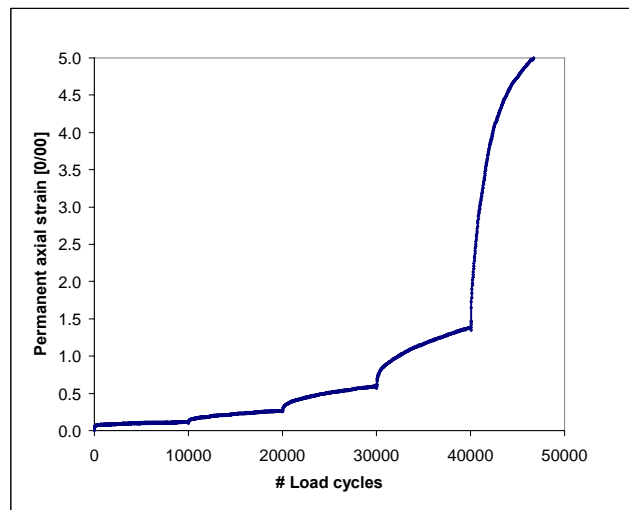

Figure 4. Axial permanent strain accumulation as a function of the number of load cycles tested at one load sequence (Uthus et al., 2007d)

In static triaxial testing with constant strain rate, the failure limit can be found by the stage of yielding, and the level of permanent strain is a key parameter for failure. In the multistage

repeated load triaxial testing procedure, the strain rate rather than the strain magnitude is found to be a suitable parameter to define failure.

Each load step (combination of confining stress and deviatoric stress) may be categorized into three ranges like in the method described by Werkmeister et al. (2001). In this study average strain rate for the last 5000 to 10000 cycle was used, and the range limits for categorization of material behaviour are found from the observed total strain / physical "failure" for the material tested. This procedure was described in Hoff et al. (2003).

Range - A: $\dot{\varepsilon} < 2.5 \cdot 10^{-8}$ Elastic range
Range - B: $2.5 \cdot 10^{-8} < \dot{\varepsilon} < 1.0 \cdot 10^{-7}$ Elasto-plastic range
Range - C: $\dot{\varepsilon} > 1.0 \cdot 10^{-7}$ Plastic/failure range

For these three ranges the steps in the elastic range are marked by square symbol, the points being in elasto-plastic range are marked by triangles and the points in the failure range is marked by circles.

All load steps shown in a σ_3-σ_d plot and categorized by the three ranges above may look like the example in Figure 5. The failure limit and the elastic limit in Figure 5 may be seen in relation to the conceptual Figure 3, which is a τ-σ plot.
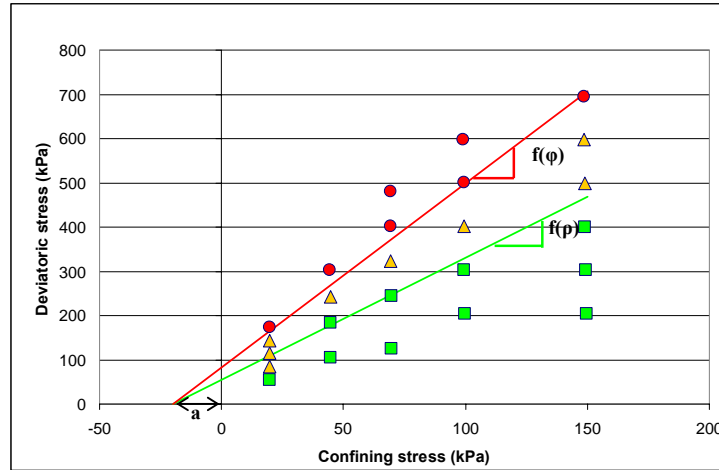
Figure 5. All load steps for one sample categorized into three categories (example)

The Coulomb criterion is used to find the stress envelope for the design stage and the failure stage, shown by the lower and the upper line respectively. The equations of these lines are:

Elastic limit: $\sigma_d = \dfrac{2sin\rho \cdot (\sigma_3 + a)}{(1 - sin\rho)}$ (Equation. 5)

Failure limit: $\sigma_d = \dfrac{2sin\varphi \cdot (\sigma_3 + a)}{(1 - sin\varphi)}$ (Equation. 6)

The apparent attraction "a" was interpreted to be close to 20 kPa for all the samples in this thesis as a simplification. This seems to be a reasonable value for the materials tested.

3.3 Cyclic load triaxial testing

Barksdale (1971) found that the repeated load triaxial test more closely simulate the stress conditions in flexible pavements than other available test methods like e.g. CBR. Still this is one of the best methods available for laboratory simulation of traffic loading on unbound materials.

The triaxial apparatus used in this thesis was developed and built during the seventies at the Department of Road and Railway Engineering, NTH, with Professor Rasmus S. Nordal as the initiator. This equipment was designed and built as a part of the doctoral work of Ivar Horvli (Horvli, 1979), who made use of this for his testing on clay. Through the work of Inge Hoff (Hoff, 1999) the equipment was further developed. Most of the analogue data acquisition and load control equipment was replaced with a PC, new and smaller LVDT's was installed and new software was developed. A picture of an instrumented triaxial sample is shown in Figure 6.

Figure 6. Instrumented triaxial sample (Dongmo-Engeland, 2005)

The triaxial chamber of this equipment is made of plexiglass, but for high stress levels a steel chamber may be used for safety reasons. Water is used as a confining medium. All samples in this study had a diameter of 150 mm and were compacted in a gyratory mould with a height of 240 mm, which means that the height of the samples were reduced compared to the EN specifications (CEN, 2000). Dongmo-Engeland (2005) studied the effect of reduced height of the samples and found that the difference was negligible with a special procedure using Teflon to reduce the friction against the end plattens. This procedure has been used in this study.

The loading procedure applied on all materials tested in this thesis was the EN 13286-7 standard (CEN, 2000), Cyclic load triaxial tests for unbound mixtures. This standard offers several procedures, but in this thesis the multistage loading procedure, high stress level, was used for all samples. The only exception was for the spheres in Paper VI. The multistage loading procedure is designed to avoid too large permanent deformations in the material. By using this procedure it is possible to obtain information about both the resilient properties and the permanent deformation behaviour from one sample. The material behaviour is in the elastic area most of the time, but at the end of each load step for all confining stresses most materials develop some permanent deformations. This happens when the axial loading reaches a certain level. The axial loading is then interrupted when the permanent axial strain reaches 0.5 %.

The results will be influenced by stress history. However, the alternative of testing one sample for each stress combination would be very time consuming.

The stress level applied is further discussed in Chapter 4.

4. DISCUSSION

This chapter discusses the findings in the papers together with those in the literature. The papers are referred to as Papers I-VI.

4.1 The effect of grain shape and surface texture

Hicks and Monismith (1971) reported that the resilient modulus was higher for a crushed material than for a partially crushed material regardless of the aggregate gradation. Allen and Thompson (1974) and Barksdale and Itani (1989) found that the resilient modulus was higher for the crushed rock tested, than for gravel. These were all well-graded materials. Barksdale and Itani (1989) also found that the gravel was more than two times more susceptible to rutting than the crushed aggregates.

Janoo (1998) concluded from a laboratory study of unbound material that rounded particles caused significantly higher permanent deformations over time than angular aggregate particles when subjected to cyclic loading. In general it was found that rounded particles were able to slip easily, whereas angular materials had to overcome higher frictional forces at the contact interfaces. From this it was concluded that the angle of internal friction, and thereby the resistance against permanent deformations, increases with increasing angularity.

Paper I presented an evaluation of different methods for characterization of grain shape for unbound granular aggregates for four different grain shapes made from the same material. Photos of the aggregates are shown in Figure 7. The rounded shapes were made by wearing the material in a Ball Mill drum for 60 minutes. The differences in grain shape were significant as the rounded aggregates had the corners worn off.

The different methods all classified the cubical material as equidimensional and disc shaped, cubic angular, non-elongated with a low flakiness. The cubical rounded aggregates were classified as being fairly spherical, equidimensional, cubic rounded, non-elongated with a low flakiness and quite low roughness, angularity and surface texture.

The flaky angular aggregates were classified as being fairly elongated, disc and blade shaped, flaky/elongated angular, elongated but with relatively low Flakiness Index. From the image analysis these aggregates were characterized as being quite rough with a low roundness, angular and with a rough surface texture. The flaky rounded aggregates were characterized as elongated, blade shaped, flaky/elongated rounded, with quite high flakiness, lower angularity than the other aggregates and a quite smooth surface texture.

Paper I concluded that the simplest methods of grain shape characterization did not distinguish well between the four grain shapes, but a combination of the Shape Index and the Flakiness Index seemed to give useful information about the grain shape, even without taking the roundness of the aggregates into account. In Paper I the Shape Index showed a higher elongation for the flaky materials than for the cubical materials, which seemed reasonable.

Cubical angular aggregates

Cubical rounded aggregates
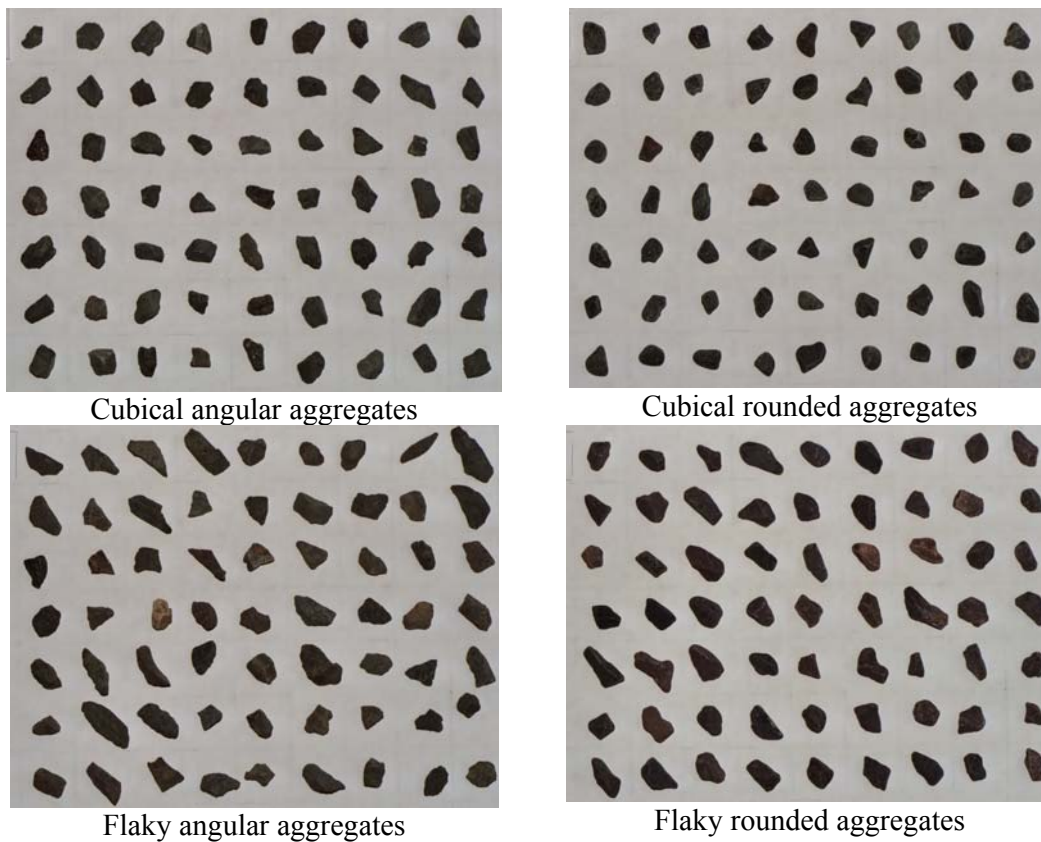
Flaky angular aggregates

Flaky rounded aggregates

Figure 7. Four different grain shapes of Askøy material 11/16 mm

The two-dimensional image analysis seemed to give good measures of the grain shapes, but the angularity and roundness were not characterized in a satisfactory way. This method also has a weakness in the fact that it only accounts for the two-dimensional projection of the aggregates, and the result will therefore depend on which direction the aggregate is placed.

The three-dimensional image analysis was found to be the best method to distinguish between the four grain shapes in this study. Both the angularity and the surface roughness are characterized from three orthogonal directions. However, the three-dimensional image analysis is still a method that is more suitable for research than for everyday laboratory characterization. Paper I questioned whether this detailed information is needed for engineering purposes and how the differences in these parameters can affect the deformation properties of unbound aggregates.

In Paper II samples with the same four grain shapes of the 11/16 mm fraction from Askøy were tested using a cyclic load triaxial apparatus to study the effect of the differences in grain shape on the deformation properties. Here the results from the triaxial testing were compared to the differences in grain shape found by three-dimensional image analysis. Paper II concluded that the rounding of aggregates in a Ball Mill drum caused significant changes in the angularity and the surface texture properties were clearly detected by the three dimensional image analysis.

The study also concluded that for low stress levels the resilient behaviour of the four grain shapes were very similar, but for higher stress levels the cubical rounded material seemed to give the highest resilient modulus. The cubical angular aggregates seemed to be less influenced by the increase in stress level as the resilient modulus did not increase as much for this grain shape for higher stress levels. The cubical rounded aggregates had a higher dry density for all the samples compared to the cubical angular aggregates, so this may be an explanation for the higher resilient modulus. It also seemed like dry density in the cubical rounded sample increased somewhat under loading and that the rounded aggregates thus have an ability to rearrange and build more stable structures.

For the flaky angular and flaky rounded aggregates the resilient modulus seemed to almost coincide for all the stress levels tested. The dry density of the flaky rounded aggregates was however higher than for the flaky angular aggregates. At equal densities the flaky angular aggregates would probably have a higher resilient modulus than the rounded aggregates. The results from the interpretation of the permanent deformation behaviour are shown in Figure 8.

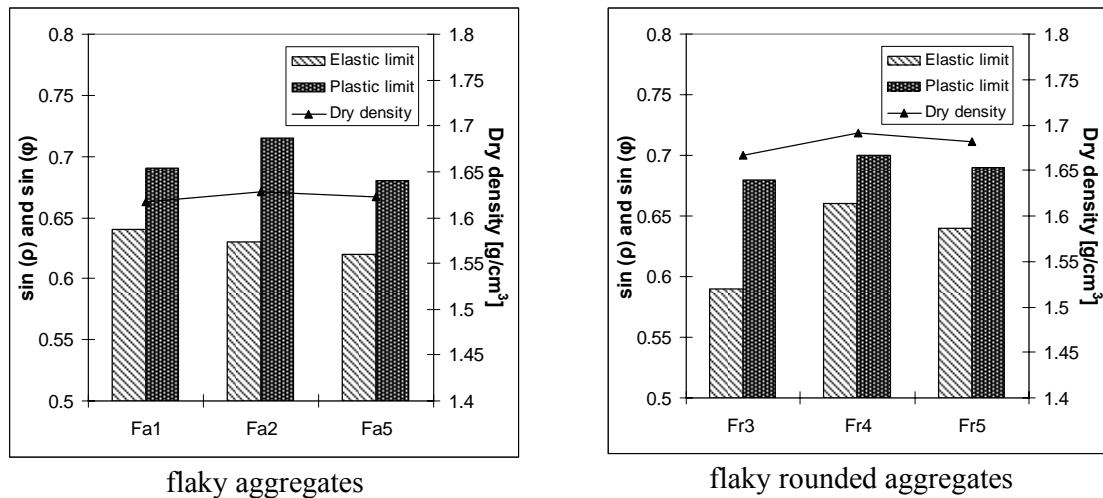flaky aggregates   flaky rounded aggregates

Figure 8. Elastic and plastic limits presented with compacted dry densities for the flaky angular and the flaky rounded aggregate samples (Uthus et al., 2007d)

The cubical angular aggregates had significantly higher resistance to permanent deformations, even when the density of the cubical rounded material was higher. This may be explained by the angularity and the surface texture, as these factors influence the internal friction in the material. Lower internal friction causes less resistance to permanent deformation and thus to rutting.

The flaky angular and rounded aggregates showed similar elastic and plastic limits for single samples, even when the flaky rounded aggregates had higher dry density for all samples. Here the same conclusion as for the cubical aggregates may be drawn, as the rounding seems to give lower internal friction in the material and lower resistance to rutting.

The intention of Paper II was to study the effect of grain shape on the deformation properties. It seems to be difficult to isolate the effect of the grain shape alone, because the grain shape also has a significant effect on the dry density achieved for the samples when the same compaction energy was applied. There also seems to be a difference between the cubical and the flaky materials, as the dry density achieved for the cubical materials was significantly higher. The flaky material might have given higher resilient modulus and resistance to permanent deformations if the same dry density was achieved. However, it may not be possible to achieve the same dry density without crushing the grains.

Paper II was a limited study using four different grain shapes from the same aggregate material. This means that the grains probably have very near the same mechanical properties. In other studies of grain shape (Barksdale and Itani, 1989; Janoo, 1998), different materials have been used to represent different grain shapes. Then the mechanical properties and other inherent properties of the materials may override the effect of the grain shape alone. In that case the mechanical strength may be a "source of error" and influence the effect of grain shape alone. This is avoided by the way the materials are selected in Paper II.

In Paper IV three materials with two different gradings were tested, one with grading coefficient n=0.35 and one with n=0.5. Two of the materials were from the same quarry in Askøy, Norway. The two materials were taken from different steps in the crushing process, as the more cubical material was more refined. The third material was an extreme material from a quarry in Sweden containing 33 % mica. The two materials from Askøy had different grain shapes, as the more flaky material had a Flakiness Index (FI) of 28 while the more cubical material had a FI of about 14. The Swedish material had a FI of 24, which is comparable to the Flaky material from Askøy. The cubical and flaky materials from Askøy had Los Angeles (LA) values of 17 and 20, respectively, while the Swedish material had an LA value of 24.

Paper IV concluded that the materials from Askøy had similar behaviour for both gradings under similar degrees of saturation and dry density. The flaky material even had a slightly higher resistance to permanent deformations and a lower dry density for the grading with n=0.5. This shows that refining a material through the crushing process seem to have negligible effect on the deformation properties for well-graded materials with grading coefficients of n=0.35 and n=0.5.

When comparing the material from Sweden with the flaky material from Askøy, the material from Askøy was stronger even if the difference in grain shape was small. Here the grain shape obviously was overruled by the effect of mineralogy and mechanical strength.

In Paper VI an extreme grain shape and grain size distribution was used as shown in Figure 9. Smooth spheres were made from the Askøy material, with a diameter of 14.4 to 15.8 mm. According to Cole et al. (in prep) the spheres had an apparent coefficient of friction - μ of about 0.28, which is a quite small value.

Figure 9. Smooth aggregate spheres from the study in Paper VI

In Paper VI the stress level from the EN multi-stage loading protocol for cyclic load triaxial testing had to be reduced to be able to get some information from the tests without collapsing the samples. The stress level needed for a more stable stress situation was so low, that the relevance to real conditions may be questioned. However, this showed that an extreme grain shape, such as spheres, has a great effect on the internal friction between grains and therefore a major influence on the deformation behaviour.

The intention of using spheres was to have a simple grain shape to describe mathematically for comparison with results from discrete element simulations. The spheres are of course only suitable for research purposes, and not for use in road structures. However, this is a first step towards more advanced simulations to model material response using a discrete element model.
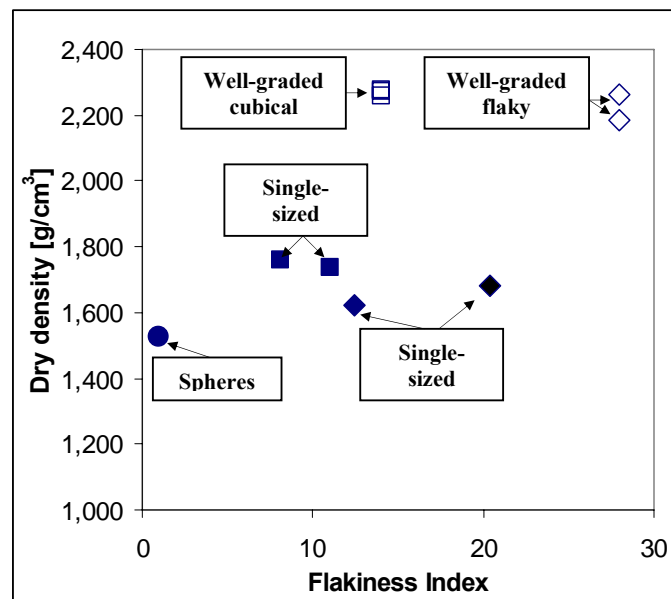

Figure 10. Dry density as a function of Flakiness Index
for single-sized and well-graded materials

Figure 10 presents the dry density as a function of the Flakiness Index of all the material from Askøy. The dot means the spherical grains that are made from Askøy material. The squares means cubical material and the diamonds mean flaky material. The filled dots, squares and diamonds are all single-sized material, while the open squares and diamonds are well-graded materials. The Flakiness Index is not a critical parameter when it comes to giving increased or decreased dry density. The gradation is a more important parameter, as the well-graded materials have significantly higher dry density regardless of the Flakiness Index. However, the well-graded materials are compacted using a vibrating hammer while the single-sized material is only lightly compacted.

4.2 The influence of grading and fines

Hicks and Monismith (1971) did not find an unambiguous effect of the gradation when testing materials with three different gradations: one coarse, one medium and one fine graded. The aggregate type seemed to affect the results, but for the crushed aggregate tested the resilient modulus seemed to increase with increasing fines content. They also found that, regardless of aggregate type, the Poisson ratio was reduced with increasing fines content.

Thom and Brown (1988) reported that the stiffness of the material decreased for excessive fines content. They also concluded that a uniform grading was stiffer than a broad grading for the same maximum particle size. This was also confirmed by Hoff (1999).

Ekblad (2004) tested four different gradations, using one material composed different curves with grading coefficients of n=0.8, 0.5, 0.3 and 0.4 (Fuller and Thompson, 1907). The study showed that the resilient modulus decreased with increasing water content and decreasing grading coefficient.

Barksdale and Itani (1989) studied the effect of the plasticity of fines on the deformation properties of a granitic gneiss by adding certain proportions of the minerals kaolinite or bentonite to the samples. Here the permanent strain was found to increase by a factor of 3 as the content of kaolinite in the fines increased from 0 to 75 %. The resilient modulus decreased with increasing kaolinite content. The bentonite only had a slight effect on the permanent deformations, but this mineral absorbs large quantities of water and was expected to have a more pronounced effect if more water was added.

Barksdale and Itani (1989) reported a decrease in the resilient modulus of 60 % as the fines content increased from 0 to 10 %. They also observed that as the fines content increased, the amount of plastic strain also increased.

Kolisoja (1997) investigated the effect of different properties on the resilient deformation behaviour. The effect of the amount of fines was investigated by adding more fines to a well-graded material. The conclusions of this work were that the resilient modulus seemed to decrease slightly with increasing fines content as the material approached a fully saturated stage.

Both the amount of fines and the properties of the fines seem to be important for the deformation behaviour. Kolisoja (1997) investigated the effect of the quality of the fines by adding fines from three different origins to two different materials. This showed that a

material could show up to 20% reduction in resilient modulus, just by adding another material as the fines fraction.

In Paper II a single-sized 11/16 mm grading was used where all material passed the 16.0 mm sieve, and no material passed the 11.2 mm sieve. The results seemed to be a little more scattered than for well-graded materials. However, the resilient modulus seemed to be slightly higher for single-sized materials except for the cubical angular aggregates from Askøy. For the permanent deformation behaviour the single-sized material seemed to give results in the same range as for the well-graded materials, even higher for some of the samples.

As mentioned earlier a well-graded material with grading coefficient n=0.35, 0/22 mm, was used in Paper III. Here the focus was on the influence of grading and fines on the deformation properties and the frost susceptibility of the three materials tested. Paper III concluded that simple frost susceptibility criteria based on gradation and fines content may be too simple to give a good classification system. Factors such as mineralogy, grading of fines and specific surface area of fines have to be taken into account to be able to predict the behaviour of the material more accurate.

In Paper IV the same three materials as described above were used, with grading coefficients of n=0.35 and 0.5, respectively. This paper concluded that the grading with n=0.5 was stronger than the material with n=0.35 and less sensitive to changes in water content for all three materials tested. It also concluded that for relatively dry conditions the grading with n=0.35 showed the highest resilient modulus and highest resistance to permanent deformations for all three materials tested. As the water content in situ varies a lot, the conclusion was that the material with n=0.5 is to be preferred for all conditions.

In Paper V the effect of grading was studied using the same two gradation curves as in Paper IV, 0/22 mm. In addition, a curve used in a PPP project in the southern part of Norway, 0/32 mm, was used. The different gradings are shown in Figure 11. Paper V concluded that for equal dry density and degree of saturation the resistance to permanent deformations decreases with increasing fines content.

When studying the triaxial test results of the aggregate spheres from Askøy in Paper VI, both the grain shape and the grain size distribution were extreme. The grain shape and surface texture of the spheres were probably the critical parameters, but also the grading was important for the behaviour of this material. The spheres were all close to the same size, which means that the structure was very unstable and dependent on the confining stress. The stress level also had to be reduced for this material, which means that this material with single-sized spheres is much weaker than all the other gradings tested from the Askøy material.
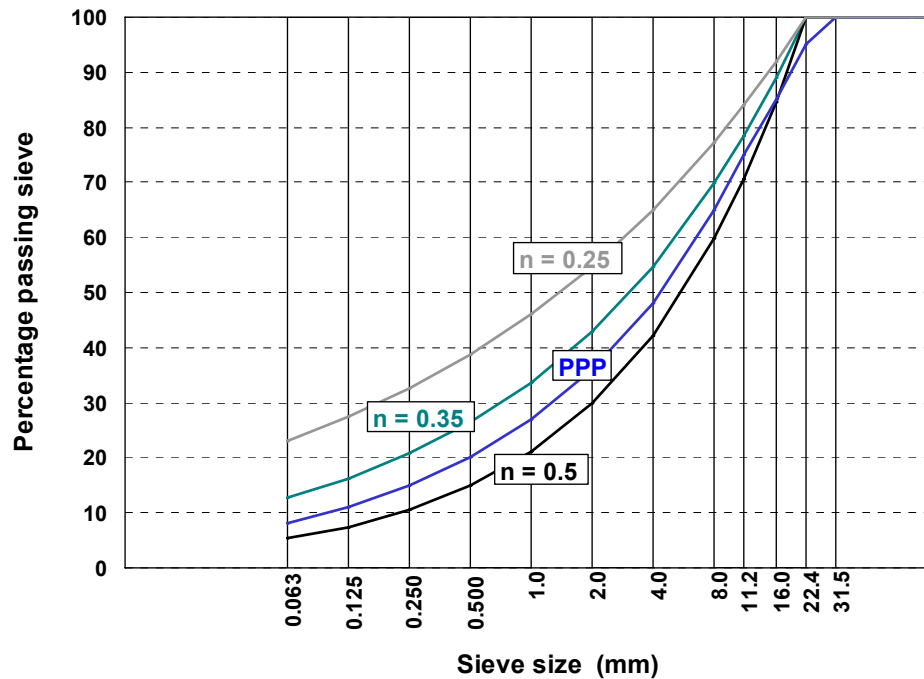
Figure 11. Grain size distributions of the material used in Paper V (Uthus, 2007a)

All together five different grain size distributions were tested in this thesis, two gradings with n=0.35 and n=0.5 0/22 mm, one relatively well-graded material used in a PPP project 0/32 mm, one single-sized grading 11/16 mm and the spheres. When comparing the different gradations just by studying the cubical angular material from Askøy, the spheres give the lowest resilient modulus followed by the single-sized cubical angular material from Askøy. The cubical single-sized material only has slightly lower stiffness than the well-graded materials and is very dependent on the confining stress.

The gradation with n=0.35 has the highest resilient modulus and resistance to permanent deformations for low water content, but the lowest for higher water content, especially close to saturation. The PPP grading has the largest maximum aggregate size, 31.5 mm, but this does not seem to affect the results much. This grading shows the highest strength for some kind of optimum water content, and then it decreases. The grading with n=0.5 shows the highest resilient modulus and the highest resistance to permanent deformations and is more dependent on the density than the degree of saturation.

4.3 The effect of mineralogy and aggregate type

The rock quality in Norway varies quite a lot. In the southern and western part of the country there is a lot of Precambrian and Cambro-Silurian gneiss and magmatic hard rock. In the eastern part and some areas in the far north there are relatively hard sandstones, and in central Norway schists and phyllites are dominant. But it is also possible to find local areas in this region with strong rock types such as gneiss, gabbro and quartzite. Scandinavia was covered by ice with interglacial periods in between. It is about 8 000 to 10 000 years since the ice cover disappeared. Therefore the weathering processes have only been acting for a short period in a geological perspective. In addition, these processes are relatively slow because of

the moderate temperature fluctuations, so the quality of the rock is generally very good, even near the surface.

The mineralogy and aggregate type are very important for the inherent properties of granular aggregates, as the mineralogy, mineral grain size and the chemical bonding between the mineral grains determine most of these properties. Crushed rock for use in base layers have to be strong to resist grain-to-grain crushing under traffic loading. The materials should also have a cubical grain shape, to avoid flaky grains that are believed to break and crush more easily and to be less compactable. The grain shape is to a certain degree determined by the mineralogy of the rock type, as foliations and cleavage planes affect the strength of the material. The mineralogical composition of the rock type may be found by thin section analysis.

In this thesis the aggregate type has not been varied much. The main material used through all papers is a relatively cubical, fine-grained gneiss from Askøy outside Bergen in Norway. In this rock, quartz and feldspar are the dominating minerals. An example from the thin section analysis is given in Figure 12. The aggregate is produced and refined by the crushing process. Some specimens are further processed in the laboratory in a Ball Mill drum. The Los Angeles (LA) value of this material is 17.

Figure 12. Example from thin section analysis of the Askøy material

In addition another material from the same quarry in Askøy is used (Papers I, II, III and IV). The difference from the first aggregate quality is mainly that this material is taken from an early step in the crushing process. However, the mineralogy and grain shape is also slightly different. The main minerals here are also quartz and feldspar like in the more cubical material, but this material contains in addition a small amount of biotite (8 %). This material has a different grain shape being more flaky and elongated as shown in Papers I, II and IV. The flakiness of this material is most visible in the well-graded material used in Paper IV. The LA value of this material is 20.

Together with the two materials from Askøy a third material is used, a mica-rich gneiss from a quarry outside Gothenburg in Sweden. This material is an extreme material for use as base course regarding mineralogy, as this material contains as much as 33 % mica

(31 % biotite and 2 % muscovite). The main minerals besides mica are plagioclase and quartz. Plagioclase is a feldspar mineral with well-defined cleavage planes, which may affect the aggregate quality. The resistance to crushing represented by the LA value is 24 for this material, which is relatively low taking the mineralogy into account. This material is used in Papers III and IV.

The cubical and the more flaky aggregate from Askøy seem to give some difference in grain shape as shown in Papers I and II, which is mostly caused by the crushing process. The cubical material has the highest resistance to permanent deformations compared to the flaky material. A significantly lower dry density for the flaky material most probably causes this difference in strength. It is difficult to isolate the effect of the material type for these two materials in Paper II, as the density, grain shape and grain size distribution overrule this parameter. The differences in LA values found for the Askøy material are so small that the mechanical strength probably has negligible effect.

The mineralogy of the fines is also of great importance, especially for materials having a high amount of fines. The fines have a high specific surface area, dependent of the mineralogy, and the minerals are exposed to water and air in the pore system of the material in situ. Some minerals interact with water, either by chemical bonding or by chemical reaction (swelling). It seems like there is a relation between the presence of certain minerals and the behaviour of the material regarding frost susceptibility and sensitivity to water.

The specific surface area of the mineral particles may be found by BET analysis (DIN, 1993), as in Papers III and IV. Rieke et al.(1983) found a strong correlation between the specific surface area of the fines and the frost susceptibility of silt materials.

The mineralogy of material less than 0.063 mm or 0.020 mm may be found semi-quantitatively by using X-ray diffraction (Mladeck, 1976) or by using a more accurate quantitative method such as scanning electron microscopy (Moen et al., 2006).

In Papers III and IV all three materials were used, and the mineralogy of both the coarse aggregate grains and the material smaller than 0.063 mm and 0.020 mm were presented. In Paper III the Austrian Mineral criterion was presented (ASI, 2001), which is a frost susceptibility criterion. Here the amount of fines <0.020 mm accepted for use in a road structure is determined by the mineralogy of the fines. If a material contains a certain amount of the minerals listed for the material <0.020 mm, then direct frost heave testing is required to see if the material will be frost susceptible in reality.

For the three materials tested in Paper III, the material from Sweden gave a high frost heave rate, as expected from the mineralogy and the Austrian Mineral criterion. This material also seemed to be less compactable than the other two materials when using a vibrating hammer. It seems that the combination between a low dry density, the mineralogy and a high water content are the critical factors resulting in the lower strength found for this material.

4.4 The effect of moisture

Water in a road structure has its origin from many sources; groundwater, surface water migrating through the shoulder, ditches or through cracks in the paved surface of the road. In many low volume roads in Norway the ditches are very shallow and the groundwater level may be very high in certain periods. In some cases the drainage system is not designed for large amount of surface water, so during a long rainy period the water level in the ditches may rise and penetrate into the road structure.

Water is a polar material, which means that the molecules have a definite positive and negative direction. This makes the molecules able to combine with the minerals in the aggregate surface. Water also tends to migrate into the pore system by capillary attraction if the pores are small enough, which is related to the grain size distribution of the material and the amount of fines.

Too much water trapped in the road structure combined with the repeated loading from traffic may cause reduced effective stress and due to excessive pore pressure in the material. This is what happens in frost susceptible materials or water sensitive materials during the spring thaw period. The consequence is reduced bearing capacity in the base and subbase leading to cracking and rutting of the asphalt pavement.

In the Tube Suction test the dielectric value is measured on a cylindrical sample of unbound granular material stored in a water bath for 10 days. Figure 13 shows a figure of the setup used in the test. The dielectric value is a measure of the amount of free water in a sample. From this the material can be classified by its susceptibility to water and frost.

Figure 13. Sample setup for Tube Suction test during
ten days of water absorption (Uthus, 2007a)

When the deformation behaviour of a material is significantly affected by changes in water content, the material is moisture sensitive or water sensitive.

Many researchers have studied the effect of water on the resilient modulus. Hicks and Monismith (1971) reported an apparent reduction in resilient modulus with increasing water

content. Barksdale and Itani (1989) observed a significant decrease in resilient modulus for four materials tested upon soaking. All samples were run under drained conditions. Raad et al. (1992) concluded that the effect of water on the resilient properties seemed to be most significant in well-graded materials with a high amount of fines.

Kolisoja (1994) performed cyclic load triaxial testing on materials with five different gradings. He reported that there was a pronounced effect of the degree of saturation for the material having the highest fines content. For the well-graded materials moisture seemed to be favourable until a certain optimum moisture content was reached, then the resilient modulus decreased towards full saturation. However, very high degrees of saturation were not reached in this study.

For the single-sized materials in Papers II and VI, about 2 % water was added to the materials. Most of this water disappeared during compaction and preparation of the samples. This means that these materials only have a moist surface, and the water only acts as a lubricant between the grains during compaction and to some degree during testing. These materials thus allow the water to drain freely. For these open-graded materials the water is not expected to have any significant effect on the results as the water does not result in any increased pore pressure under loading. However, if a weak material is used, there is a risk that the grading of the material will change over time because of interparticular crushing. This may make the material frost susceptible and water sensitive. In the laboratory series described in Papers II and IV the interparticular crushing was negligible.

In Paper III the frost susceptibility and water sensitivity of three materials were tested by laboratory frost heave testing and cyclic load triaxial testing, respectively. This paper also evaluated the materials by using several criteria for frost susceptibility based on grading and mineralogy. Paper III concluded that the simple criteria for frost susceptibility, based on gradation only may give useful information for frost susceptibility classification of materials. However, these criteria do not account for the mineralogy of the materials and other properties of importance. The Austrian Mineral criterion adds another dimension to this, as this criterion allows a higher amount of fines if the content of certain minerals is below specified levels. For the materials tested in Paper III the material giving the highest frost heave rate was also detected by the Austrian Mineral criterion.

All three materials tested in Paper III were more or less water sensitive, as they all gave a reduced resilient modulus for increased water content. An example of this is shown in Figure 14. The material with a high amount of mica also was the most water sensitive material. The resistance to permanent deformations seemed to be more influenced by the changes in water content than the resilient modulus for these materials.
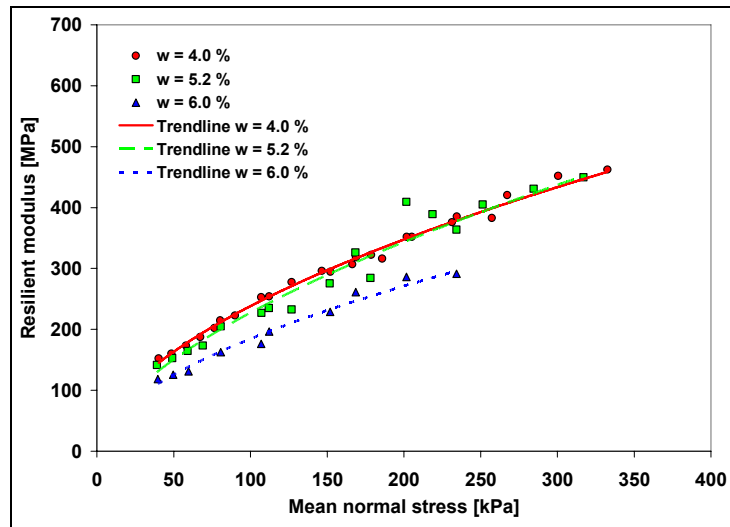
Figure 14. Resilient modulus as a function of mean stress
for a Swedish gneiss (Example) (Uthus et al. 2006)

A material is frost susceptible if it has a pore structure and a mineralogy that attracts water to the frost front, making possibilities for creating ice lenses. A material being sensitive to water has the ability to suck up water and to keep water in the pore structure. The Austrian Mineral criterion is an example of a criterion that limits the amount of certain minerals in materials for use in road structures. These minerals all (to a certain degree) interact with water.

It may be questioned whether it is the frost susceptibility or the water sensitivity that is the most critical factor of a material in a road structure. Frost heave cannot occur without water present in the road structure, and if water is present and trapped inside the pore structure, the material certainly is water sensitive. The water sensitivity of a material seems to be the critical factor leading to most damage. However, the frost may also give problems with cracks in the pavement directly caused by frost heave.

In Paper IV the same three materials and grain size distributions as in Paper III was used. This paper also concluded that the sensitivity to water increased with increasing fines content. The most well-graded material with n=0.5 seemed to be less sensitive to water.

Paper V presented a study of the cubical Askøy material sieved and recomposed into three different gradations, as mentioned earlier. The materials were tested using the Tube Suction test and cyclic load triaxial testing. It seems like a degree of saturation over a certain level affect the resilient modulus of the different gradations tested in Paper V, as the resilient modulus decreased when the degree of saturation was over a certain level. Increasing fines content made the resilient modulus decrease at a lower degree of saturation. Paper V concluded that both the resilient modulus and the resistance to permanent deformations seemed to decrease for increasing fines content for equal dry densities.

4.5 The effect of dry density

The achieved dry density of a compacted material is dependent on a number of factors. First of all the grain size, grain shape, grain size distribution and amount of fines are material properties of importance together with the moisture content. Secondly, external factors like compaction method and compaction energy are also of importance (Hoff, 2003).

Hicks and Monismith (1971), Allen and Thompson (1974), Rada and Witczak (1981), Thom and Brown (1988), Barksdale and Itani (1989) and Kolisoja (1994) all found that density played a dominant role on the resilient response of the materials tested.

Hicks and Monismith (1971) also reported that the effect of density on the resilient modulus was greater for a partially crushed material that for a crushed material. They also found that the effect of density decreased with increasing fines content.

An increasing dry density increases the shear strength of a material (Thom and Brown, 1988; Barksdale, 1991). A material having high shear strength may be more difficult to compact, as they also resist the shear stresses induced by the compaction.

In Paper II aggregates with four different grain shapes were produced from the same quarry. The intention of this paper was mainly to study the effect of different grain shapes on the resilient and permanent deformation behaviour. However, the conclusion of this paper was that dry density seemed to be the dominant parameter, overriding the possible effect of different grain shapes with respect to the resilient modulus and the permanent deformation behaviour.

The rounded aggregates achieved a higher dry density than the more angular aggregates, hence giving a higher strength. Also the flaky materials had a significantly lower dry density than the cubical aggregates. Since these were all single-sized materials, dry density was even more dependent on the compactability of the materials and the ability to fill the voids in the structure. Only light compaction using a vibrating table was applied, with the same energy, dead weight, layer thickness and compaction time for all the samples. The dry densities obtained then show us that the different grain shapes do have different compactability.

In Paper III a higher dry density was achieved than obtained by Modified Proctor for the samples of Material 1, as shown in Figure 15. This is probably caused by the compaction method, as the samples for triaxial testing were compacted by a vibrating hammer, while the Modified Proctor samples were compacted with a Proctor hammer. The vibrating hammer seemed to be a suitable method for compaction of Material 1. For Material 2 slightly lower dry densities were achieved for the triaxial samples compared to the Modified Proctor. This shows that the grain shape might influence the optimum compaction method.
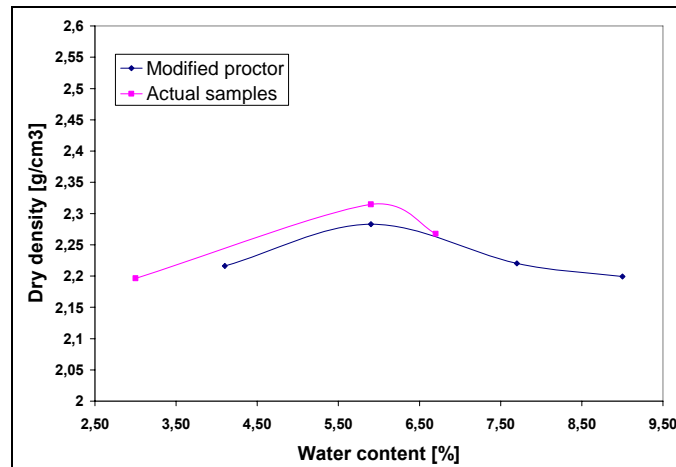
Figure 15. Modified Proctor and actual dry density and water content for
Material 1 in Paper III (Uthus et al, 2006)

For Material 3 the dry densities achieved by the vibrating hammer were significantly lower
that the Modified Proctor curve. This may be caused by the high amount of mica in this
material, which is known to affect the compactability of materials. The proctor hammer
seemed to be a better method for compaction of this material. A kneading compactor might
have been able to compact this material even better.

The conclusions from Paper III was that the dry density may be an influencing factor on the
apparent strength of Material 3, as the dry density achieved was significantly lower than for
the other two materials.

In Paper IV the same three materials as in Paper III was tested, with grading coefficients
n=0.35 and 0.5. Here it seemed like the dry density was a critical parameter for the gradation
with n=0.5, as the strength of the samples followed the dry density achieved for most of the
single samples, even if the degree of saturation increased. An example of the behaviour for
different degrees of saturation is shown in Figure 15 for the flaky material. For the n=0.35
gradation the degree of saturation overrode the dry density at high degrees of saturation.
Within the same degree of saturation however, the behaviour seemed to be mostly influenced
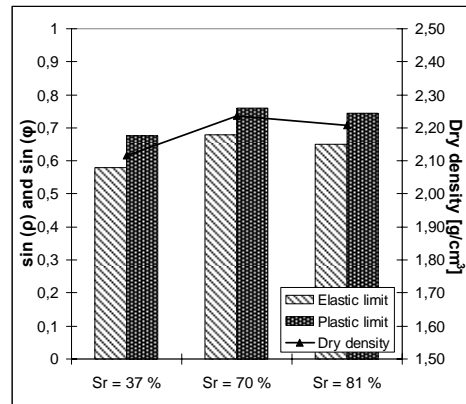by the dry density.

Figure 16. Elastic and plastic ("Failure") limits for
Askøy flaky n= 0.5 (example) (Uthus, 2007b)

In Paper V the cubical material from Askøy was used to compose three different grain size distributions as mentioned earlier. Here the grading with grading coefficient n=0.5 had the highest resistance to permanent deformation compared to the other two grain size distributions, and the PPP grading had the second highest resistance to permanent deformations. The samples with grading n=0.35 did not seem to be significantly influenced of the dry density.

From the findings in Paper V a well-graded material is mostly influenced by the dry density up to a certain level of fines content. The dry density of a material with a relatively high amount of fines seems to be important under dry conditions, but as the fines increases the degree of saturation seems to override the effect of the dry density of the samples. For equal dry densities the resilient and permanent deformation seems to increase as the fines content increases. Hence a high amount of fines gives a lower resilient modulus as well as lower shear strength.

In Figure 17 the dry density is presented as a function of C_u number for the different gradings tested with cubical material from Askøy. The C_u number is a measure of the uniformity of the grading.

Here the single-sized material (11/16 mm) has the lowest C_u number of about 1, while the more well-graded materials ranges from 36 to 167 in C_u number. For the lowest C_u number to the next the increase is quite large, while the well-graded materials seem to have similar dry densities.

This shows that the dry density is dependent on the grading to some extent, but for well graded materials the variations in dry density with increasing C_u number seems to be very small compared to the difference between the single-sized and the well-graded materials.
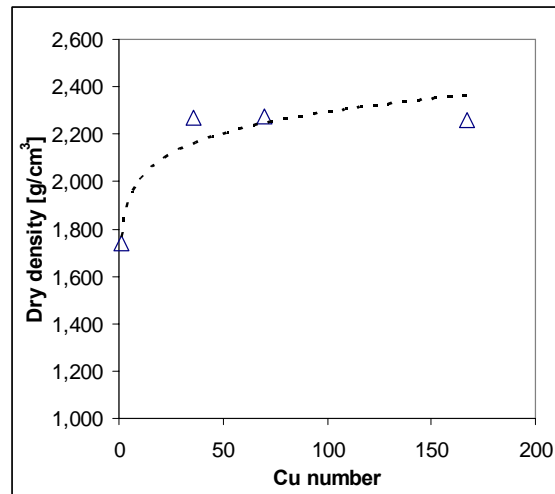
Figure 17. Dry density as a function of C_u number
for cubical material from Askøy

In Paper VI the dry density for the sample with spheres is low compared to all other grain size distributions tested. Here a dry density of about 1.5 g/cm^3 is achieved without using any compaction, only some vibration by hand. One of the differences between the simulations in Paper VI and the laboratory samples is that the laboratory samples is run continuously without unloading the sample, this means that the laboratory sample may have experienced a densification throughout the testing period that may influence the results and give a stronger material over time. The simulations are all run from an equilibrated state for each confining stress.

4.6 The effect of stress level

The response of a material to cyclic loading is very dependent on the stress level. Hicks and Monismith (1971) reported that the stress level affected the resilient modulus most significantly. They found that in all cases the resilient modulus increased considerably with increasing confining stress, and slightly with increasing axial stress. Allen and Thompson (1974) also found that the testing variable that affected the resilient modulus the most was the applied state of stress.

In this thesis the European standard for cyclic load triaxial testing of unbound mixtures EN 13286-7 was applied on all materials tested. The multistage loading procedure was chosen in order to get as much information as possible from a sample. The objective of this procedure is to determine stress limits to avoid the development of excessive permanent deformations. The procedure applies different stress paths, with constant confining pressure (CCP), on the same specimen.

Table 1. EN 13286-7 Multi stage loading procedure (CEN, 2000)

Sequence 1			Sequence 2			Sequence 3			Sequence 4			Sequence 5		
Confining stress, σ_3 (kPa)	Deviator stress, σ_d (kPa)		Confining stress, σ_3 (kPa)	Deviator stress, σ_d (kPa)		Confining stress, σ_3 (kPa)	Deviator stress, σ_d (kPa)		Confining stress, σ_3 (kPa)	Deviator stress, σ_d (kPa)		Confining stress, σ_3 (kPa)	Deviator stress, σ_d (kPa)	
Constant	min	max	Constant	min	max	Constant	min	max	Constant	min	max	Constant	min	max
20	0	50	45	0	100	70	0	120	100	0	200	150	0	200
20	0	80	45	0	180	70	0	240	100	0	300	150	0	300
20	0	110	45	0	240	70	0	320	100	0	400	150	0	400
20	0	140	45	0	300	70	0	400	100	0	500	150	0	500
20	0	170	45	0	360	70	0	480	100	0	600	150	0	600
20	0	200	45	0	420	70	0	560						

Two different loading procedures are provided, one with high stress level and one with low stress level. In Papers II through V the high stress level was applied as shown in Table 1. The axial loading was interrupted when the permanent axial strain reached 0.5 % and the next confining stress was applied. The same loading procedure was used for all the samples, which makes it possible to compare the results for the test series.

In Paper VI the stress level had to be reduced from the level in the EN standard, and even lower than the low stress level procedure. The combinations of stresses were chosen to allow the samples to run for some load steps without collapsing. The samples were very unstable, so initially it was very difficult to find a stress level. Even preparing the samples was a great challenge.

Table 2. Stress level for testing of the spheres

Sequence 1			Sequence 2			Sequence 3			Sequence 4			Sequence 5		
Confining stress, σ_3 (kPa)	Deviator stress, σ_d (kPa)		Confining stress, σ_3 (kPa)	Deviator stress, σ_d (kPa)		Confining stress, σ_3 (kPa)	Deviator stress, σ_d (kPa)		Confining stress, σ_3 (kPa)	Deviator stress, σ_d (kPa)		Confining stress, σ_3 (kPa)	Deviator stress, σ_d (kPa)	
Constant	min	max	Constant	min	max	Constant	min	max	Constant	min	max	Constant	min	max
20	0	25	45	0	50	70	0	75	100	0	110	150	0	100
20	0	30	45	0	55	70	0	80	100	0	120	150	0	150
20	0	35	45	0	60	70	0	85	100	0	140	150	0	200

For all samples the general trend is that the resilient modulus and the resistance to permanent deformations increases with an increasing mean stress and increasing confining stress. In Paper II the effect of deviatoric stress and confining stress was studied. The paper indicates that the stiffness and strength of the sample is more dependent on the confining stress than the deviatoric stress. In Paper II the confining stress seems to be 3-5 times as powerful as the deviatoric stress. When using bulk stress or mean stress the confining stress is the dominant parameter, as the expression are $\sigma_m = 1/3(\sigma_d+3\sigma_3)$ for the mean stress and $\theta=3\sigma_m$ for the bulk stress. It was found reasonable to interpret the resilient modulus as a function of mean stress or bulk stress.

4.7 The effect of stress history and the number of load applications

Allen and Thompson (1974) found that the resilient response of a well-graded material was independent of the stress pulse duration in the range of moving wheel loads. They also found that the resilient modulus value was independent of the number of load applications, as they achieved the same resilient modulus after 25 stress repetitions as after several thousand stress repetitions.

The effect of stress history and the number of load applications is not studied in particular in this thesis. However, some testing on this aspect has been done for one of the cubical rounded samples from Paper II. At the end of the test the confining stress was reduced from 150 to 45 kPa and the load sequence of 45 kPa confining stress was repeated.

The resulting resilient modulus from the first load sequence with 45 kPa confining stress and the same sequence run at the end of the test is shown in Figure 18 as (1) and (2), respectively. The effect of load history seems to be that the resilient modulus increases up to a certain mean stress for the second load step and then it decreases, while the first load step with a confining stress of 45 kPa has the highest resilient modulus for the lowest mean stress. The maximum value for resilient modulus is found for the second load step of 45 kPa confining stress. This may be explained by the fact that the material in this case has experienced a higher stress level earlier. The change in resilient modulus may be explained by a densification and a rearrangement of grains through the heavy loading. However, this was only done for one sample, so this need to be confirmed by more tests.

In Figure 19 the plastic limit, or failure limit from the Coloumb interpretation of the triaxial results is shown conceptually. Here the result of the densification is seen, as the failure limit will be moved, maybe parallel to the original failure limit, to a higher level as the material undergoes higher stress levels.

The number of load applications is important for the material response. In this thesis this factor has not been studied in particular. In Paper VI the number of load applications had to be reduced for the simulations compared to the laboratory samples, from 10 000 cycles per load step in the experiments to 100-200 cycles for the modelling. It is indicated in Paper VI that the resilient modulus increased at the beginning of the load step, and that the resulting resilient modulus may be somewhat higher for the laboratory samples than the DEM simulations for corresponding stress levels.
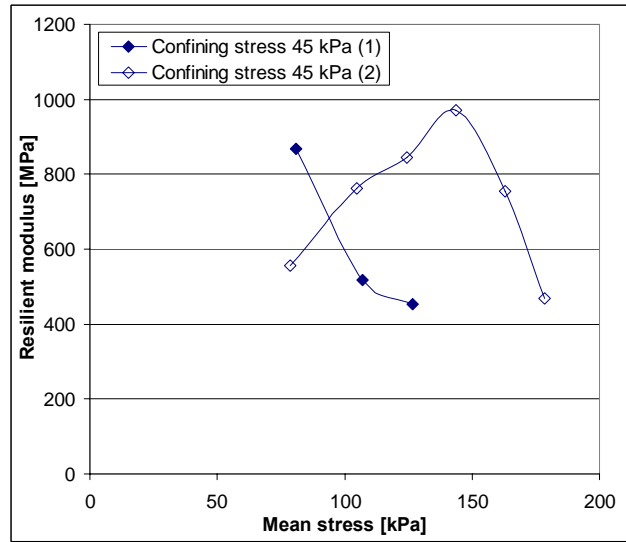
Figure 18. Resilient modulus as a function of mean stress for the load sequence of 45 kPa confining stress for a cubical rounded material, 11/16 mm (an example)
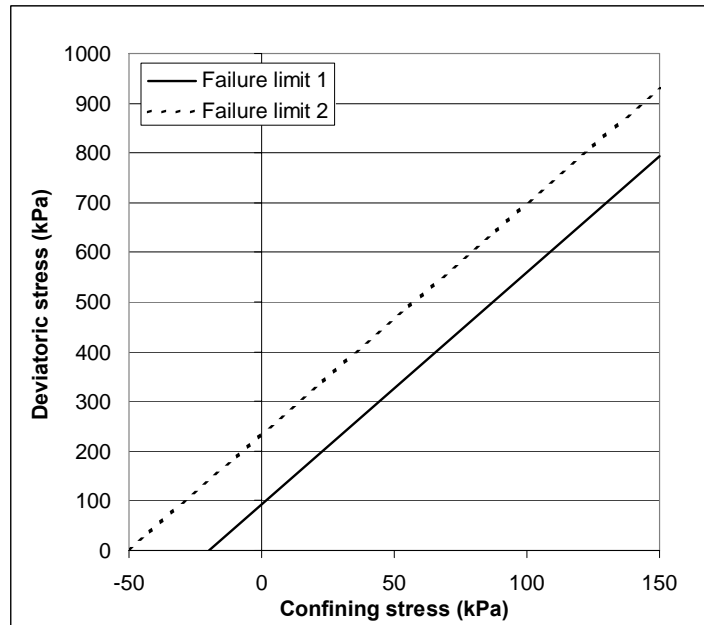

Figure 19. Failure limit for the material as an effect of load history (conceptual)

4.8 The effect of principal stress rotation

When a vehicle is moving over a pavement the orientation of the principal stress axes is gradually rotated. When looking at a small element of material in the road structure, the vertical stress reaches its maximum as the wheel is directly above the element. This is a mechanism that needs to be considered when looking at in situ conditions.

The effect of the reorientation of principal stresses was not studied in this thesis, even if this is found to be of some importance for the deformation properties. The triaxial equipment at NTNU is modified to switch principal stress direction between the axial and lateral direction. In this thesis the triaxial procedure is chosen to be equal for all samples, except for the aggregate spheres, to minimize the number of variable factors. The limits for the permanent deformations may be overestimated compared to traffic loading, which includes the effect of stress rotation.

4.9 Using DEM for simulation of unbound granular aggregates

Unbound granular materials are typically modelled as continuous materials, but in reality they exhibit discontinuous behaviour as the individual grains only interact at the contact points where sliding is common. Observations from the testing of aggregate materials show that they do not always fit even the advanced continuum models based on non-linear behaviour very well. Discrete element modeling (DEM) allows discontinuity in a material and is therefore more realistic for simulation of the behaviour of unbound materials.

One of the advantages of a DEM model compared with real laboratory testing is that all parameters may more easily be varied to study the effect of the different parameters. Another advantage is that the effect of aggregate type is strictly controlled by the grain shape, surface friction and contact stiffness of the grains. This makes it easier to isolate the effect of stress level, grain shape and friction without any disturbance from the effect of aggregate type. However, in reality the aggregate grains will always have some anisotropic behaviour because of mineralogy and foliation. This is so far not included in the model.

From the findings in Paper VI it was concluded that the DEM simulations using the Hertzian contact force model were suitable for simulation of the behaviour of idealized aggregate grains under cyclic loading. The modelling was verified by comparison to laboratory data from triaxial testing of aggregate spheres. The use of a flexible confining membrane in the simulations gave increased realism and accuracy, however, with a significant increase in computation time.

In Figure 20 discrete elements formed by octoids is shown as an example of the future in modelling. This is a more realistic grain shape than the ellipsoids that is currently used.
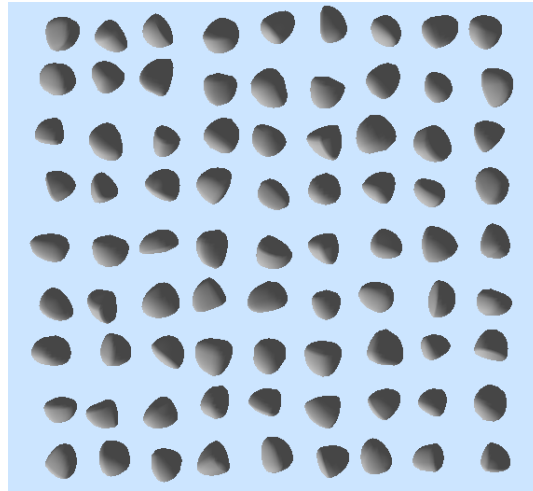
Figure 20. Elements made by octoids (Mark Hopkins)

4.10 Sources of variation in triaxial testing

Cyclic load triaxial testing is currently the most useful laboratory method for determination of the deformation behaviour of unbound aggregates under traffic loading. However, this method also has several sources of variation that needs to be considered.

Sample preparation
Compaction of the materials and the obtained density has a major impact on the sample properties. The resulting dry density of the sample is dependent on the compaction energy and also the compaction method. Measurements of the sample height and diameter are the basis of the calculation of dry density, so the accuracy of these measurements is important

Another source of variation connected to the compaction is the use of Modified Proctor to find the optimum water content and dry density. The dry density found by Modified Proctor may not be the optimum for another compaction method. This is seen in Paper III.

Applying a rubber membrane to a cylindrical unbound aggregate sample without causing any disturbance is very difficult. There are several methods to apply the rubber membrane to a triaxial sample; one method is to use a split mould and another is to use vacuum and push the sample into the rubber membrane. (The last technique is used in this work)

When using a split mould it may be possible to compact the sample of a well-graded material with the rubber membrane inside the walls of the mould, but then the rubber membrane is easily damaged. Another possibility with a split mould is to apply the rubber membrane after the sample is compacted, by splitting the mould and applying the membrane to the sample. Then the sample needs to be made of a material that has certain amount of cohesion to keep the sample together. The disadvantage of this last method is that the sample is fully relaxed after the compaction, which this may affect the initial behaviour of the sample.

At NTNU most of the samples are made in a gyratory mould and a vacuum is applied while the sample is pushed from the mould and into the rubber membrane. The vacuum is turned off

when the sample is mounted in the triaxial chamber with some confining pressure. With this method the sample is not relaxed after compaction and it is possible to make samples of single-sized material, like the material in Paper II and the spheres in Paper VI.

The instrumentation of the samples is important for accurate measurements. In a triaxial apparatus the measurement of radial and axial deformations is usually done by LVDTs, like in this work. The LVDTs may be mounted on the sample or sometimes also the end platens and the wall of the triaxial chamber. When mounting the LVDTs it is important that they are not loose and that the LVDT is mounted normal to the platen or other devices that the LVDT rests against. These factors may all cause some errors that are important to minimize.

Testing
The membrane stiffness may be of some importance, as the membrane keeps the sample in place. However, the stiffness of the membrane was in Paper VI estimated to approximately 4 MPa. The effect of the membrane stiffness at lateral expansion of the sample is estimated below.

The influence of the rubber membrane

This is an estimate of the influence of the rubber membrane at the maximum strain situation at the end of the last load sequence with the confining stress of 150 kPa.

The following assumptions form the basis for the calculations:

Stiffness of membrane:

$E_{membrane}$= 4 MPa (from Paper VI)

Maximum strain on the membrane:

The maximum permanent axial strain on the sample will determine the expansion of the sample in the radial direction. For each confining stress he sample is allowed to develop 0.5 % axial permanent strain, 2.5 % in total for five load sequences. From this we assume a maximum radial strain on the membrane of about 1.5 %.

ε_θ = 1.5 %

Thickness of the membrane:

t = 1 mm = 0.001 m

In Figure 21 the forces on the rubber membrane are shown. The intention of the calculations is to find the effect of the inner pressure from the lateral expansion of the sample, denoted P, giving a contribution to the confining stress on the sample.
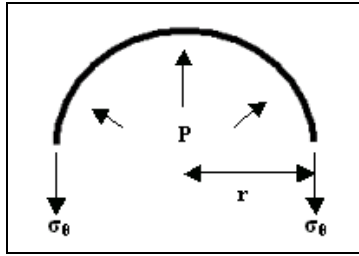
Figure 21. Forces on a cylindrical wall with inner pressure (Irgens, 2002)

$$\sigma_\theta = E_{membrane} \cdot \varepsilon_\theta \qquad \text{(Equation. 7)}$$

$$\sigma_\theta = \frac{r}{t} \cdot P \qquad \text{(Equation. 8)}$$

$$P = \left(\frac{t}{r}\right) \cdot E_{membrane} \cdot \varepsilon_\theta = \left(\frac{0.075\,m}{0.001\,m}\right) \cdot 4 \cdot 10^6\,Pa \cdot 0.015 = 800Pa = \underline{0.8\,kPa}$$

The calculations show that the effect of the lateral expansion of a sample on the rubber membrane at a confining stress of 150 kPa is very low, only 0.8 kPa, and therefore negligible. For the lower confining pressures the strain of the rubber membrane will be also be lower, giving even less contribution from the membrane

The LVDTs used at NTNU are manufactured by RDP. The axial LVDTs are of the type D5/300AW and the radial LVDTs are of the type D5/200AW. The accuracy of these LVDTs is within the requirements of the EN standard (CEN, 2000). The amplifier is manufactured by Hottinger, and the type of amplifier is ME 50.

The measurements by the LVDTs may in some cases be sources of variations. One example is if one of the LVDTs is not working, then the results needs to be calculated from the LVDTs that are working well. To check the LVDTs the results from all of them may be plotted together to see if they give the same result.

Another indication of error is when parallel samples show scattered results. In these situations more samples needs to be run. If all samples tested show a scatter, then this is probably the correct recording of the material behaviour. This behaviour may occur especially when testing single-sized materials, which are more sensitive to variation in grain shape, grain orientation and dry density than the well-graded materials.

One possibility to cope with a high variation between single samples is to increase the number of samples to form a good base for statistical analyses. However, as the work required per sample is high in this case it is not feasible. To compensate for the lack of statistical analyses some "engineering judgement" must be used in the interpretation. This introduces risk of drawing too rigid conclusions from only a few tests.

5. CONCLUSIONS

The conclusions are based on the findings from the different papers in this thesis combined with findings from the literature. Most of the conclusions are related to the deformation properties, but other conclusions regarding the material behaviour are also given.

5.1 Grain shape and surface texture

It is difficult to isolate the effect of grain shape. The deformation behaviour of unbound granular aggregates is connected to several other properties of the materials, such as mechanical strength and dry density. The dry density seems to be a key parameter that is being influenced by the grain shape as shown in Paper II. For the same compaction energy the dry density is different for samples with varying grain shape.

Rounded materials are more compactable than angular materials, but because of the smooth surface of each grain the internal friction is low. The resistance to permanent deformation is therefore lower for rounded than for angular materials as shown in Paper II. The flaky materials in Paper II also seem to be harder to compact than the cubical materials.

The effect of the material grading seems to interact with the effect grain shape. As shown in Paper IV the influence of grain shape on the deformation properties is less pronounced for well-graded materials than single-sized materials. Samples with different grain shape have almost the same deformation behaviour for all the stress levels tested.

Extreme grain shapes, such as smooth spheres, have a considerable effect on the material properties. This is because the internal friction between the particles is extremely low. However, this grain shape is only of interest for research purposes in order to better understand material behaviour.

5.2 Grading and fines

Papers IV and V indicate that well-graded materials with a high fines content are more sensitive to changes in water content. A material with high fines content may be the strongest material under dry conditions, but as the material is subjected to a water content above a certain limit, the resilient modulus and the resistance to permanent deformations clearly decreases.

Paper III shows that it is not only the content of fines that is important, but also the properties of fines like the specific surface area, mineralogy and grading.

Papers II and V state that single-sized materials may have almost the same deformation properties as well-graded materials, but this is dependent on the mechanical strength of the particles.

5.3 Moisture

In well-graded materials the sensitivity to water seems to increase with rising fines content. The resistance to permanent deformation is strongly affected by high fines content in combination with high water content. The content of certain minerals, such as mica, affects the sensitivity of a material to water.

Water is not expected to affect the deformation properties of coarse single-sized materials significantly. This is because the water is not "trapped" in the pore system, but is more or less on the surface of the particles. The only effect of the water here would be as a lubricant. However, over time a uniformly graded material may be subjected to interparticular crushing. The accumulation of fines may change the grading of the material and make it more sensitive to water. By using strong materials the risk of this is reduced.

The Tube Suction test seems to be a good method to detect materials that are susceptible to moisture and frost.

5.4 Dry density

The dry density is affected by parameters like grain shape, grain size distribution, fines content and compaction method. A single graded material usually has a lower dry density than a well-graded material because the latter can fill the voids in the structure more easily as shown in the discussion chapter.

The findings in Paper V indicate that the deformation properties of a well-graded material are mainly influenced by the dry density up to a certain amount of fines. The dry density of a material with a high amount of fines seems to be important under dry conditions, but as the amount of fines increases, the degree of saturation seems to override the effect of the dry density of the samples under wet conditions.

The dry density is one of the key parameters for the deformation behaviour of unbound granular aggregates. The resilient modulus increases with increasing dry density and the resistance to permanent deformations increases with increasing dry density.

The dry density may be a measure of the compactability of a material, when materials with the same grading and specific density are compacted with the same compaction energy, as shown in Paper II.

5.5 Stress level

In this thesis the same loading procedure is applied to all samples, the EN 13286-7 standard, multistage loading procedure, high stress level. The only exception to this was the loading procedure for the spheres. Here the stress level had to be significantly reduced to avoid an immediate collapse of the sample.

The stiffness and strength of an unbound granular aggregate seems to be more dependent on the confining stress level than the deviatoric stress level. This observation seems to fit well with the Coulomb failure envelope theory.

5.6 Stress history and the number of load applications

The permanent deformation behaviour of unbound granular aggregates is very dependent on the stress history, as a material that previously has experienced higher stress levels show significantly higher resistance to permanent deformations, and higher failure limit. This is probably caused by a densification and reorientation of individual aggregate grains. This is considered in the discussion chapter.

For the resilient modulus the stress history also seems to have some impact, but this is not as pronounced as the permanent deformation behaviour. The maximum resilient modulus of the material studied seems to have increased slightly after high stress levels, and the resilient modulus function of a sample subjected to previous high loading is different than originally.

5.7 Using DEM for simulation of unbound granular materials

With increased computer capacity DEM is probably a future method for modelling the behaviour of bound and unbound materials. The possibilities are numerous, when it is possible to describe the problem mathematically. This method can possibly help to give a better understanding of the deformation behaviour of unbound granular aggregates.

The micromechanical properties of an unbound granular material are known to have great importance for the deformation behaviour.

6. PRACTICAL CONSEQUENCES AND RECOMMENDATIONS FOR FURTHER RESEARCH

6.1 Practical consequences of the results from this thesis

The results from this work cannot be used directly as guidelines for practical pavement design. However, some of the results may be used as rules of thumb for quality control and observation of the critical factors in order to obtain a long service life.

- It is recommended to take the mineralogy into account in the requirements regarding the amount of fines in unbound layers. A criterion similar to the Austrian Mineral criterion is recommended. The current Norwegian requirements regarding the amount of fines seem reasonable to avoid both water- and frost susceptible materials. The access to water in a road structure should be reduced to a minimum by good drainage.

- The dry density of the materials is found to be one of the most important factors to avoid permanent deformation. New procedures and methods for compaction control in situ are recommended to assure optimum dry density of the material in situ.

- Cyclic load triaxial testing seems to be a good method for the characterization of the permanent deformation behaviour. Design methods based on the resistance to permanent deformations from triaxial testing is recommended in special cases for a more realistic material characterization.

6.2 Recommendations for further research

It is recommended to collect all the research on unbound granular aggregates done in Norway as a basis to identify the needs for further research.

- The triaxial testing procedures still needs further development. The current procedures are very time consuming, especially considering the preparation of samples and instrumentation.

- More materials should be tested in the triaxial apparatus to study the effect of different factors on the deformation properties, particularly the permanent deformations.

- More materials should be tested by the Tube Suction test and by direct frost heave testing in combination with in-situ observation of the same materials. In this way it is possible to obtain more knowledge about the effect of water and the frost mechanisms in unbound materials. The effect of mineralogy should be studied in particular.

- This thesis shows that the Flakiness Index is not a critical parameter for the deformation properties for well-graded materials. This conclusion should be further investigated for other materials.

- Discrete element modelling offers a variety of possibilities, and the work presented in this thesis is only a start. More simulations should be done and verified with real laboratory data. Factors such as grain shape, grain size distribution and also the presence of water should be further investigated.

REFERENCES AND LITERATURE

Aksnes, J. (2001). A Study of Load Responses towards the Pavement Edge. IVJ-Medd. 35. Thesis, Norwegian University of Science and Technology (NTNU), Trondheim, Norway.

Allen, J.J. and Thompson, M.R. (1974). Resilient Response of Granular Materials Subjected to Time-Dependent Lateral Stresses. Transportation Research Record 510, Transportation Research Board, Washington DC, USA. pp 1-13.

Angen, E. (1978). Fukttransport i jordarter (in Norwegian). IVJ-Medd. 28. Thesis, Norwegian University of Science and Technology (NTH), Trondheim, Norway.

ASI - Austrian Standards Institute (2001). "Gesteinskörnungen für ungebundene Tragschichten im Straßen- und Flugplatzbau - Beurteilung der Frostsicherheit" (in German) Önorm B 4811.

Barksdale, R. (1971). Compressive Stress Pulse Times in Flexible Pavements for Use in Dynamic Testing. Highway Research Record 345, Highway Research Board, Washington DC, USA. pp 32-44.

Barksdale, R. (1991). The Aggregate Handbook. National Stone Association, Washington DC, USA.

Barksdale, R. and Itani, S. Y. (1989). Influence of Aggregate Shape on Base Behaviour. Transportation Research Record 1227, Transportation Research Board, Washington DC, USA.

Berntsen, G. (1993). Reduksjon av bæreevnen i teleløsningsperioden (in Norwegian). IVJ-Medd. 25. Thesis, Norwegian University of Science and Technology (NTH), Trondheim, Norway.

Casagrande, A. (1932). "A new theory of frost heaving: discussion". Proceedings of US Highway Research Board. Vol. 11, Pt. I,. pp. 168–172.

CEN - European Commite for Standardization , (2000). EN 13286-7 Unbound and hydraulically bound mixtures – part 7: Cyclic load triaxial tests for unbound mixtures. Brussels.

Cole, D., Uthus, L. and Hopkins, M (in prep). Normal and Sliding Contact Experiments on Smooth Spherical Grains of Gneiss. (unpublished).

Collins, I.F., Wang, A.P. and Saunders, L.R. (1993). Shakedown in Layered Pavements Under Moving Surface Loads. International Journal for Numerical and Analytical Methods in Geomechanics, vol 17. pp 165-174.

Coulter Corporation (1994). Product Manual for Coulter LS 2300. Miami, Florida, USA.

Dawson, A.R., Arnold, G., Werkmeister, S., Hughes, D. and Robinson, D. (2003). Using a shakedown approach as a simple means of predicting rutting in unsealed and chip-sealed pavements. Paper Proceedings for the 21st ARRB (Australian Road Research Board)/ 11th REAAA Conference.

DIN - Deutches Institut für Normung (1993). Bestimmung der spezifiscen Oberfläche von Feststoffen durch Gasadsporption nach Brunauer, Emmet und Teller (BET). DIN 66131, Germany.

Dongmo-Engeland, B.(2005). GARAP Influence of sample´s height on the development of permanent deformations. STF50 A05075. SINTEF Technology and Society, Road and Railway Engineering,Trondheim, Norway.

Ekblad, J. (2004). Influence of Water on Resilient Properties of Coarse Granular Materials. Licentiate Thesis, Kungliga Tekniska Högskolan (KTH), Stockholm, Sweden.

Fuller, W and Thompson, S. E, (1907). The laws of proportioning concrete. Transactions of the American Society of Civil Engineers. Paper no 1053, pp 67-143

Garba, R.S. Permanent Deformation Properties of Asphalt Concrete Mixtures. IVJ-Medd. 35. Thesis, Norwegian University of Science and Technology (NTNU), Trondheim, Norway.

Hauck, C. (1988). Grusmaterialers vannømfindtlighet (in Norwegian). Cand. Scient thesis, University of Oslo (UiO), Oslo, Norway.

Hauck, C. (1988). Water susceptibility of base gravel materials (In norwegian). Cand. Scient thesis, University of Oslo (UiO), Oslo, Norway.

Hicks, R.G and Monismith, C.L, (1971). Factors Influencing the Resilient Response of Granular Materials. Highway Research Record 345, Highway Research Board, Washington DC, USA. pp 15-31.

Hoff, I. (1999). Material Properties of Unbound Aggregates for Pavement Structures. IVJ-Medd. 28. Thesis, Norwegian University of Science and Technology (NTNU), Trondheim, Norway

Hoff, I., Nordal, S. and Nordal, R. (1999). Constitutive model for unbound granular materials based on hyperelasticity. Paper, Proceedings of an International Workshop on Modelling and Advanced Testing for Unbound Granular Materials, Lisbon, Portugal. pp187-196.

Hoff, I., Bakløkk, L. and Aurstad, J. (2003). Influence of Laboratory Compaction Method on Unbound Granular Materials. Paper, Proceedings for the 6th International Symposium on Pavements Unbound (UNBAR 6) (CD-ROM), University of Nottingham, Great Britain.

Horvli, I. (1979). Dynamisk prøving av leire for dimensjonering av veger (in Norwegian). IVJ-Medd. 20. Thesis, Norwegian University of Science and Technology (NTH), Trondheim, Norway.

Huang, Y.H. (1993). Pavement Analysis and Design. University of Kentucky, USA.

Irgens, F. (2002). Kontinuumsmekanikk (in Norwegian). Textbook in Continuum Mechanics, Norwegian University of Science and Technology, Trondheim, Norway

Janoo, V. (1998). Quantification of Shape, Angularity, and Surface Texture of Base Course Materials. Special Report 98-1, US Army Corps of Engineers, Cold Regions Research & Engineering Laboratory, Hanover NH, USA.

Johnson, K.L. (1985). Contact mechanics. Cambridge University Press, Great Brittain.

Kolisoja, P. (1994). Large Scale Dynamic Triaxial Test with Coarse Grained Aggregates. Paper, Proceedings for the 4th International Conference on Bearing Capacity of Roads and Airfields, Volume 2, Minneapolis, Minnesota, USA.

Kolisoja, P. (1997). Resilient Deformation Characteristics of Granular Materials. Publication 223. Thesis, Tampere University of Technology, Tampere, Finland

Lees, G. (1964). The measurement of particle shape and its influence in engineering materials, Journal of the British Granite and Whinestone Federation, London, , pp 1-22.

Lekarp, F. (1999). Resilient and Permanent Deformation Behaviour of Unbound Aggregates under Repeated Loading. TRITA-IP FR 99-57. Thesis, Kungliga Tekniska Högskolan (KTH), Stockholm, Sweden.

Melby, K. (1977). Repeterte belastninger på leire (in Norwegian). IVJ-Medd. 16. Thesis, Norwegian University of Science and Technology (NTH), Trondheim, Norway.

Mladek, M.H. (1976). Mineralidentifikasjon ved røntgenmetoder (In Norwegian). Universitetsforlaget, Oslo, Norway.

Moen, K., Malvik, T., Breivik, T. and Hjelen, J. (2006). Particle Texture Analysis in Process Mineralogy. Paper, Proceedings for the XXIII International Mineral Processing Congress, Istanbul, Turkey.

Mork, H. (1990). Analyse av lastresponsar for vegkonstruksjonar (in Norwegian). IVJ-Medd. 24. Thesis, Norwegian University of Science and Technology (NTNU), Trondheim, Norway.

Myre, J. (1988). Utmatting av asfaltdekker (in Norwegian). IVJ-Medd. 23. Thesis, Norwegian University of Science and Technology (NTH), Trondheim, Norway.

Noss, P.M. (1978). Poresug i jordarter (in Norwegian). IVJ-Medd. 14. Thesis, Norwegian University of Science and Technology (NTNU), Trondheim, Norway.

Nordal, R.S. (1960). Berelag for vegar (in Norwegian). Medd.nr. 12. Norwegian Road Research Laboratory, Oslo, Norway.

Nordal, R.S and Hansen, E.K. (1987). The Vormsund Test Road – Part 4: Summary report. Medd. Nr. 58. Norwegian Road Research Laboratory, Oslo, Norway.

Nordiska ministerrådets sekretariat (1976). STINA – Samarbetsprojekt för tillämpning i Norden av AASHO-undersökningen (in Swedish). Oslo, Norway.

Raad, L., Minassian, G. and Gartin, S. (1992). Characterization of saturated granular bases under repeated loads. Transportation Research Record 1369, Transportation Research Board, Washington DC, USA. pp 73-82

Rada, G. and Witczak, M. W. (1981). Comprehensive Evaluation of Laboratory Resilient Moduli Results for Granular Materials. Transpoertation Research Record 810, Transportation Research Board, Washington DC, USA. pp 23-33.

Refsdal, G. (2007). Kjellstadveien forsøksvei (in Norwegian). Note, Oslo, Norway.

Rieke, R., Vinson, T.S. and Mageau, D.W. (1983). The role of specific surface area and related index propertiesin the frost heave susceptibility of soils. Paper, Proceedings of the 4th International Conference on Permafrost, Fairbanks, Alaska

Seed, H.B., Chan, C.K and Lee, C.E. (1962). Resilience characteristics of subgrade soils and their relations to fatigue in asphalt pavements. Proceedings of International Conference on Structural Design of Asphalt Pavements. Ann Arbor, USA. Vol 1, pp 611-636.

Senstad, P. (1994). Sluttrapport for etatssatsningsområdet Bedre utnyttelse av vegers bæreevne (in Norwegian). Publikasjon nr 75, Vegdirektoratet, Oslo, Norway.

Sharp, R.W. (1985). Pavement Design Based on Shakedown Analysis. Transportation Research Record 1022, Transportation Research Board, Washington DC, USA. pp 99-107.

Slyngstad, T. (1977). Filler i bituminøse dekker (in Norwegian). IVJ-Medd. 15. Thesis, Norwegian University of Science and Technology (NTH), Trondheim, Norway.

Standard Norge (1997). Prøvingsmetoder for geometriske egenskaper for tilslag Del 3: Bestemmelse av kornform Flisighetsindeks (Flakiness Index) (In Norwegian). NS-EN 933-3.

Standard Norge. Prøvingsmetoder for mekaniske og fysiske egenskaper for tilslag Del 2: Metoder for bestemmelse av motstand mot knusing. (Los Angeles method) (In Norwegian). NS-EN 1097-2. 1998.

Statens vegvesen (1977). Vegnormalene - Håndbok 018 Vegbygging (in Norwegian). Oslo, Norway.

Statens vegvesen (1980). Håndbok 018 Vegbygging (in Norwegian). Oslo, Norway.

Statens vegvesen (1992). Håndbok 018 Vegbygging (In Norwegian). Oslo, Norway.

Statens vegvesen (1999). Håndbok 018 Vegbygging (In Norwegian). Oslo, Norway.

Statens vegvesen (2005a). Håndbok 014 Laboratorieundersøkelser (In Norwegian). Oslo, Norway.

Statens vegvesen (2005b). Håndbok 018 Vegbygging (in Norwegian). Oslo, Norway.

Thom, N. H. and Brown, S.F. (1988). The effect of grading and density on the mechanical properties of a chrushed dolomitic limestone. Paper, Proceedings 14th ARRB Conference, Vol 14, Part7, pp 94-100.

Uthus, L., Hoff, I. and Horvli, I. (2005). Evaluation of grain shape characterization methods for unbound aggregates. Paper, Proceedings 7th International Conference on the Bearing Capacity of Roads, Railways and Airfields, Trondheim, Norway. (PAPER I)

Uthus, L., Hermansson, Å., Horvli, I. and Hoff, I. (2006). A study on the influence of water and fines on the deformation properties and frost heave of unbound aggregates. Proceedings of the 13th Intl. Conference on Cold Regions Engineering (CD-ROM), Orono, Maine. (PAPER III)

Uthus, L. (2007a). Effect of Grading and Moisture on Deformation Properties of Unbound Aggregates. (Will be submitted for the TRB conference 2008). (PAPER V)

Uthus, L. (2007b). Material Properties of Unbound Granular Aggregates and the Effect on the Deformation Behaviour. International Journal of Pavements. Submitted. (PAPER IV)

Uthus, L., Hopkins, M. and Horvli, I. (2007c). Discrete Element Modelling of Unbound Aggregates Using Dilated Particles. International Journal of Pavement Engineering. Submitted. (PAPER VI)

Uthus, L., Tutumluer, E., Horvli, I. and Hoff, I. (2007d). Influence of grain shape and surface texture on the deformation properties of unbound aggregates in pavements. International Journal of Pavements. Submitted.

Utvalg for Frost i Jord (1976). Frost i Jord – Sikring mot teleskader (in Norwegian). Nr. 17. Oslo, Norway

Uzan, J. (1985). Characterization of Granular Material. Transportation Research Record 1022, Transportation Research Board, Washington DC, USA. pp 52-59.

Våre Veger (2000). Pukk og grusbransjen: Verdiskaper og naturforvalter (in Norwegian). (Periodical) Nr. 2, 2000. Oslo, Norway.

Werkmeister, S., Dawson, A. and Wellner, F. (2001). Permanent Deformation Behaviour of Granular Materials and the Shakedown Concept. Transportation Research Record 1757, Transportation Research Board, Washington DC, USA. pp 75-81.

Werkmeister, S. (2003). Permanent Deformation Behaviour of Unbound Granular Materials in Pavement Constructions. Thesis, Techniscen Universität Dresden, Germany.

PAPER I

Evaluation of grain shape characterization methods for unbound aggregates

L. Uthus
Norwegian University of Science and Technology, Department of Civil and Transport Engineering, Trondheim, Norway

I. Hoff
SINTEF Technology and Society, Road and Railway engineering, Trondheim, Norway

I. Horvli
Norwegian University of Science and Technology, Department of Civil and Transport Engineering, Trondheim, Norway

ABSTRACT: A laboratory study is performed on an unbound aggregate of gneiss commonly used as base course in road pavements. Aggregate samples with four different grain shapes from the same quarry have been tested. The objective of this study was to evaluate different methods of grain shape characterization to see which methods that gives the most reliable results for the same materials on the parameters describing shape, angularity and surface texture.

One group of methods for grain shape characterization is simple petrologic methods in combination with physical measurements of the aggregate shape. These methods are based on visual classifications of rock type and measurement of the aggregate dimensions giving several shape characteristics as flatness and elongation ratio, angularity, degree of sphericity, flakiness index, shape index etc. The most common test in this group is the flakiness index test.

Image analyses are more sophisticated in their characterization of the aggregate shape. These methods are also more powerful in their ability to characterize surface roughness. Two dimensional analysis give a picture of each grain in only two dimensions, i.e. the projection of the grain on one plane in a random position. The most advanced methods are the three dimensional image analysis.

KEY WORDS: Grain shape characterization, aggregate shape, image analysis

1. INTRODUCTION

The geometrical irregularities of an aggregate particle are of great importance for the behaviour of the aggregates. Aggregate particles appear in different shapes depending on its origin and later processes. Aggregate particles worn by wind, water or glaciers appear rounded while particles from crushed rock appear angular (Wadell 1932).

The grain shape of aggregates influences the material gradation obtained by sieving. According to Lees (1964) flaky particles tends to pass diagonally through the sieves with square holes. The shape also has a significant influence on the volume of the particles retained on each sieve. As shown by Lees (1964) the rod-shaped particles are about 2.5 times the volume of the disc shaped particles.

1

Requirements in design guidelines for grain shape give limitations for flaky and elongated particles; hence promoting equidimensional or cubic aggregates. Parameters as roundness, angularity and surface texture are only given in the guidelines as a requirement for percentage of crushed and broken surfaces. More sophisticated methods as image analysis are not yet practical or accepted for everyday engineering work, but they have been used by researchers.

There are many methods for quantification of the grain shape; from the simple visual methods and physical measurements to complex three dimensional image analysis. The manual methods are laborious and tedious measurements, and the more sophisticated methods are expensive but more effective and easier to operate. Some of the methods available have been evaluated with respect to quality of output.

2. METHODS FOR QUANTIFICATION OF AGGREGATE GRAIN SHAPE

2.1 Visual methods and sieving

Wadell (1932) questioned the use of measurements to quantify the shape of aggregate particles: *How is it possible to define the breadth and thickness of an irregular particle?* These types of characterizations will always be estimates and approximations. However, they are easy to perform and widely used.

2.1.1 Description of particle shape, angularity and surface texture

The grain shape is one of many important parameters influencing the response of unbound aggregates. Lees (1964) Barksdale and Itani (1989) categorized the grains in 4 different shapes; disc, equidimensional, blade or rod shaped. Janoo (1998) organized the description of the different shapes in a table.

Table 1: Description of aggregate shape

Aggregate shape	Description
Disc	Slabby in appearance, but not elongated
Equidimensional	Neither slabby appearance nor elongated
Blade	Slabby appearance
Rod	Elongation, but not slabby in appearance

Lees (1964) found that these 4 broad categories permitted quite a large range of particle shape characteristics within each classification. He concluded that this classification was not suitable for research purposes and that it would probably be better to classify the particle shape by the flatness and the elongation ratio.

The flatness ratio (p) is the ratio of the short length (thickness) to the intermediate length (width). The elongation ratio (q) is the ratio of the intermediate length to the longest length (length). By combining the flatness- and the elongation ratio, the shape of the aggregates can be described by a shape factor (F) and the sphericity (ψ). The shape factor is the ratio of the elongation ratio and the flatness ratio (Eq. 1).

$$F = \frac{p}{q}$$ (Eq. 1)

A round or cubical particle will have a shape factor equal to 1. If the shape factor is less than 1, the particle is more elongated and thin. A blade shaped particle will have a shape factor greater than 1.

The sphericity is defined as the ratio of the surface area of a sphere having the same volume as the aggregate particle. The sphericity can also be expressed by the flatness- and elongation ratios as shown in Equation 2. The sphericity varies from values near 0 to values near 1.0 for perfect spheres.

$$\psi = \frac{12.8(\sqrt[3]{p^2 q})}{1 + p(1+q) + 6\sqrt{1 + p^2(1+q^2)}}$$ (Eq. 2)

The flatness- and elongation ratio and the shape factor and the sphericity are combined in the diagram below. In the diagram the aggregates can be classified as disc, equidimensional, blade- and rod shaped as described in Table 1. Equidimensional means either cubic or round particles.
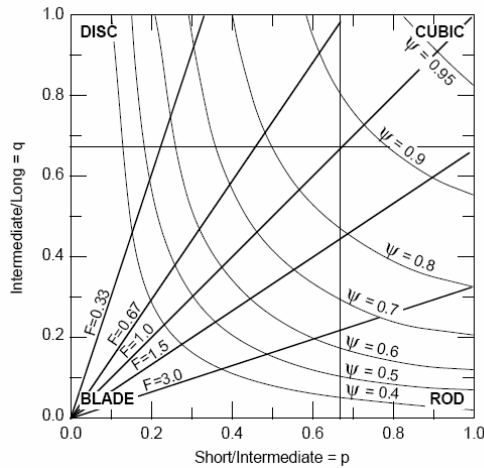
Figure1: Aggregate classification chart (Lees, 1964, Janoo, 1998)

2.1.2 Norwegian classification of aggregates for concrete

The aim of this testing procedure is to determine the percentage of flaky and elongated grains in a sample (Norwegian Control Board for Concrete Products, 2001). For use in concrete the grain shape of the material is of importance to the workability of the concrete mass and also the amount of water needed.

The procedure gives 3 different groups of grain shape: cubic, flaky and elongated in combination with rounded/subrounded and angular/subangular. For measuring the grains a slide calliper is used in combination with visual characterization.

Flaky and elongated grains are determined by the relation between the length, width and thickness of the grain. The length is defined as the longest axis of the grain. The width is the second longest axis of the grain and the thickness is the shortest axis.

A grain is classified as **flaky** if: $\dfrac{width}{thickness} > 2.0$

A grain is classified as **elongated** if: $\dfrac{length}{thickness} > 2.5$

A grain is classified as **cubic** if it is not flaky or elongated, that means:

$$\frac{width}{thickness} < 2.0 \text{ and} : \frac{length}{thickness} < 2.5$$

3

The cases of doubt are then measured by a slide calliper to determine the grain shape.

2.1.3 Shape Index

The shape index (EN 933-4:1999) is a method for determining the elongation of coarse aggregate grains. The test is performed on aggregate with grain size ranging from 4 mm and up to 63 mm. Particle length is described as the maximum dimension of a particle as defined by the greatest distance apart of two parallel planes tangential to the particle surface. Particle thickness is described as the minimum dimension of a particle as defined by the least distance apart of two parallel planes tangential to the particle surface

A special made particle slide gauge is used for determination of the category for each aggregate grain. This is made with the use of two openings or slots, one to measure the length and another opening that is 1/3 of the opening for the length. In this way it is easy to find if the length is more or less than 3 times the thickness. According to the result for each particle the sample is divides into the two categories; cubical and non cubical, where the non cubical is the particles where the thickness is less than 1/3 of the length. The shape index is calculated as the ratio between the mass of non-cubical particles and the total mass of particles tested

2.1.4 Flakiness Index

This method (EN-933-3:1997) is commonly used in the European countries with requirements for aggregates for several material types in road pavements. The test consists of two sieving operations. During the first operation test sieves are used to separate the sample into various particle size fractions. Each of the fractions are then sieved using bar sieves.

The flakiness index can be calculated for each fraction within the sample and for the whole sample. The overall index is calculated as the total mass of particles passing the bar sieves expressed as a percentage of the total dry mass of the whole sample.

2.2 Image analysis

Digital image processing for characterization of aggregate shape has been used for research purposes in many years. Several researchers have used both 2D and 3D image analysis methods to quantify the grain shape parameter.

Digital image processing is a technique of using pictures on a digital form and applying various mathematical procedures to get digital information from the image.

2.2.1 Two dimensional quantification of grain shape by the QMOT image analysis system

Image analysis is an advanced way to evaluate and quantify the shape of an aggregate. In the simplest form this is to arrange grains on a white background and take pictures. Then the pictures shows a two dimensional projection of the aggregate grain shape.

By using a computer with a suitable programme for processing the pictures, it is possible to calculate almost any geometrical parameter in two dimensions. The Quebec Ministry of Transportation (QMOT) uses image analysis on a regular basis to verify the angularity of its hot-mix aggregates (Janoo 1998).

From the two dimensional image analysis two different parameters are found; the roundness and the roughness of the aggregates. An image analysis programme is used to track the two dimensional projection of the aggregates and get rid of shades and other disturbance.

For the image analysis the following basic measurements are made:
  1) Area
  2) Perimeter

3) Ferets
4) x-y coordinates

The area is calculated as the number of pixels of an object that form an object and the perimeter is determined by counting the number of pixels touch the background or the projection of the object. This parameter will depend on the resolution of the image, it is more sensitive to variations in texture at high resolutions and to changes in angularity at relatively low resolution.
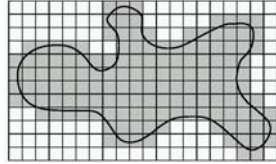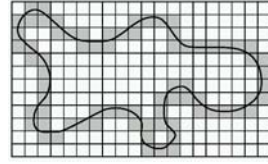

Figure 2a: Area of an aggregate (Janoo 1998)

Figure 2b Perimeter of an aggregate (Janoo 1998)

Ferets are straight-line measurements made between two tangents as shown in figure 3a. From these measurements it is possible to obtain expressions for both the roundness and the roughness of an aggregate.
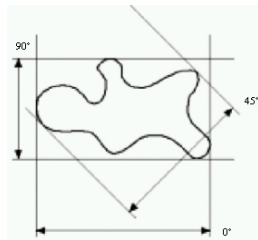
Figure 3a: Feret measurement (Janoo 1998)
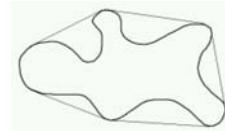
Figure 3b: Illustration of convex perimeter (Janoo 1998)

The roundness/angularity index (Janoo 1998) is calculated by the following formula:

$$R_n = \frac{4\pi A}{p^2}$$ (Eq. 3)

where,
R_n= Roundness index
A= area of aggregate
p = perimeter of aggregate

This parameter typically has a value less than 100. A perfectly circular object will have a value of 100, but because of the square pixel simplification the best that can be obtained is 95. An object with irregular surface will have a smaller value.

The roughness of the grains is calculated by the following formula (Janoo 1998):

$$r = \frac{p}{p_c}$$ (Eq. 4)

where,
r = roughness
p= perimeter of aggregate
p_c= convex perimeter of aggregate

5

The roughness of an aggregate grain is defined by the ratio of perimeter to the convex perimeter. For a smooth material the roughness factor equals 1.00, the roughness factor increases by the increasing roughness of a particle.

2.2.2 Three dimensional quantification of grain shape by the UI-AIA system

An aggregate particle has three dimensions in nature, so a two dimensional projection will not tell the whole truth. The method presented is one of the sophisticated and advanced methods available. This type of equipment demands a lot of money and effort to build up, but over the years many methods have been developed with different approaches.

An image analyzer has been developed at the University of Illinois to provide a reliable means of automating the determination of coarse aggregate size and shape properties. Flat and elongated ratio, gradation and angularity are the factors investigated in a fast and efficient way.

The apparatus uses three cameras to collect aggregate images from three orthogonal directions. The particles that are analyzed are fed on to a conveyor belt system, which carries the particles – one by one – towards the orthogonally placed cameras. Each particle will be detected by the cameras as they travel into the field of view of a sensor. The cameras are synchronized so the three pictures are taken at the exact same time.

The angularity index described by Rao et al. (2002) was developed as a part of the UI-AIA analysis package. The basis theory has been carefully verified with typical coarse aggregate shapes in order to develop an objective tool to characterize aggregate grain shape.

The image analysis procedure first provides an angularity value for each of the three 2D images collected from the three views. Then the angularity is established as a weighed average of all three views.

$$AI_{Particle} = \frac{Ang.(front) \cdot Area(front) + Ang.(top) \cdot Area(top) + Ang.(side) \cdot Area(side)}{Area(front) + Area(top) + Area(side)}$$
(Eq. 5)

where;
$AI_{Particle}$ = Angularity index for the particle
Ang. = Angularity for one view
Area = Area for one view

The AI for a sample is the average of the AI for all grains weighed by weight. The unit for AI is degrees.

The UI-AIA system can also be used to determine the surface texture of coarse aggregates by using an erosion-dilation technique (Rao et al. 2003). This is a well known technique in image analysis where the erosion operation is a procedure to obtain the first imaging morphologic parameter. Masad et al. (1999) used the erosion-dilation technique to determine the surface texture of fine aggregates.

Erosion is a morphologic operation by which all boundary pixels are removed from a binary picture, leaving the object one pixel less dense along the boundary. Dilation is the reverse of erosion, where a layer of pixels is added to the object boundary to create a simplified form of the original object. The area lost under the erosion-dilation process as a percentage of the total area of the original image is denoted by the surface parameter ST:

$$ST = \frac{A_1 - A_2}{A_1} \cdot 100$$
(Eq. 6)

where;
A_1 = Area (in pixels) of the two dimensional projection before erosion-dilation
A_2 = Area of object after erosion-dilation

6

The surface texture ST is calculated as the average of the surface texture values for each view weighed by their individual areas as shown in Equation 7.

$$ST_{particle} = \frac{ST(front) \cdot Area(front) + ST(top) \cdot Area(top) + ST(side) \cdot Area(side)}{Area(front) + Area(top) + Area(side)} \qquad \text{(Eq. 7)}$$

where;
$ST_{Particle}$ =Surface texture for the particle
ST = Surface texture for one view
Area = Area for one view

3. RESULTS

3.1 Visual methods and sieving

The characterization of grain shape according to Lees (1964), and Barksdale and Itani (1989) is used to characterize aggregate from Askøy with 4 different aggregate shapes. Table 4, Table 5 and Figure 4 shows the results from the Lees method for the different grain shapes. As can be seen both from Table 4 and Figure 2 the results are not giving any clear distinction between the series. However, from a statistical point of view the results are significant when testing in a 95% confidence interval. Only the two values for the form factor, which is almost similar, are not significant.

Table 4: The flatness- and elongation ratio of the series (Lees, 1964)

| Material type / sample | Aggregate shape (analysis result) | | | | | |
| | Flatness Ratio (p) | | | Elongation Ratio (q) | | |
	Mean	Variance	Std. dev.	Mean	Variance	Std. dev.
Cubic	0.65	0.00017	0.013	0.74	0.00011	0.011
Cubic Rounded	0.69	0.00016	0.013	0.78	0.000096	0.0098
Flaky	0.52	0.00026	0.016	0.68	0.00016	0.013
Flaky Rounded	0.63	0.00017	0.013	0.62	0.00014	0.012

Table 5: The shape factor and sphericity of the series

| Material type / sample | Aggregate shape (analysis result) | | | | | |
| | Shape factor | | | Sphericity | | |
	Mean	Variance	Std. dev.	Mean	Variance	Std. dev.
Cubic	0.92	0.00070	0.026	0.86	0.000021	0.0046
Cubic Rounded	0.92	0.00087	0.029	0.88	0.000016	0.0039
Flaky	0.83	0.0013	0.036	0.77	0.000075	0.0086
Flaky Rounded	1.08	0.0014	0.037	0.82	0.000034	0.0059
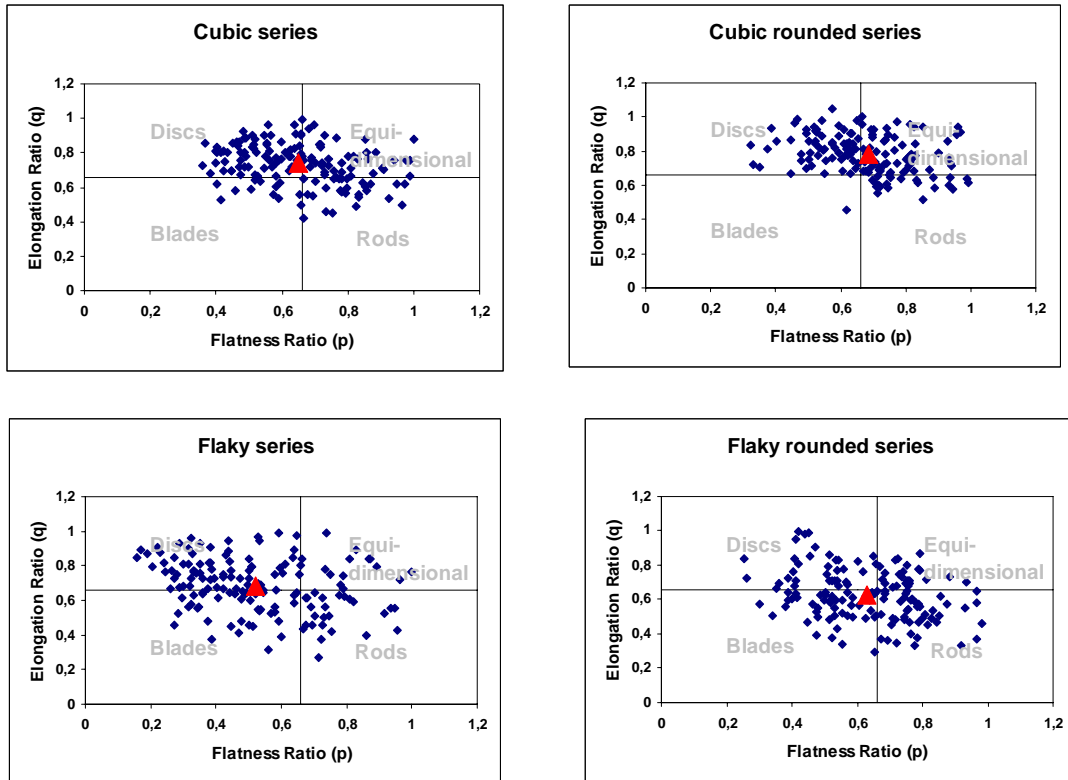
Figure 4: Results from characterization of grain shape after Lees (1964) method

The main part of the cubic series fall in the category of disc shape, while cubic rounded series tends more to be equidimensional. The flaky series falls in between the categories of disc and blade shape while the flaky rounded material tends to be more blade shaped. These results are expected results from the known differences in the grain shapes. The shape factor and sphericity in Table 5 does not give any clear difference between the series.

3.1.3 The Norwegian method for classification of aggregates for concrete

The Norwegian method for classification of aggregates for concrete is a visual method, so it will not give results to analyze statistically. As can be seen from Table 6 the cubic material tends to be cubic angular (69 %), while a smaller portion is flaky/elongated and angular (26 %). The cubic rounded material tends to be cubic rounded/subrounded (75%) while some grains are flaky/elongated and rounded/subrounded (25 %). For the flaky series most of the grains falls under the category of flaky/elongated and angular (60 %), but some grains are cubic angular (36 %). A large portion of the flaky rounded grains are flaky/elongated and rounded/subrounded (61 %) and some are cubic angular (39 %).

8

Table 6: Results from the Norwegian method for classification of aggregates for concrete

Material type / sample	Aggregate shape (analysis result)			
	Cubic Rounded/subrounded	Cubic Angular	Flaky/elongated Rounded/subrounded	Flaky/elongated Angular
Cubic	2	69	3	26
Cubic Rounded	75	0	25	0
Flaky	3	36	1	60
Flaky Rounded	39	0	61	0

3.1.4 Shape Index and Flakiness Index

The shape and flakiness indexes according to the EN standard (EN-933-3:1997 and EN 933-4:1999) seems to distinguish relatively well between the materials, see Table 7. Here we observe considerably lower shape index for the cubic rounded material than for the cubic, and considerably higher shape index for the flaky rounded than for the flaky. The same tendency is shown also for the flakiness index. The shape indexes are three orders of magnitude lower for the cubic and cubic rounded materials than for the flaky and flaky rounded. The flakiness indexes are also relative lower for the cubic variants than for the flaky, but this parameter does not show such big a difference. In this case is it impossible to use a statistical approach, as these tests are bulk tests, and only two parallels are tested.

Table 7: Results from the shape index and flakiness index

Material type / sample	Aggregate shape (analysis result)	
	Shape Index	Flakiness Index
Cubic	0.083	10.99
Cubic rounded	0.056	8.08
Flaky	55.5	12.42
Flaky rounded	63.3	20.34

3.2 Image analysis

Results from the applied two dimensional image method frequently used by The Quebec Ministry of Transportation are shown in Table 8. The results are as expected both for the roundness and the roughness. The roundness results shows that the cubic rounded series is the one with highest roundness and the flaky series is the most angular. The flaky rounded series have a lower roundness than the cubic series. This probably has to do with the elongation of these grains which gives a high perimeter value. The results of the roughness value shows that both the rounded series has a lower roughness than the more angular series, with the flaky series giving the highest roughness value.

The differences in the roundness and roughness parameters are relatively small compared to the accuracy of the method, however the results are significantly different when testing for significance for a 95 % confidence interval. The method should distinguish better between such different grain shapes.

Table 8: Results from the two dimensional image analysis

| Material type / sample | Aggregate shape (analyse result) | | | | | |
| | Roundness | | | Roughness | | |
	Mean	Variance	Std. dev	Mean	Variance	Std. dev.
Cubic	76	43	6.5	1.048	0.00011	0.01
Cubic rounded	80	31	5.6	1.037	0.00042	0.02
Flaky	67	140	11.8	1.10	0.035	0.2
Flaky rounded	74	47	6.9	1.044	0.0000070	0.003

3.2.2 Three dimensional image analysis (UI-AIA analysis)

Table 8: Results from the three dimensional image analysis

| Material type / sample | Aggregate shape (analyse result) | | | | | |
| | Angularity Index (AI) | | | Surface Texture Index (ST) | | |
	Mean	Variance	Std. dev.	Mean	Variance	Std. dev.
Cubic	369.9	82.5	9.1	0.83	0.0011	0.033
Cubic Rounded	270.0	86.5	9.3	0.54	0.0042	0.065
Flaky	417.1	86.8	9.3	1.06	0.0023	0.048
Flaky Rounded	317.2	129.38	11.4	0.79	0.0043	0.066

A three dimensional image analyse developed on the University of Illinois (Rao et al, 2001, 2002) is used to analyse the material from Askøy. The angularity index as well as the surface texture index is significantly different for all the material types; Cubic, cubic rounded, flaky, flaky rounded according to this method when testing for a 95 % confidence interval. The method is therefore capable to distinguish very well between all material types in this study

4. DISCUSSION

In this study many different methods has been applied on four different grain shapes of the same material. It is difficult to say something about the quality of the methods because of the big differences in the way they are treating the data.

- Lees method
As can be seen from the results the method does not clearly separate the different series. Statistically this method is also not a good method as some of the values are not significantly different for the different series. This method is based on physical measurements of the length, breadth and width, which according to Wadell (1932) is difficult when working with irregular particles.

- The Norwegian method for classification of aggregates for concrete
This method is subjective, which means that the results are to some degree dependent on the operator. It is therefore important to use the same operator for all the series to ensure that the results can be compared. As shown in the results this method clearly separated the different series. However the categories are not detailed, so it will not distinguish well between series that is almost similar in grain shape.
- Flakiness and Shape Index
The results show that the flakiness index separates the series to some extent, but there were expected to be a larger difference between the flaky and the cubic series. An explanation could

be that the flaky series are not that flaky, only elongated. The results from the shape index shows a big difference between the flaky and the cubic series, which was expected. These tests distinguishes well between materials with i.e. typically flaky or typically elongated grain shapes, but will not separate material with minor differences in grain shape.

- Two dimensional image analysis
Janoo (1998) found that the two dimensional image analysis (QMOT image analysis system) did not distinguish well between crushed and rounded aggregates regarding roundness and angularity. It must be noted that this study was done on a very limited range of materials with no additional material performance testing.

In this study the same conclusions may be drawn. The method separates the series with significant differences, but does not give a clear distinction between the materials witch can easily be separated visually. One of the disadvantages of the method is that you only measure the two dimensional projection of the aggregates is measured. As aggregates tend to lay with the flat side down, this will give some problems to the quality of the output. The elongation is always measured, but a proper measure for the flatness or the combination of flatness and elongation will be more difficult.

The resolution of the images is of great importance in image analysis. As found by other researchers, the resolution is of importance to the quality of the output depending on the parameter investigated. The lower resolution, the less accurate the analysis will be.

- Three dimensional image analysis
The results clearly show that this method is the best method for characterizing this series. For the two parameters chosen (angularity index and surface texture index) the results are as expected and correspond to what can be observed visually.

A disadvantage of the UI-AIA method is the fact that it is not able to analyze dark colored aggregates. This is because of the black colour of the conveyor belt transporting the aggregates. This problem could be avoided by using a light conveyor belt. It is also a method that demands expensive equipment.

4. CONCLUSIONS

Simple methods of grain shape characterization distinguish well between aggregates with a clear difference in grain shape, but do not separate materials which has almost similar grain shape. A combination between several methods, e.g. flakiness and shape index, may give the information needed on grain shape.

The two dimensional image analysis (QMOT image analysis system) performed on the processed aggregates did not distinguishing good enough between crushed and rounded aggregates.

As can be seen from the results the three dimensional image analysis is the best method for good quality output. There may also be some resistance from the industry to use new tests that do not give the same results as traditional tests, even though the image analysis is more accurate. The question is how detailed information is needed to separate materials, and how the differences found would affect the behaviour of the material in a base layer.

REFERENCES

American Society for Testing and Materials (ASTM), 2000. *Standard test method for index of aggregate particle shape and texture* , ASTM Designation D 3398-00, Philadephia.

American Society for Testing and Materials (ASTM), 2000. *Standard practice for description and identification of soils* (Visual-Manual Procedure), ASTM Designation D 2488-00, Philadelphia

Barksdale, R and Itani, S, 1989. *Influence of Aggregate shape on Base Behavior,* Paper Transportation Research Record 1227, Transportation Research Board, National Research Council, Washington DC, pp 173-181

Barksdale, R, Kemp, M.A., Sheffield, W. J. and Hubbard, J. L., 1991. *Measurement of Aggregate Shape, Surface Area and Roughness ,* Paper Transportation Research Record 1301, Transportation Research Board, National Research Council, Washington DC, pp 107-116.

European Committee for Standardization, 1997. *Tests for geometrical properties of aggregates. Part 3: Determination of particle shape, Flakiness Index.* EN-933-3:1997.

European Committee for Standardization, 1999. *Tests for geometrical properties of aggregates. Part 4: Determination of particle shape, Shape Index.* EN 933-4:1999.

Janoo, V, 1998. *Quantification of Shape, Angularity, and Surface Texture of Base Course Materials.* Special Report 98-1,US Army Corps of Engineers, Cold Regions Research & Engineering Laboratory

Janoo, V and Bayer II, John J, 2001. *The Effect of Aggregate Angularity on Base Course Performance.* Technical Report TR-01-14,US Army Corps of Engineers, Cold Regions Research & Engineering Laboratory

Lees, G., 1964. *The measurement of particle shape and its influence in engineering materials.* Journal of the British Granite and Whinestone Federation, London, pp 1-22

Maerz, N. H, 1998. *Aggregate Sizing and Shape Determination Using Digital Image Processing.* Center For Aggregate Research (ICAR) Sixth Annual Symposium Proceedings, St Louis Missouri, pp 195-203.

Masad, E. and Button, J. W, 2000. *Unified Imaging Approach for Measuring Aggregate Angularity.* The International Journal of Computer-Aided Civil and Infrastructure Engineering. Vol 15 No 4. pp 273-280

Norwegian Control Board for Concrete Products, 2001. *Metoder for proving av betongtilslag.* Klasse P Betongtilslag (In Norwegian).

Rao, C., Tutumluer, E. and Stefanski, J.A., 2001. *Coarse Aggregate Shape and Size Properties Using a New Image Analyzer.* ASTM Journal of Testing and Evaluation, Vol. 29, No. 5, pp 79-89

Rao, C., Tutumluer, E. and Kim, I. T., 2002. *Quantification of Coarse Aggregate Angularity Based on Image Analysis.* Paper Transportation Research Record 1787, Transportation Research Board, National Research Council, Washington DC.

Rao, C., Pan, T. and Tutumluer, E, 2003. *Determination of Coarse Aggregate Surface Texture Using Image Analysis.* Paper for the 16th ASCE Engineering Mechanics Conference, University of Washington, Seattle.

Rex, H. M. and Peck, R. A., 1956. *A Laboratory Test to Evaluate the Shape and Surface Texture of Fine Aggregate particles.* Public Roads 29, pp 118-120

Wadell, H., 1932. *Volume, shape and roundness of rock particles.* The Journal of Geology. Volume 40, pp 443-451.

PAPER II

The Equations 5 and 6 in the text should be corrected to:

Elastic limit: $\sigma_d = \dfrac{2\sin\rho \cdot (\sigma_3 + a)}{(1 - \sin\rho)}$ (Equation. 5)

Failure limit: $\sigma_d = \dfrac{2\sin\varphi \cdot (\sigma_3 + a)}{(1 - \sin\varphi)}$ (Equation. 6)

INFLUENCE OF GRAIN SHAPE AND SURFACE TEXTURE ON THE DEFORMATION PROPERTIES OF UNBOUND AGGREGATES IN PAVEMENTS

Lillian Uthus
Research Fellow, NTNU Norwegian University of Science and Technology, Department of Civil and Transport Engineering, NO-7491 Trondheim, Lillian.Uthus@ntnu.no

Erol Tutumluer
Associate Professor, University of Illinois, Department of Civil and Environmental Engineering, Urbana, IL 61801, tutumlue@uiuc.edu

Ivar Horvli
Professor, Dr.ing, NTNU Norwegian University of Science and Technology, Department of Civil and Transport Engineering, NO-7491 Trondheim, Ivar.Horvli@ntnu.no

Inge Hoff
Research Director, Dr.ing, SINTEF Roads and Transport, NO-7034 Trondheim, Inge.Hoff@sintef.no

ABSTRACT: Aggregate shape and texture affect shear strength of granular materials by influencing the particle interlock and the load distribution properties. The objective of this study was to investigate the influence of grain shape, angularity and surface texture on the deformation properties of unbound granular materials. Only one type of granular material was tested in the laboratory, gneiss from Askøy outside Bergen, Norway. This is a hard-rock, commonly used in road construction in Norway. To study the effect of grain shape and texture only, the same test procedures were consistently followed for a given level of compaction. By choosing a uniformly-graded material, it was expected that the impact of grain shape would be more pronounced and discernible. Aggregate samples with four different particle shape characteristics were produced from the Askøy gneiss. Both flat and cubical aggregates were obtained from various stages in the crushing process. The texture and angularity properties were also changed by wearing the crushed rock in the Nordic ball mill test drum. A three-dimensional (3-D) image analysis approach was adopted for an accurate characterization of the grain shape, texture and angularity properties. The aggregate samples were tested for resilient modulus and permanent deformation characteristics by applying a multistage loading procedure using the cyclic load triaxial test. The cubical aggregates were easier to compact when compared to the flaky aggregates. The cubical rounded aggregates gave the highest resilient moduli when tested at high stress levels. For the cubical aggregates, the angularity and surface texture seemed to have a significant effect on both the elastic and plastic shakedown threshold limits.

KEY WORDS: Unbound aggregates, triaxial testing, resilient modulus, permanent deformation, grain shape, texture, angularity

1. INTRODUCTION

The aggregate grain shape is controlled by the geological properties of the parent rock and the crushing process. By using different types of crushers and going through several stages in the crushing process, a more cubical particle can be produced. In general, aggregates with more cubical grains are considered to be more suitable for road building purposes than those granular materials with flat and elongated particles. Cubical particles show more resistance to crushing and abrasion than flat and elongated aggregates in laboratory tests [1].

Barksdale and Itani [1] studied the influence of grain shape on unbound base behaviour by using repeated load triaxial testing. Five different types of crushed rock with different grain shapes were used. They concluded that blade- and disc shaped aggregates performed almost as well as cubical aggregates with

respect to permanent deformation resistance. The rounded gravel tested was two times more susceptible to rutting than the crushed aggregates.

The aggregate shape also has a considerable influence on the gradation properties. Lees [2] found that rod-shaped particles in reality were about twice the size of disc-shaped particles retained on the same sieve. This would affect both the specific surface area and the ability to fill voids properly.

A study by Lekarp [3] showed that a single sized material was more susceptible to permanent deformations than a well-graded material. Also an angular rock was shown to be less susceptible to permanent deformation accumulation than a rounded aggregate material. Similarly, rough particles were also proven to have better inter-particular friction properties.

This paper focuses on the influence of grain shape, texture and angularity on the deformation behaviour of a granular material. The aggregate material used is a single-sized fraction with different shape, texture and angularity properties. Resilient modulus and permanent deformation characteristics of aggregate samples with different shape, texture and angularity properties are determined from repeated load triaxial testing and linked to aggregate morphology by the use of imaging based shape indices.

2. MATERIAL CHARACTERIZATION

2.1 Material preparation

Granular material samples with four different grain shape, texture and angularity properties were processed from one rock type, gneiss from Askøy outside Bergen, Norway. Two grain shapes were produced directly from field manufacturing of aggregates in the crushing plant, flat and elongated and cubical shapes. The other two samples produced were rounded variants of these processed in the Nordic Ball Mill test drum.

To produce different texture and angularity properties from the same Askøy gneiss, the Nordic Ball Mill was used to process the original cubical and the flat and elongated samples from the crushing plant to further give the two abraded and rounded shape properties. This simulates in a way the fluvial process in nature producing gravel deposits. According to earlier work [4] done with Ball Mill drum, the rounding of aggregates was best accomplished by conducting the Nordic Ball Mill test drum test for duration of about 60 minutes.

The resulting four aggregate test samples, all being single-sized fractions, were:
Cubical angular (Ca): cubical material obtained from production and optimized through the crushing process;
Cubical rounded (Cr): cubical material rounded in the Nordic Ball Mill drum for 60 minutes;
Flaky angular (Fa): flat and elongated material obtained from an early stage in the production process; and
Flaky rounded (Fr): flat and elongated material rounded in the Nordic Ball Mill drum for 60 minutes.

2.2 Grain shape characterization using three-dimensional (3-D) image analysis

There are several methods to characterize the morphological grain shape properties of aggregate material, i.e. simple visual methods, physical measurements, three-dimensional (3-D) visualization from image analysis, laser detection techniques and x-ray computer tomography. The 3-D image analysis offers both a practical approach and an advanced methodology to evaluate and quantify the shape of an aggregate particle. Although may not be needed for routine testing, this method gives reliable results in research applications [5].

The method adopted for 3-D image analysis of aggregate samples is the use of University of Illinois Aggregate Image Analyzer (UIAIA). This is an imaging system based on photos taken from three cameras, top, front and side, positioned in orthogonal directions. Individual aggregate particles are transported into the position of the cameras by a conveyor belt, and three pictures from the different views are taken simultaneously [6,7]. The shape indices are then computed from the three orthogonal 2-D projections of the aggregate image using algorithms written in a graphical language as part of the virtual instrument computer

program. The data are analyzed in two main categories. The first category is for the particle sizes, which includes determination of maximum, intermediate and minimum dimensions, gradation properties, and the volume of the particle. The second category is for the particle shape characterization for which the developed shape indices mainly include the flat and elongated ratio (F&E ratio), the angularity index (AI) and the surface texture (ST) index. The three indices were developed to represent the three key morphological properties of an aggregate particle, i.e., shape, angularity and surface texture (see Figure 1). In this study, the focus will be on the use of the particle shape indices to investigate how these factors influence the deformation properties of the unbound aggregate samples.
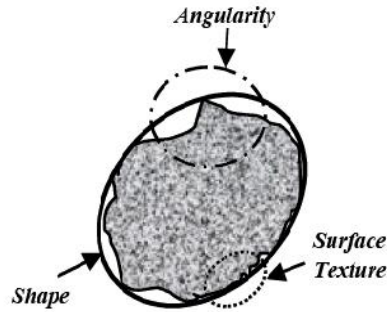
Figure 1. Key morphological properties of an aggregate particle [6]

Flat and Elongated ratio

Aggregate particle flatness and elongation, sometimes also referred to as flakiness or slenderness, is determined in the UIAIA system using the Flat and Elongated (F&E) ratio as given in Equation 1 [6, 8]:

$$\text{F\&E Ratio} = \frac{\text{Longest Dimension}}{\text{Shortest Perpendicular Dimension}} \tag{1}$$

Traditionally the dimensions of a particle for flatness and elongation are determined by manual measurements using a proportional caliper according to ASTM D4791. Using the UIAIA system, the F&E ratio is computed by determining the longest and the shortest perpendicular dimensions of each of the three views, whereas the ratio of the longest dimension to the shortest finally gives the F&E ratio for the aggregate grain. All aggregate samples evaluated were separated into classes as shown in Table 1.

Table 1. Aggregate Flatness and Elongation Determined from Flat and Elongated (F&E) Ratio

Aggregate Sample	F&E Ratio < 3:1 (% by weight)	F&E Ratio 3:1 to 5:1 (% by weight)	F&E Ratio > 5:1 (% by weight)
Cubical	85.7	12.9	1.4
Cubical rounded	91.8	8.2	0.0
Flaky	67.2	27.3	5.4
Flaky rounded	68.2	30.9	0.9

From the results of the 3-D image analysis the cubical particles tend to have low F&E ratio since approximately 86 % of the sample is classified with aspect ratios less than 3:1. This means that most of the particles are close to being equidimensional. The wear of corners and edges apparently made the aggregate particles more equidimensional compared to the more angular samples. As expected from visual observations the flaky materials are in general less equidimensional than the cubical aggregates with lower percentages listed in Table 1 under the different F&E aspect ratio ranges.

Angularity Index
Traditionally, angularity of an aggregate particle can be determined directly by counting the number of fractured faces on the grain surface. There are also other methods, such as the particle index and uncompacted void test (ASTM D3398-00 and AASHTO TP56) to give results for the combined shape, angularity and texture properties. There is not a single standard test to adequately define and quantitatively determine the aggregate shape, angularity and surface texture properties for quantifying the angularity based on more advanced and less labor intensive techniques.

The angularity index (AI) based on the images captured by the UIAIA system provides a means to adequately define and quantitatively determine the aggregate angularity. The AI image analysis procedure first provides an angularity value for each 2-D images collected from the top, front and side views. The outline each 2-D aggregate projection is then approximated by an n-sided polygon as shown in Figure 2. Next, AI for one particle, which measures overall degree changes of the boundary particle, is computed as a weighed average of the angularity values obtained from all three views with respect to the 2-D projection areas. The final AI value in degrees for the entire aggregate sample is simply an average of the angularity values of all the particles weighed by the particle weight.
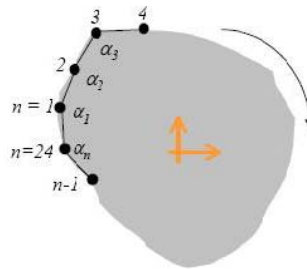
Figure 2. Aggregate projection as an n-sided polygon [7]

Surface Texture Index
The UIAIA system can also be used to determine the surface texture of coarse aggregates by using an image processing method known as the erosion-dilation technique [6, 9]. Erosion is a morphologic operation by which all boundary pixels are removed from a binary picture, leaving the object one pixel less dense along the boundary. Dilation is the reverse of erosion, where a layer of pixels is added to the object boundary to create a simplified form of the original aggregate projection. The area lost during an optimized number of the erosion-dilation cycles is given as a percentage of the total area of the original image and denoted by the surface texture (ST) parameter:

$$ST = \frac{A_1 - A_2}{A_1} \cdot 100 \qquad (2)$$

where;
A_1 = Area (in pixels) of the 2-D projection before erosion-dilation process is applied
A_2 = Area of object after erosion-dilation process is applied

The aggregate surface texture, $ST_{particle}$, which measures overall degree of surface irregularities of a particle, is computed as the weighed average of each ST determined from all three views weighed by their individual areas. The final ST index for the entire aggregate sample is simply an average of the angularity values for all particles weighted by the particle weight.

Figure 3 shows the AI and ST index results of all four aggregate test samples. The results of the sample evaluations give the expected results that the cubical and the flaky materials are generally more angular, having rougher surface textures than the rounded samples. The analyses in addition show that the flaky category has the highest values of AI and SI. Significant differences are indicated between the AI and ST index values before and after aggregate rounding and abrading using the Nordic Ball Mill drum. The

differences in the shape indices between the original and the rounded/abraded aggregates are typically in the order of 20 to 30% as reductions from the original shape indices.
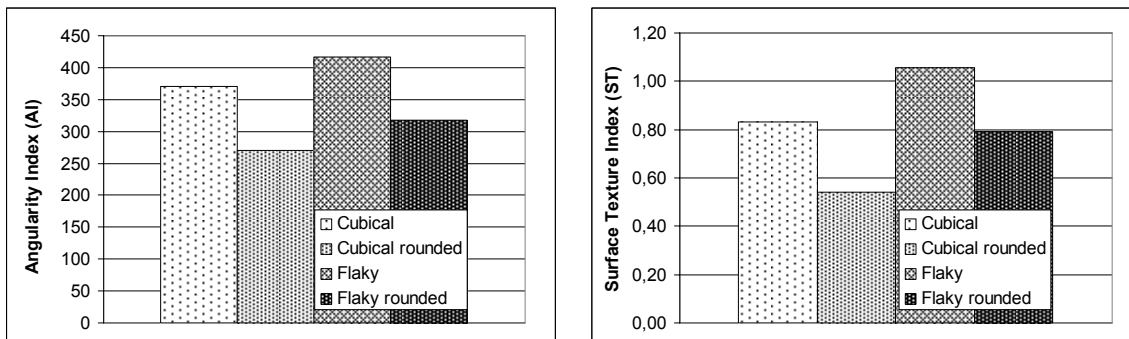
Figure 3. Angularity index (AI) and surface texture (ST) index results for all four aggregate samples

3. CYCLIC LOAD TRIAXIAL TESTING

3.1 Sample preparation

Laboratory triaxial testing was undertaken to determine resilient modulus and permanent deformation properties of the four aggregate samples. All specimens were compacted in gyratory moulds by applying the same compaction energy and following the same sample preparation method. The compaction was performed in five equal layers using a vibratory table. Each layer was compacted for 30 seconds with a dead weight on top, and the amplitude of the vibrating table was 10 mm.

The samples were conveniently compacted using a gyratory mould, which could produce 220 mm tall cylindrical specimens with 150 mm diameter. This differs from the recommendations in the European CEN-standard [10] where the height is recommended to be twice the diameter of the sample. A study on the influence of sample height on permanent deformation behaviour of unbound aggregates was performed by SINTEF [11]. It was concluded that samples with a height to diameter ratio ranging from 1:1 to 1.5:1 showed little difference, with respect to resilient modulus and the resistance against permanent deformations. To compensate for the reduced height and the end effects in the sample, a finer grained material from the same quarry was used at the ends of the specimen. The 11-16 mm grains did not touch the top and bottom plate and the grain size was gradually reduced in a 10 mm layer at the top and bottom. In addition, lubricated Teflon foils were used in both ends to reduce friction.

3.2 Test procedure

The testing procedure followed was taken from the CEN-specifications [10]. The multistage loading procedure with high stress level was chosen to give as much information as possible from each sample tested. The objective of this procedure is to determine stress limits or threshold limits to avoid the development of excessive permanent deformations.

The loading was performed in five different sequences, with five different confining stresses applied. In each loading sequence there were up to six different deviator stresses applied with stress magnitudes increasing with load steps. Each load step consisted of applying 10 000 load pulses. This procedure gave the elastic response of the material as well as the permanent deformation behaviour. The loading was interrupted if the axial permanent deformation reached 0.5 %, and then the next confining stress was applied.

4. RESILIENT BEHAVIOUR

Under traffic loading, granular material deformation behaviour in a base layer is typically a non-linear response with partly resilient (recoverable) and partly accumulation of plastic/permanent deformations. Figure 4 shows in principle the response in a granular material during one load cycle, where the resilient strain is fully recovered and some permanent deformation is also developed. For typical use as base or sub-base material in a pavement structure the elastic strain would be several orders of magnitude larger than permanent strains. This means that it is possible to treat the two strain types separately.
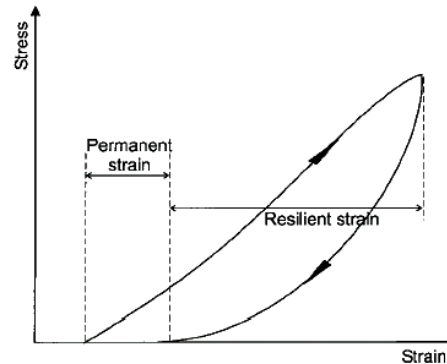
Figure 4. Resilient and permanent strains in granular materials during one cycle of load application [3]

4.1 Resilient Modulus

The theory of elasticity traditionally defines the elastic properties of a material by the modulus of elasticity, E, and the Poisson's ratio, ν. The bulk and shear moduli can also be used alternatively. Dealing with unbound aggregates in base layers the elastic modulus E is replaced by the resilient modulus, M_R, to indicate that the elastic, recoverable behaviour is actually realized in these trafficked pavements not at a stress and/or strain free state but together with the accumulated permanent deformations or ruts in the granular layer. The resilient modulus M_R behaviour is known to be nonlinear and stress dependent.

By running a repeated load triaxial test at constant confining pressures, one can compute the resilient modulus M_R at an applied wheel load dynamic stress using the following equation:

$$M_R = \frac{\sigma_d^{dyn}}{\varepsilon_a^e} \qquad (3)$$

where,

M_R = resilient secant modulus;

σ_d^{dyn} = applied dynamic deviator stress;

ε_a^e = axial resilient strain.

The resilient modulus has been found to be influenced by several factors of which the stress level and moisture content are commonly accepted as the predominant variables. Previous research studies have shown that resilient modulus increases greatly with increased confining pressure or increased sum of principal stresses (bulk stress) and only slightly with deviator stress [3, 12, 13, 14].

Figure 5 shows the resilient modulus test results plotted with deviator and bulk stresses on the x-axis respectively. The influences of the deviator stress levels on the resilient moduli are clearly seen from the first graph for different confining pressures. Overall, the influence of the deviatoric part of the stress is much less pronounced than the effect of the confining stress. Evaluating the factors $\Delta M_R/\Delta \sigma_d$ and $\Delta M_R/\Delta \sigma_3$, which can

be found from Figure 5, we find that the influence of the confining stress is 3-5 times more powerful than the influence of the deviatory stress. When plotting these data as a function of the bulk stress however, all data fits reasonably good within a curved line, indicating that the k-θ model might work reasonably well for our data.
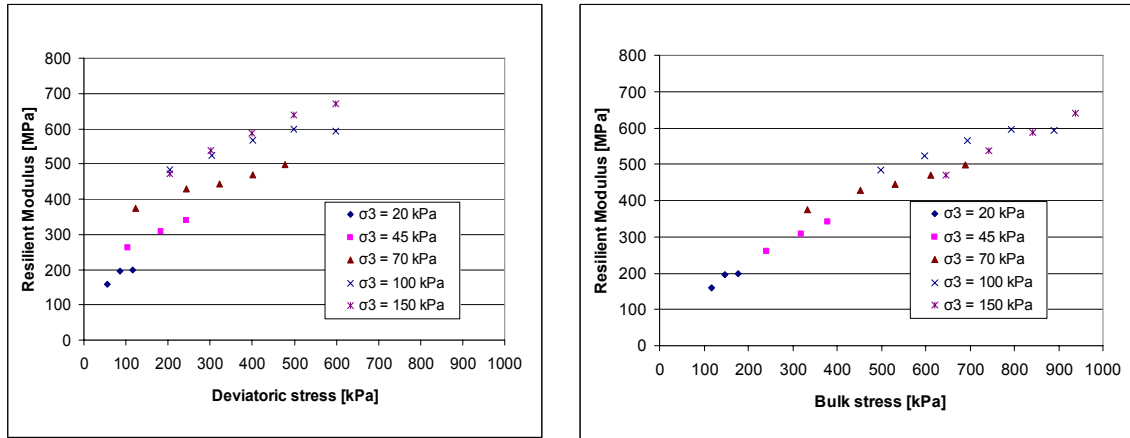
Figure 5. Resilient modulus variations with deviator and bulk stresses
for one cubical aggregate sample (example)

In Figure 6, each combination of applied confining pressure and deviator stress for the cubical angular aggregates are separated into two categories of deformation behaviour under two stress regimes. The figure to the left contains data where the material exhibited purely elastic response, and the figure to the right contains only data after some permanent deformations occurred in the specimen. The resilient modulus seems to be almost the same whether the material is subjected to stresses within the elastic or the plastic stress regimes. As observed in all the tests conducted the resilient modulus did not change significantly from the elastic to the plastic stress stage, even when considerable amounts of permanent deformation or rutting accumulated.

cubical aggregate - elastic stress regime   cubical aggregate - plastic stress regime
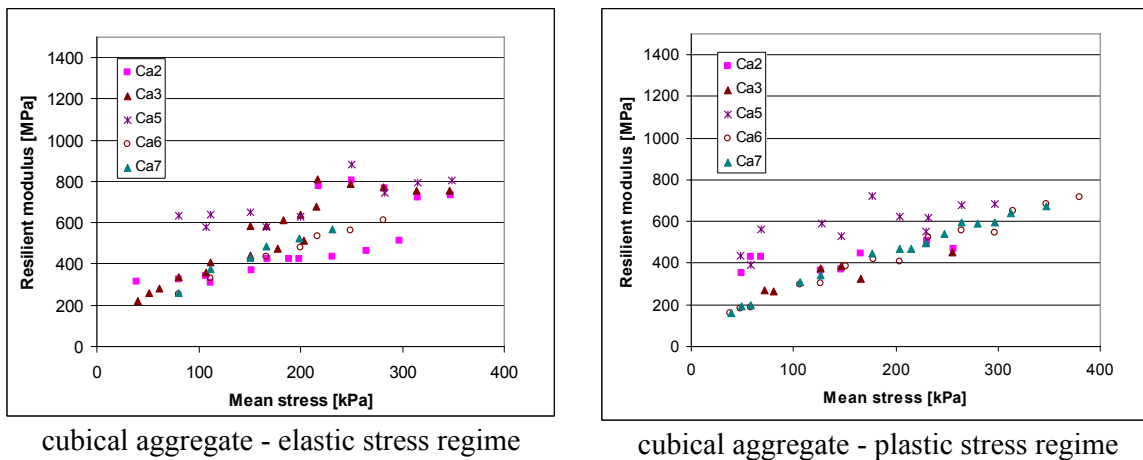
Figure 6. Resilient modulus versus mean stress for the cubical angular aggregates

K-θ-model
Many researchers have developed models to describe the stress dependency of the resilient modulus. A well-known curve-fitting model based on the sum of principal stresses or bulk stress is named the k-θ model. The k-θ model is a non-linear, stress-dependent power function model, described by Seed et al. [13]. This is a

commonly used model to account for the stress dependency of resilient modulus. In its dimensionless form, the model is given as follows:

$$M_r = k_1 \cdot \sigma_a \left(\frac{\theta}{\sigma_a} \right)^{k_2} \tag{4}$$

where,

M_r = Resilient modulus;
θ = bulk stress; $\theta = \sigma_1 + \sigma_2 + \sigma_3$
k_1 and k_2 = model parameters from regression analyses of triaxial test results;
σ_a = reference pressure (100 kPa);

The original k-θ model has several shortcomings. It considers the all-around bulk stress to represent triaxial stress states and does not account for the confining pressure and deviator (or shear) stress individually. By doing that, stress level is only accounted for by the bulk stress, which assigns the sum of all the different combinations of principal stresses to have the same influence on the moduli. Further, the model is often used with a constant Poisson's ratio to calculate the specimen radial strain. Earlier work [14, 15] showed that Poisson's ratio does not stay constant, but varies with applied stresses as well.

Figure 7 shows the resilient modulus results by the fitted k-θ model for all aggregate samples tested. Each line represents one sample tested. There are considerable differences in the shape of the curves between the original cubical aggregates and those of the cubical rounded ones. The cubical materials show a lower dependence on the bulk stress than the cubical rounded aggregates. For high stress levels, the resilient modulus curves for the cubical materials seem to level off, while the cubical rounded aggregates have much steeper curves and seem to give steadily increasing resilient moduli with increasing bulk stresses. This was also highlighted previously by Janoo [16] who found that the angularity of aggregates had a considerable influence on the resilient modulus. Natural gravel gave higher resilient modulus properties than crushed materials prepared and tested about the same density levels, which was explained by the ability of rounded gravel particles to better rearrange, in some cases to more stable structures.

The flaky materials do not show any significant differences in the M_R behaviour as all M_R curves for both series are within the same range. Here, the rounding of the grains does not seem to have any significant effect on the resilient response of the material. However, the rounded materials in this case had significantly lower dry densities. Naturally, this makes it harder to single out the impact of abrading and rounding of the flaky aggregate particles.

Table 2 lists the mean values of the k-θ model parameters determined to establish resilient modulus characterizations as a function of bulk stress for all test series. Figure 8 shows the characterization results for the mean resilient moduli predicted from the k-θ curve fitting models. Figure 8 clearly underlines some of the tendencies observed in Figure 7. The cubical rounded and flaky rounded materials have about the same bulk stress influence, but the cubical rounded series results in the highest resilient moduli at high stress levels.
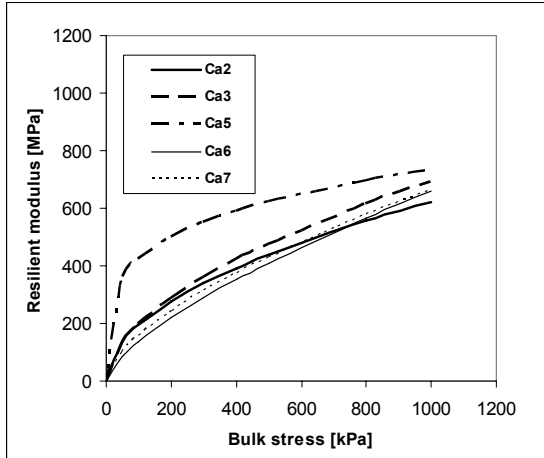
cubical aggregates
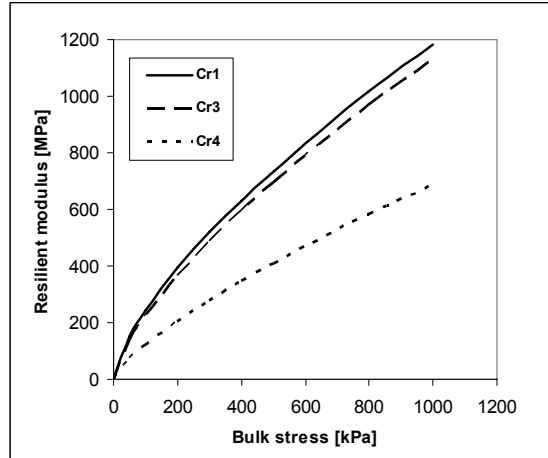
cubical rounded aggregates
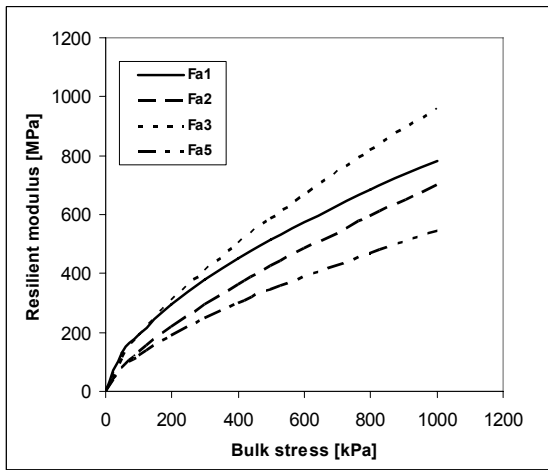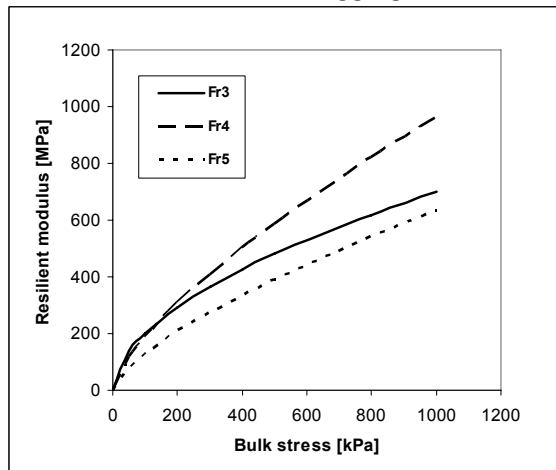
flaky aggregates

flaky rounded aggregates

Figure 7. Curve fitting by k-θ model for all series
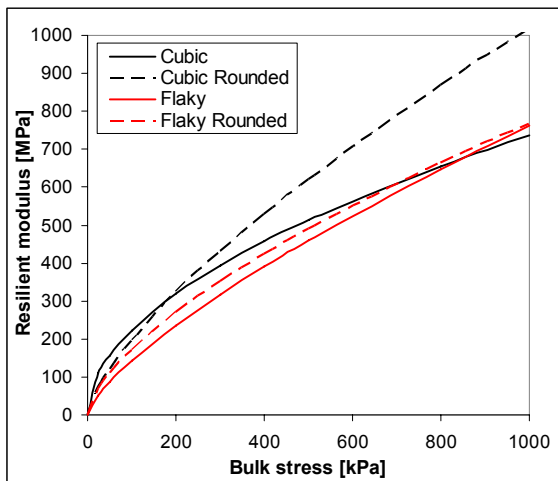
Figure 8. Mean resilient modulus results from
k-θ model curve-fitting

Table 2. k_1 and k_2 for all series, mean values

Series	k_1	k_2
Cubical	2.2	0.518
Cubical rounded	2.0	0.711
Flaky	1.4	0.727
Flaky rounded	1.7	0.648

5. PERMANENT DEFORMATION BEHAVIOUR

5.1 Interpretation of permanent deformation behaviour

The strain rate $\dot{\varepsilon}$ is a measure of the speed of permanent deformation. In this paper, the term is used for development of permanent deformation per cycle. The strain rate is normally highest for the first few pulses at a load magnitude or step and decreases gradually towards the end of that step. Figure 9 shows per step the permanent strain accumulation as a function of the number of cycles for one load sequence.

In static triaxial testing with constant strain rate, the failure limit can be found by the stage of yielding, and the level of permanent strain is a key parameter for failure. In the multistage repeated load triaxial testing procedure, the strain rate rather than the strain magnitude is found to be a more suitable parameter to define failure.
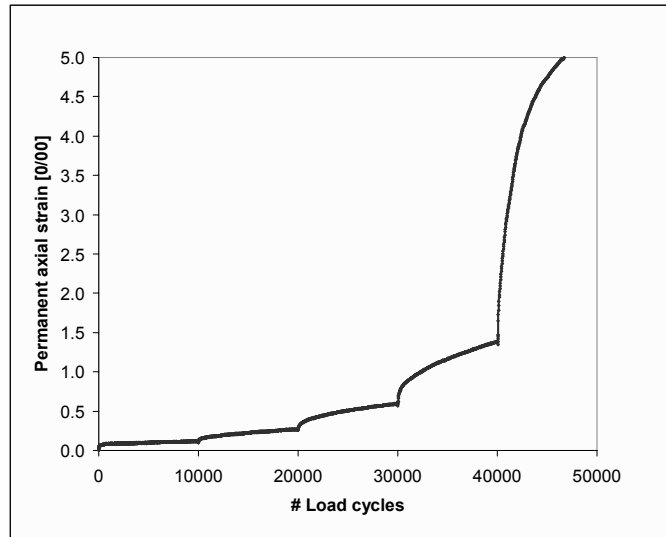
Figure 9. Axial permanent strain accumulation with load cycles tested at one load sequence

Werkmeister [17] proposed to use the average strain rate between load pulses 2000 and 5000 as a criterion for characterizing granular materials' resistance to permanent deformation. To consider all the information gathered from applying up to 5000 load pulses, Hoff et al. [18] used the average strain rate response together with the concept of modified range limits according to the observed total strain and the physical "failure" for the material tested. This method was applied in this paper, and the ranges were;

Range - A:	$\dot{\varepsilon} < 2.5 \cdot 10^{-8}$	Elastic range
Range - B:	$2.5 \cdot 10^{-8} < \dot{\varepsilon} < 1.0 \cdot 10^{-7}$	Intermediate Response
Range - C:	$\dot{\varepsilon} > 1.0 \cdot 10^{-7}$	Incremental failure

The permanent deformation test data from all load steps were analyzed and classified in range A, B and C and plotted as shown in Figure 10, with different symbols, each characterizing one strain rate range. The Coloumb-criterion was used to find the limiting stress envelopes for the design stress stage and the failure stage. These are represented by the two straight lines in Figure 10. The criteria used are defined by the threshold limits for the strain rate of the last 5000 load cycles of each load step ($N = 10^4$) defined as ranges A, B and C defined above. The equations of these lines are:

Elastic limit: $\sigma_3 = \sin\rho(\sigma_1 - \sigma_3) + a$ (5)

Failure limit: $\sigma_3 = \sin\varphi(\sigma_1 - \sigma_3) + a$ (6)

where,
σ_1 and σ_3 = principal stresses;
ρ and φ = angles of the elastic and plastic limit lines;
a = apparent attraction in the material given by the relationship;

$$a = \frac{c}{\tan \rho} \text{ or } \frac{c}{\tan \varphi}, \text{ where c is the apparent cohesion in the material.}$$

The apparent attraction "a" showed very little variation and was fixed at 20 kPa for all series to simplify the interpretations. The results for each test series are shown in Figures 9 and 10.

The samples in these series were only lightly compacted, which influenced the permanent deformation results of the first two load sequences in the CEN procedure. Hence, the two first sequences, 20 kPa and 45 kPa confining stress, are less valid for material characterization with respect to permanent deformation than the three last sequences. The first load sequence could rather be assessed as part of the compaction procedure of the material. Thus, in Figure 10, the first load sequence is not shown because of the big scatter caused by the effect mentioned.

Table 3. Symbols for σ_3-σ_d-plot

Range – A points:	■
Range – B points:	▲
Range – C points:	●
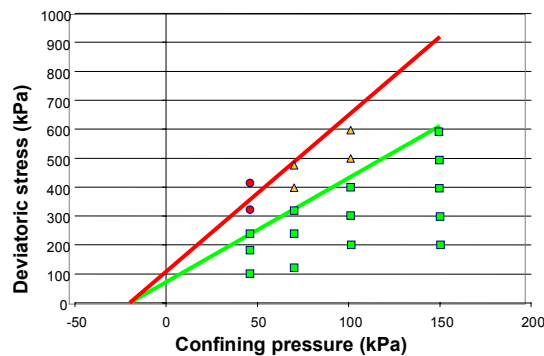
Figure 10. Interpretation of results by the Coulomb approach

Figure 11 shows the elastic (sin ρ) and failure limits (sin φ) for all samples together with the dry densities. The cubical and cubical rounded series show that the rounding has a pronounced effect on both the elastic response and the development of permanent deformations. Here, the sample compacted dry densities are close to each other, and the differences in strength properties are mainly influenced by the different grain shapes.

For the flaky materials the rounding apparently does not seem to have any significant effect on the material strength. But in this case, the dry density is higher for the rounded material. Higher density normally gives higher material strength, while rounding (less angularity) should theoretically give lower strength for the cubical material. The effect of densification seems to cancel out the effect of the rounding.

As Figure 11 shows, different dry densities were achieved for the different samples compacted using the same energy input. The reason for this is probably different ability to fill the voids. The cubical materials seem to be the easiest materials to compact compared to the flaky materials. The angularity of the aggregate sample also controls the compactibility. By comparing the cubical and the cubical rounded materials as well as the flaky and the flaky rounded aggregates, one can observe that the rounded aggregates in general result in higher dry densities.

When comparing the mean values for the cubical and the flaky test series in Figure 12, there is a significant difference only between the two original angular materials. The cubical aggregates show significant higher resistance against permanent deformations as they have a larger range of elastic behaviour and a higher failure limit compared to the rounded aggregates. However, the rounded aggregates indicate similar values for the failure limit, as the original angular material. The flaky rounded aggregates show a bit higher range and a higher elastic limit than the original material, but this is probably due to a higher density.
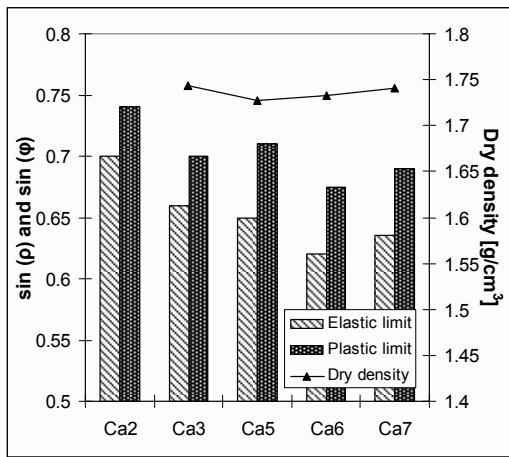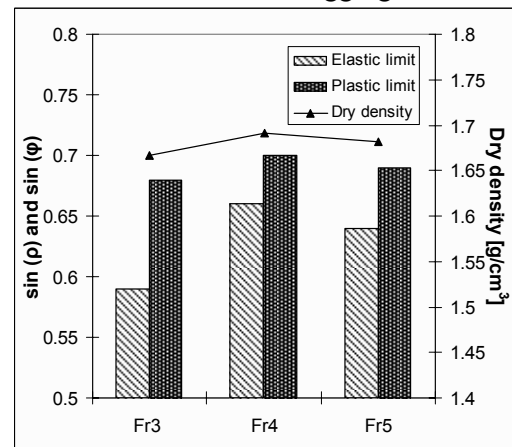
cubical aggregates
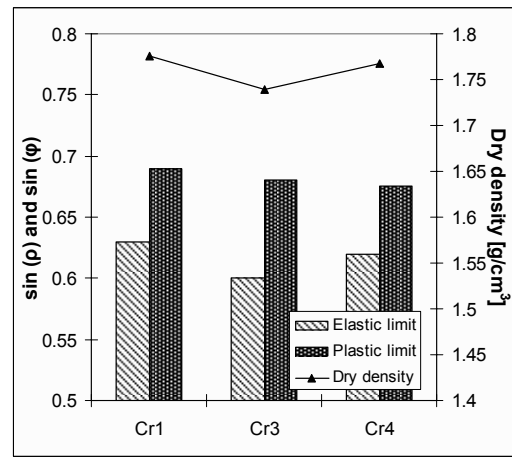
cubical rounded aggregates
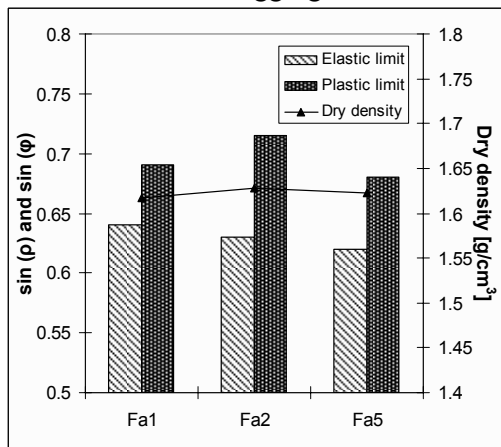
flaky aggregates

flaky rounded aggregates

Figure 11. Elastic and plastic limits presented with compacted dry densities for all samples
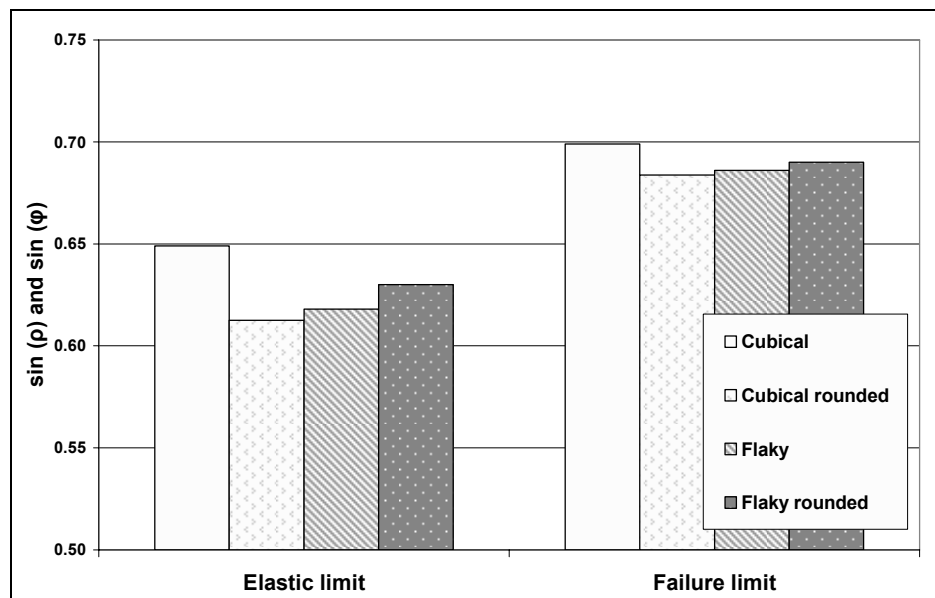

Figure 12. Elastic and failure limit for the test series

6. CONCLUSIONS

Rounding of aggregate in a Ball Mill drum causes significant changes in the angularity and the surface texture properties. The University of Illinois Aggregate Image Analyzer (UIAIA) using three orthogonal views of each aggregate particle properly distinguished in this study rounded particles from the original angular ones for the same Askøy gneiss from Norway. The imaging based angularity and surface texture indices adequately quantified changes in shape properties in agreement with the visual observations. The biggest advantage was the complete characterization of the grain shape key morphological properties by the quantifiable indices, which established meaningful relationships with strength, modulus and permanent deformation properties.

Using the bulk stress for establishing stress dependency of the resilient modulus seemed to work reasonably well for these samples. All aggregate samples had close to the same resilient responses at low stress levels. At high stress levels, the resilient responses for the cubical aggregates seemed to be less influenced by the stress level than observed for the cubical rounded aggregates. The cubical rounded aggregates gave the highest resilient moduli at high stress levels, and were thereby highly influenced by the level of applied stresses. This could be explained by the ability of rounded aggregate grains to rearrange for building more stable structures.

The flaky angular and the flaky rounded aggregates showed approximately the same resilient responses within the applied stress levels. However, the flaky rounded aggregates had significantly higher dry densities, which made it very hard to distinguish the impact of particle rounding from the effect of different densities. The flaky (flat and elongated) and angular grains were harder to compact during sample preparation.

For the cubical aggregates, the angularity and surface texture seemed to have a significant effect on both the elastic and plastic aggregate shakedown threshold limits. For the flaky materials, the rounded aggregates showed the same strength as the angular ones. However, the dry densities achieved were higher for the rounded samples. When compared at similar dry densities, it is highly probable that the rounded material would give more permanent deformation than the angular at high deviator stress levels.

The dry density of the aggregate samples seemed to have an effect on both the elastic and failure limits for all the materials tested. The cubical aggregates were easier to compact when compared to the flaky aggregates. The cubical aggregate samples achieved higher densities for the same applied compaction energy.

REFERENCES:

[1] Barksdale, R, and S. Itani. Influence of Aggregate shape on Base Behaviour, Paper Transportation Research Record 1227, Transportation Research Board, National Research Council, Washington,1989, pp 173-182.
[2] Lees, G. The measurement of particle shape and its influence in engineering materials, Journal of the British Granite and Whinestone Federation, London, 1964, pp 1-22.
[3] Lekarp, F. Resilient and Permanent Deformation Behaviour of Unbound Aggregates under Repeated Loading. TRITA-IP FR 99-57, Kungliga Tekniska Högskolan, Royal Institute of Technology, Stockholm, 1999.
[4] Stensland, K. A laboratory evaluation of the Ball mill method. Diploma thesis, NTNU Norwegian University of Science and technology, Study Programme in Earth Sciences and Petroleum Engineering, 2003.

[5] Uthus, L., I. Hoff and I. Horvli. Evaluation of grain shape characterization methods for unbound aggregates. Paper 154, CD Proceedings. 7th International Conference on the Bearing Capacity of Roads, Railways and Airfields, Trondheim Norway, 2005.

[6] Pan, T. and Tutumluer, E. Imaging Based Evaluation of Coarse Aggrgate Size and Shape Properties Affecting Pavement Performance. Paper ASCE Geotechnical Special Publication 130, 2005.

[7] Rao, C., E. Tutumluer, and I. T.Kim. Quantification of Course Aggregate Angularity Based on Image Analysis. Paper, Transportation Research Record 1787, Transportation Research Board, National Research Council, Washington DC, 2002.

[8] American Society for Testing and Materials, ASTM. Standard Test Method for Flat Particles, Elongated Particles, or Flat and Elongated Particles in Coarse Aggregate. ASTM D 4791-99, 1999.

[9] Rao, C., T. Pan and E. Tutumluer. Determination of Course Aggregate Surface Texture using Image Analysis. Paper, 16th ASCE Engineering Mechanics Conference, University of Washington, Seattle, 2003.

[10] CEN. Unbound and hydraulically bound mixtures – part 7: Cyclic load triaxial tests for unbound mixtures. EN 13286-7. Brussels, 2000.

[11] Dongmo-Engeland, B. GARAP Influence of sample´s height on the development of permanent deformations. STF50 A05075. SINTEF Technology and Society, Road and Railway Engineering, 2005.

[12] Uzan, J. Characterization of Granular Material, Paper Transportation Research Record 1022, Transportation Research Board, National Research Council, Washington DC, 1985, pp 52-59.

[13] Seed, H.B., Chan, C.K and Lee, C.E. (1962). Resilience characteristics of subgrade soils and their relations to fatigue in asphalt pavements. Proceedings of International Conference on Structural Design of Asphalt Pavements. Ann Arbor, USA. Vol 1, pp 611-636.

[14] Hicks, R.G and C.L. Monismith, Factors influencing the resilient response of granular materials. Paper Highway Research Record Number 345, Highway Research Board, National Research Council, Washington DC, 1974, pp 15-31.

[15] Kolisoja, Pauli. Resilient Deformation Characteristics of Granular Materials. Thesis Tampere University of Technology Publication 223. Tampere, 1997.

[16] Janoo, V. and J.J. Bayer II. The Effect of Aggregate Angularity on Base Course Performance. Technical Report ERDC/CRREL TR-01-14, Cold Regions Research and Engineering Laboratory, 2005.

[17] Werkmeister, S., Permanent Deformation Behaviour of Unbound Granular Materials in Pavement Constructions, *Thesis,* Technischen Universität Dresden. 2003.

[18] Hoff, I., Bakløkk, L. and Aurstad, J. Influence of Laboratory Compaction Method on Unbound Granular Materials. Paper, Proceedings for the 6th International Symposium on Pavements Unbound (UNBAR 6) (CD-ROM), University of Nottingham, UK, 2003.

PAPER III

The value 6.4 % for material less than 0.2 mm for Material 1 in Table 4.
should be corrected to 20.4 %

A study on the influence of water and fines on the deformation properties and frost heave of unbound aggregates

L. Uthus[1], Å. Hermansson[2], I. Horvli[1] and I. Hoff[3]

[1]Department of Civil and Transport Engineering, Norwegian University of Science and Technology, NTNU, Høyskoleringen 7A 7491 Trondheim, Norway; PH (0047) 73595000; FAX (0047) 73591478; email: Lillian.Uthus@ntnu.no, Ivar.Horvli@ntnu.no

[2]VTI, SE-58195 Linköping, Sweden, PH (0046) 13204072 ; FAX (0046) 13141436; email: Ake.Hermansson@vti.se

[3]SINTEF Building and Infrastructure, Road and Railway engineering, Trondheim, Norway,; PH (0047) 73594731; FAX (0047) 73591478; email: Inge.Hoff@sintef.no

Abstract

Damages caused by frost heave as well as rutting caused by loss of bearing capacity in the spring thaw period are serious problems in most countries that experience frost in the winter time. In order to keep a road network in frost affected areas with minimum total costs for road users and owners, a proper use of materials which serves winter and spring thaw conditions is essential. The choice between extensive utilization of local materials and the use of high quality material, transported a long distance, is an important issue. In this context it is important to avoid severe differential frost heaves, and to keep a high bearing capacity throughout the year. For unbound material, the mineralogy, fines content and permeability are key factors to determine the frost susceptibility. In this project one grading of unbound material from three different rock types was investigated; one relatively weak mica-rich gneiss from Sweden and two typical hard rock types from Norway. The potential for frost heave was investigated by laboratory frost heave tests. Repeated load triaxial testing was used to study the resilient modulus and the permanent deformation properties under influence of different water contents. This investigation improves the knowledge on the behavior of unbound aggregate used in road construction in regions with cold climates.

Introduction

The frost heave of a material is dependent on a variety of factors. The characteristics of the material, like fines content, gradation, mineralogy, texture, pore water chemistry, are all important variables concerning frost heave. Other influencing parameters are the access to water, drainage, heat flux and internal stress.

There are two conditions necessary for frost heave to occur. The ground temperature has to be low enough over a certain period of time for the pore water to freeze, and the soil has to be susceptible to the segregation of ice. Moreover, it is often stated that the water table has to be close to the frost front

to feed a significant frost heave (Ladanyi 1994). Field studies though show severe frost heave with the water table as deep as five meter below the frost front, indicating that frost susceptible soils hold water enough to feed the heave. This observation is supported by laboratory frost heave tests where no external water was added (Hermansson and Guthrie 2005).

Criteria for frost susceptibility in soils for road purpose are in its simplest way based on the grain size distribution characteristics of the soil. Such a criterion is typically connected to the amount of material finer than a certain grain size, and also the shape of the grain size curve. The background of the gradation specifications are often empirical results.

Other methods have been proposed, like pore size distribution, saturated moisture content, capillary rise and permeability. In Austria, the mineral content plays an important role for the specification of frost susceptibility. However, none of the indirect methods available gives a good prediction for all soils. In special cases, like for recycled materials (Aurstad et al 2005), and also when a material is not clearly non frost susceptible the best method for prediction of frost susceptibility is the direct testing.

The scope of this paper is to investigate the sensitivity to water and the frost susceptibility of three different materials with almost the same gradation curve. The sensitivity to water is connected to the deformation behavior. Water contents were chosen close to the optimum Modified Proctor, and also on the dry and wet side of the optimum water content.

There is a link between frost susceptibility giving frost heave and the water sensitivity resulting in loss of shear strength as well as reduced resilient modulus under high water contents which may occur in the spring thaw period. The focus in this paper is on the factors that influence the frost heave of granular materials and criteria regarding the suitability of granular materials for use under frost conditions and spring thaw.

Materials

Three granular materials were used in this study, two materials from Norway and one from Sweden. All three materials were first separated into narrow fractions and then recomposed to give equal gradation curves. This means that a criterion, based on gradation only, would predict the three materials to show similar properties regarding frost heave. The gradation chosen is a fuller curve with gradation number - n equal to 0.35. This is a curve giving about 13 percent fines < 63 µm. The gradation of the material < 63 µm, the specific surface area of the material < 63 µm and also the mineralogical distribution in both thin sections and bulk samples were investigated to see if observed differences in the susceptibility to water and frost were caused by differences in these parameters.

The specific surface area of the material < 63 µm was investigated using BET analysis (BET means Brunauer, Emmet and Teller), Table 1. Material 1 has a specific surface area of 1.58 m^2/g, which is the lowest compared to the two other materials. Material 2 and 3 have similar specific surface areas of 4.88 m^2/g and 4.73 m^2/g respectively. The specific surface area of fines influences the ability to bond with water molecules, as a higher specific surface area gives more area to cover with water.

Table 1. Quantification of the main minerals in thin sections in %

Sample	Material 1	Material 2	Material 3
Quartz	47	40	19
Feldspar	44	50	37
Mica		8	33
Epidote			9
Amphibole	5		
Titanite	2		
Unidentified minerals	2	2	2

Table 1 shows the results from the analysis of thin sections from hand specimens. Material 1 and 2 have similar mineralogy and all three materials have a large amount of the two minerals feldspar and quartz. Material 3, contrary to the other materials, contains a lot of mica, approximately 33 %. It must be kept in mind that neither thin section analysis nor x-ray diffraction (XRD) are accurate, and the percentages of each mineral must be seen as more relative values.

The results from the XRD analysis on bulk material < 20 μm are presented in Table 2. Here the mineral contents are different compared to the thin sections. Material 1 and 2 still have quartz and feldspar as their main minerals, but the amount of quartz is lower and the amount of feldspar is higher in the fines. Quartz and feldspar are very strong and hard minerals, and not expected to accumulate in the fines. Mica however is a soft and more "lose" mineral, with weaker chemical bonds between the sheets of mica (Prestvik 1992). Mica would therefore be expected to accumulate in the fines as it is more easily crushed than the other minerals.

Table 2. Quantification of the minerals in % of material <20 μm by XRD and SEM analysis

Sample	Material 1	Material 2	Material 3	
	XRD	XRD	XRD	SEM
Quartz	27	21	21	28
Plagioclase	31	37	53	27
Alkali feldspar	31	16	11	8
Mica	6	17	11	24
Chlorite	2	4	3	1
Pyrite	T	T		
Epidote			T	3
Amphibole	3	5		
Other minerals				9

T= Traces of the mineral

It can be seen that the content of mica is different in Material 1 and 2 compared to Table 1. In the thin sections, Material 1 contained no mica and Material 2 approximately 8 %, and in the fines the mica content is 6 % and 17 % for Material 1 and 2 respectively. These two materials are from the same quarry but the mica content may vary within the quarry.

Material 3 contains about the same amount of quartz in the material < 20 μm as in the thin sections, but the content of feldspar is higher than in the thin sections. Feldspar contains two mineral groups, plagioclase and alkali feldspar, so in Table 1 those minerals are classified as feldspar. It can also be seen that the content of mica in Material 3 has decreased from a value of 33 % from the thin section to

only 11 % in material < 20 μm. We did not expect this, but it may indicate that most of the mica is bound in the coarser particles.

Many of the minerals possibly causing sensitivity to water and frost heave are not original minerals, but minerals transformed through different processes. These minerals are not always easy to detect using the XRD, but by using a scanning electron microscope (SEM) all those minerals can be detected. Table 2 shows the results from a SEM analysis on Material 3, performed on bulk material of the partition < 20 μm.

The XRD and the SEM analyses on Material 3 show somewhat different results, as the SEM analysis detected significantly more mica in the sample. Some of the variation may be caused by the difference between samples.

Frost susceptibility criteria

Many different criteria for frost susceptibility of soils have been developed over the years. Most of them are based on the grain size distribution. Empirically there is a correlation between the frost susceptibility of soils and the grain size distribution, as it affects the pore structure in the material and thereby the suction and permeability. Each criterion is mainly based on the quantification of the material less than a certain critical grain diameter. Different methods of research on the frost susceptibility of soils have resulted in different critical grain diameter.

Here only a selection of the available criteria is used to describe the frost susceptibility of the materials studied.

Casagrande Criterion. Arthur Casagrande (Casagrande 1932) proposed a rule-of-thumb criterion for use as engineering guidelines regarding frost susceptibility. He connected the frost susceptibility to the size of pores in the granular materials. He found that soils are non frost susceptible if the so called characteristic pore size is greater than 0.01 mm. The pore size in the structure is connected to the grading and the fines content, so the following criteria were set. This criterion turned out to be really useful, as it proved to identify about 85 % of the frost susceptible soils correctly (Kaplar 1974).

According to the Casagrande Criterion all the three materials studied are frost susceptible. However Material 1 is close to non frost susceptible with a fines content of 3.1 %, Table 3.

Table 3. Characterization of frost susceptibility by Casagrande

Materials	Cu	Fines < 0.02 mm	Classification
Material 1	167	3.1 %	Frost susceptible (low)
Material 2	167	6.1 %	Frost susceptible
Material 3	167	6.1 %	Frost susceptible

Norwegian classification system. The Norwegian classification system regarding frost susceptibility is developed from work done by Nordal (Nordal 1960) and also from the Casagrande Criterion. The criterion is based on grading and limits the amount of fines in a material to be regarded as non frost susceptible. This classification system is designed to take both the frost susceptibility and the bearing

capacity during spring thaw into consideration. This method is a bit more sophisticated than the Casagrande Criterion, as it has several classes from non frost susceptible materials to highly frost susceptible materials.

Table 4 shows the classification according to the Norwegian classification system. All the three materials tested are classified as low frost susceptible.

Table 4. Characterization of frost susceptibility by the Norwegian Classification system

Materials	Percent by weight of material ≤ 20 mm			Classification
	< 0.002 mm	< 0.02 mm	< 0.2 mm	
Material 1	0.4	3.2	6.4	Low frost susceptible – T2
Material 2	0.4	6.4	20.0	Low frost susceptible – T2
Material 3	0.4	6.4	20.0	Low frost susceptible – T2

The Swedish criterion for frost susceptibility is somewhat similar to the Norwegian, based on the amount of material passing different sieves.

The Mineral Criterion. In Austria the Mineral Criterion (ASI 2001) is used for the specification of frost susceptibility. This criterion is based both on the quantification of fines, both < 63 μm and < 20 μm and the content of active minerals in the material < 20 μm. The analysis is done on the material after road construction or after proctor compaction.

If the material contains more than 4 percent by mass less than 63 μm, the material < 20 μm has to be quantified. Furthermore, if the quantity of the material < 20 μm is 3 percent by mass or more the soil has to be analysed regarding mineral content.

If a material has no active minerals or passes the Mineral Criterion, it is considered to be frost resistant. If it fails the Mineral Criterion frost heave test should be performed to determine if the material is frost susceptible or not.

The Mineral Criterion is proved successful, as materials which passes it really turns out to be frost resistant in practical use. However, Kugler (Kugler et. Al. 2005) found that the mineral criterion in some cases is too strict, as materials that failed the criterion might show frost resistant behaviour during frost heave tests.

Work done by Konrad and Lemieux (Konrad et. Al. 2005) supports the Mineral Criterion as they found that the frost susceptibility of well graded crushed base course materials increased linearly with increasing fines content and content of the mineral kaolinite.

From the quantification of minerals by XRD analysis and also SEM analysis for Material 3 (Table 2) the materials can be classified according to the Mineral Criterion, Table 5. The classification by the Mineral Criterion indicates that Material 3 requires frost heave testing and Material 2 is close to the limit (if the content of mica + chlorite is approximately 25 % for a material with fines content 6.1%, then it should undergo frost heave test).

Table 5. Characterization of frost susceptibility by the Mineral criterion

Materials	Material < 0.02 mm in percent by mass	Active minerals found by XRD	Active minerals found by SEM	Classification
Material 1	3.1	6 % mica 2 % chlorite		Frost resistant
Material 2	6.1	17 % mica 4 % chlorite		Frost heave test almost needed according to XRD
Material 3	6.1	11 % mica 3 % chlorite	24 % mica 1 % chlorite	Frost heave test needed according to SEM

Frost Heave Test. The most reliable method for characterizing the frost susceptibility of a soil in the laboratory is the direct frost heave test. The frost heave tests on the samples presented in this paper were performed by VTI in Sweden. Specimens, approximately 600 mm in length, are frozen from the top and water is fed at the bottom. Just slightly more than the upper 100 mm are frozen at testing and the lower 500 mm of the specimen simulates capillary rise of water to the freezing front to feed the frost heave (Hermansson and Guthrie 05).

The frost heave rate determines how susceptible the material is to frost heave. Figure 1 shows the frost heave from the testing of Material 1, 2 and 3. Each specimen was frozen twice, i.e. freezing was restarted directly after thawing. The frost heave for Material 1 and 2 were similar and the rate during the second freezing did not differ significantly from the first freezing. However, Material 3 showed significantly higher heave rate than the other materials even though the second freezing gave a lower rate.
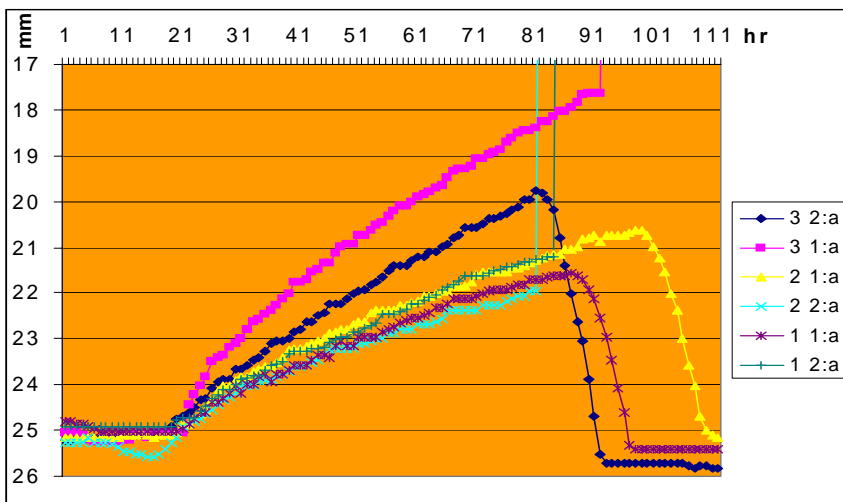
Figure 1. Results from frost heave testing(VTI)

The Swedish classification system is currently being revised and no exact limits for frost heave rate are available. However, we know that the highest frost heave rate seen for materials tested by this method is 0.25mm/h, which must be classified as highly frost susceptible. This value is about three times the highest value of frost heave rate observed for our samples, shown in Table 6.

Table 6. Average rate of heave from frost heave test

Materials	Average rate of heave [mm/h]	Suggested classification
Material 1	0.045	Non to low frost susceptibility
Material 2	0.045	Non to low frost susceptibility
Material 3	0.076	Low frost susceptibility

The suggestion based on these results, and also by looking at the frost heave ranges in the CRREL classification system (Kaplar 1974), is that Material 1 and 2 is non to low frost susceptible and that Material 3 is a low frost susceptible material.

Deformation properties

Sensitivity to water, which is especially connected to the thaw period, can be tested by looking at both resilient response and development of permanent deformations in a material at different water contents.

The deformation properties of Material 1, 2 and 3 were tested using a repeated load triaxial apparatus. For information on both the resilient properties and the permanent deformation behaviour of the materials, the tests were run using the multistage loading procedure for high stress levels according to the CEN- specifications (CEN 2000). Results are presented for both the resilient modulus and the permanent deformation behaviour.

The resilient modulus is presented as a function of the mean normal stress, for all load steps. For the permanent deformation behaviour the constant confining stress of 150 kPa and an increasing deviatory stress is chosen for presentation. However, the samples may have experienced slightly different load history at the four first load sequences, with constant confining stresses of 20, 45, 70 and 100 kPa.

The samples were compacted close to Modified Proctor level using a Kango vibrating hammer. Water contents close to the optimum with variations on the dry and wet side were used.

Material 1. Figure 2a shows the Proctor curves from the Modified Proctor compaction together with the density data for the samples tested of Material 1, and Figure 2b shows the resilient modulus function for the three samples. The sample with 3.0 % water content shows the highest level of resilient modulus, while the samples with 5.9 % and 6.7 % water contents, show the same moduli.
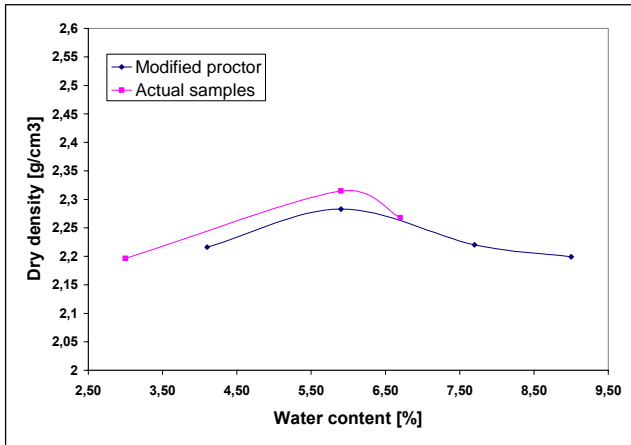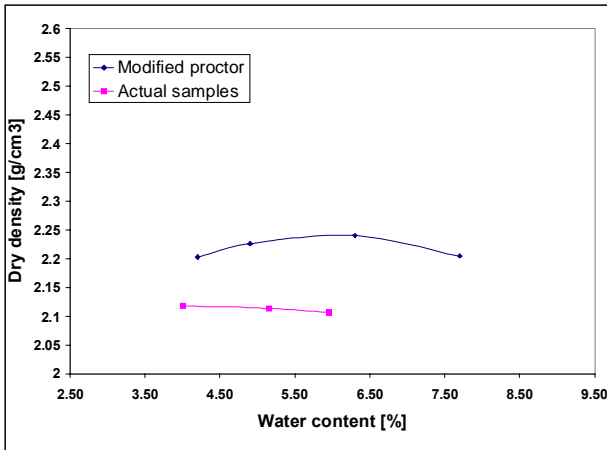
Figure 2a. Modified Proctor and actual dry density and water content for Material 1
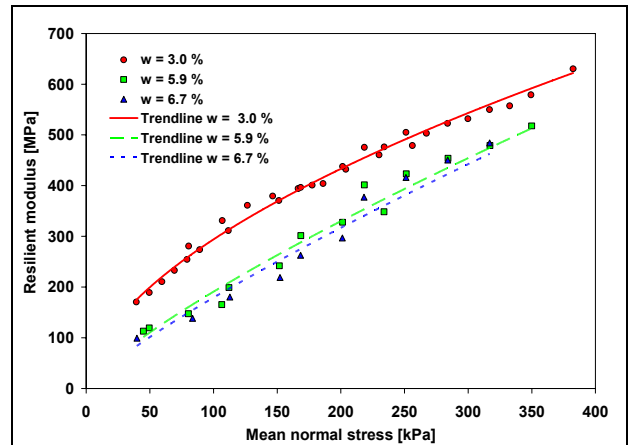
Figure 2b Resilient Modulus vs mean normal stress for Material 1

Figure 3 shows the cumulative permanent strain for Material 1 under constant confining stress of 150 kPa and an increasing axial loading.
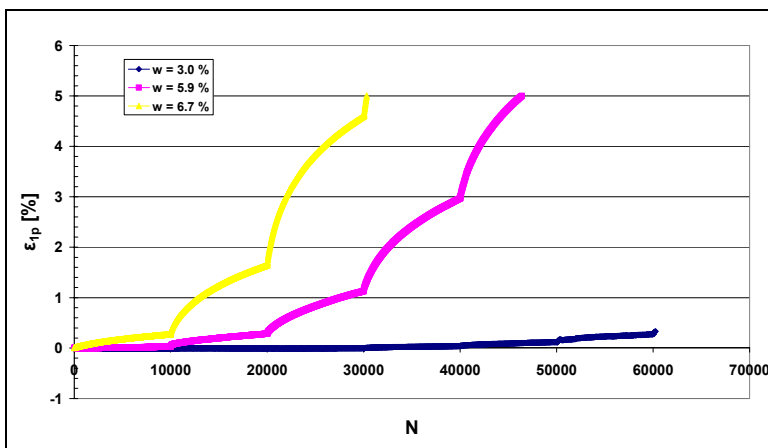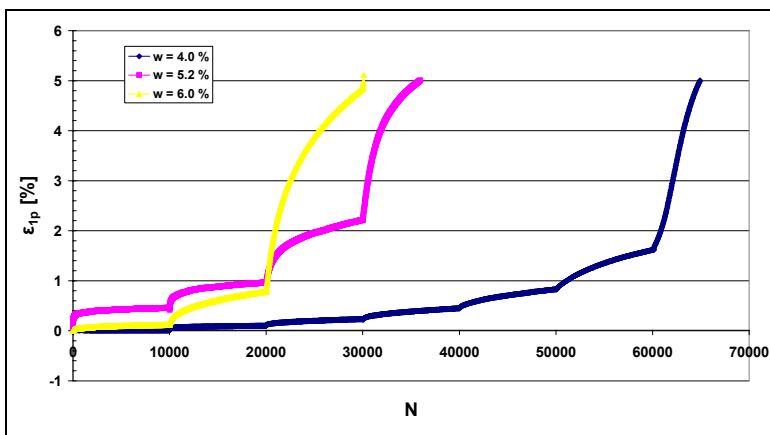

Figure 3 Cumulative permanent deformations Material 1

Here the sample with 3 % water content shows no severe development of permanent deformation for the applied stress levels, while the samples with water contents 5.9 % and 6.7 % both show significant permanent deformations. The water susceptibility is more pronounced here than for the resilient modulus.

Material 2.   Also for Material 2 the Proctor curve for the samples follows the Modified Proctor curve fairly well, Figure 4a. For the highest water content (5.9 %) the samples deviates slightly from the Modified Proctor curve.

8

Figure 4b shows the resilient modulus versus mean normal stress. Again the lowest water content shows the highest resilient response. There is no significant difference between the two samples with water contents of 5.5 % and 5.9 %.
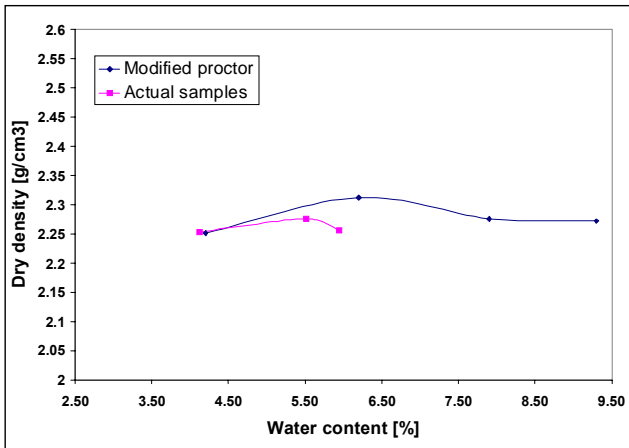
Figure 4a. Modified Proctor and actual dry density and water content for Material 2
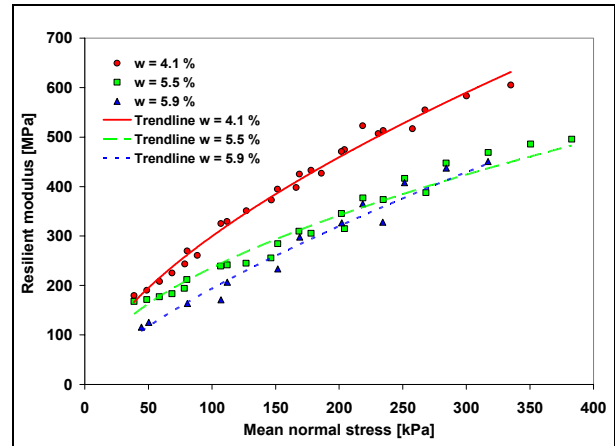
Figure 4b Resilient Modulus vs mean normal stress for Material 2

Figure 5 shows the cumulative permanent strain for the three samples of Material 2. The sample with 4.1 % water shows almost no permanent deformation for the constant confining stress of 150 kPa and an increasing axial load. The sample with 5.5 % water shows a higher susceptibility to permanent deformations, and the sample with slightly higher water content shows dramatically higher permanent deformations.
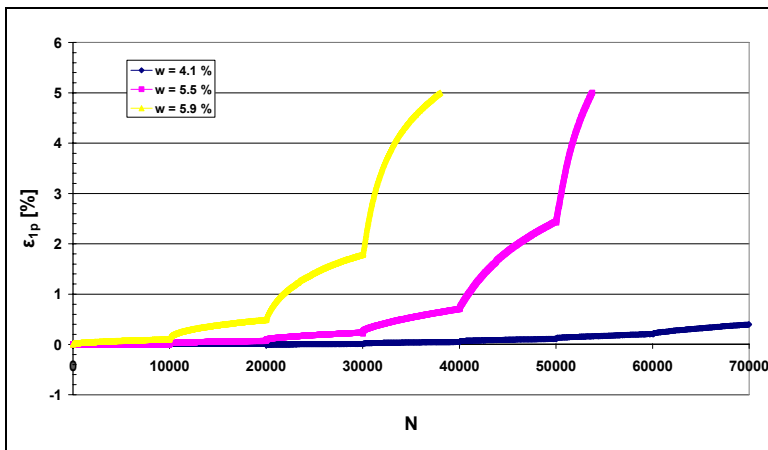
Figure 5 Cumulative permanent deformations Material 2.

Material 3.   In Figure 6a the dry density for the samples of Material 3 is presented together with the Modified Proctor curve. Here the samples have a lower dry density than for the Modified Proctor

compaction. This is expected to affect the results compared to the other two materials with higher dry density close to the Modified Proctor values for the materials.

Figure 6b shows the resilient response for the three samples. The samples with a water content of 4.0 % and 5.2 % show similar behaviour, while the sample with 6.0 % water shows a significantly lower resilient modulus for the same load application. The slight increase from 5.2 % to 6.0 % water gives a significant decrease in the resilient modulus.

Figure 6a. Modified Proctor and actual dry density and water content for Material 3
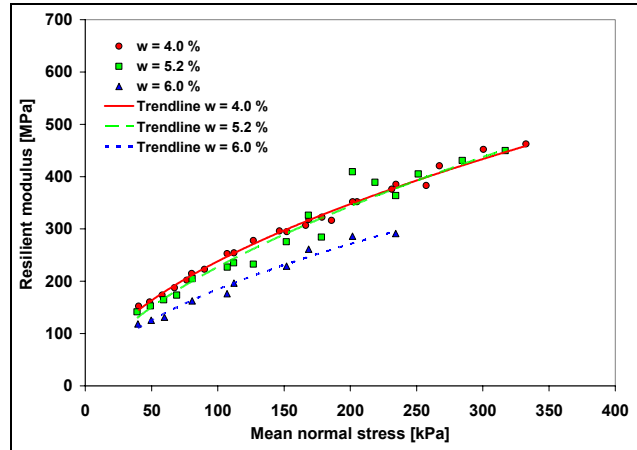
Figure 6b. Resilient Modulus vs mean normal stress for Material 3

The cumulative permanent axial strain for Material 3 at a confining stress of 150 kPa is shown in Figure 7. The sample with a water content of 6.0 % shows significant higher permanent deformations than the sample with a water content of 5.2 %. The samples with 5.2 % and 6.0 % water had pronounced higher permanent deformation rates than the sample with 4.0 % water, even though the resilient modulus for 4.0% and 5.2 % water were about the same.

Figure 7. Cumulative permanent deformations Material 3

The sample with a water content of 6.0 % shows a slower development of permanent deformations than the sample with a water content of 5.2 % in the early steps. At the third increase in axial load the sample develops high permanent deformations. The sample with 5.2 % water shows a little more stable behavior, but goes to large permanent axial strain during the fourth load increase.

Conclusions

It seems that a simple criteria for frost susceptibility, based only on gradation, gives some useful information for frost classification of materials. However, frost heave tests resulted in significantly different heave rates for almost equally graded materials.

The Austrian Mineral Criterion seems to add some aspects of importance. Several different methods were used to analyze the mineral content. The methods gave different results, but they all indicated a high content of so-called active minerals for Material 2 and 3. This was especially true for Material 3 which also showed the highest frost heave rate in the laboratory testing

All three materials studied were more or less water sensitive, as an increase in water content affected the resilient modulus function of the materials when subjected to the same stress level. Material 3 was the most water sensitive, as the permanent deformation increased dramatically after a relatively small increase of the water content, from 4.0 to 5.1 %. The resilient modulus was generally lower for Material 3 than for the other two materials, for a similar stress level. This behavior, may be influenced by the slightly lower level of compaction achieved for Material 3. All the materials tested showed higher resilient modulus for low water contents.

The susceptibility to water was also shown by the development of permanent axial strains, as an increase in water content caused a higher strain rate and an accelerated development of permanent deformations. For the materials tested the permanent deformation function was affected more by the water content than was the resilient modulus. This was especially true for Material 3. The slightly lower density for this material may however have influenced the results.

References

Aurstad, J and Hoff, I. (2005). ”Finstoffinnhold i resirkulert tilslag” (In norwegian). *Gjenbruksprosjektet rapport nr 15 (preliminary).* Statens Vegvesen.

ASI - Austrian Standards Institute (2001). "Gesteinskörnungen für ungebundene Tragschichten im Straßen- und Flugplatzbau - Beurteilung der Frostsicherheit" *Önorm B 4811.*

Casagrande, A. (1932). "A new theory of frost heaving: discussion". *Proceedings of US Highway Research Board. Vol. 11, Pt. I,. pp. 168–172.*

CEN – European Committee for Standardization (2000). "Unbound and hydraulically bound mixtures – part 7: Cyclic load triaxial tests for unbound mixtures". *prEN 13286-7.*

Chamberlain, E. J. (1981). "Frost susceptibility of soils – Review of index tests". *CRREL Monograph 81-2.* United States Army Corps of Engineers, Cold Regions Research and Engineering Laboratory, Hanover New Hampshire.

Hermansson, Å and Guthrie, S (2005), Frost Heave and Water Uptake Rates in Silty Soil Subject to Variable Water Table Height During Freezing. *Cold Regions Science and Technology* 43 (2005) 128-139.

Kaplar, C. W. (1974). " Freezing test for evaluating relative frost susceptibility of various soils". Technical Report 250. Cold Regions Research and Engineering Laboratory, Hanover, New Hampshire.

Konrad, J M. and Lemieux, N (2005). "Influence of fines on frost heave characteristics of a well-graded base-course material". *Canadian Geotechnical Journal*, Volume 42, Number 2, 1 April 2005, pp. 515-527(13)

Kugler, H., Ottner, F., Schwaighofer, B. and Strasser, W. (2005). "Frost suceptibility of Unbound Bases - An Improved Mineralogical Assessment". *Scientific note International Journal of Road Materials and Pavement Design.* 6/2005, 119-138.

Ladanyi, B and M. Shen (1989). "Mechanics of freezing and thawing in soils". *Proceedings for VTT symposium 94 Frost in Geotechnical Engineering,* Volume 1, Saariselkä, Finland.

Nordal, R. (1960). "Berelag for vegar" (In Norwegian). *Meddelelse nr 12.* Statens Vegvesen, Veglaboratoriet

Prestvik, T. (1992) " Mineralogi" (In Norwegian). Trondheim, Norway.

In Figure 11 the angles of the elastic and the plastic limits are functions of ρ and φ, respectively

The Equations 3 and 4 in the text should be corrected to:

Elastic limit: $\sigma_d = \dfrac{2sin\rho \cdot (\sigma_3 + a)}{(1 - sin\rho)}$ (Equation. 3)

Failure limit: $\sigma_d = \dfrac{2sin\varphi \cdot (\sigma_3 + a)}{(1 - sin\varphi)}$ (Equation. 4)

MATERIAL PROPERTIES OF UNBOUND GRANULAR AGGREGATES AND THE EFFECT ON THE DEFORMATION BEHAVIOUR

Lillian Uthus *
Research Fellow, Department of Civil and Transport Engineering, Norwegian University of Science and Technology, Norway.
* NTNU, Department of Civil and Transport Engineering, Høgskoleringen 7A, 7491 Trondheim, Norway.
Lillian.Uthus@ntnu.no

ABSTRACT: Material properties like grain size distribution, grain shape, mineralogy and mechanical strength are important for the deformation properties of unbound granular materials when subjected to cyclic loading. The properties of the fines, like specific surface area, mineralogy and grading, are also important for the material behaviour because of the interaction with water. Water plays an important role in the compaction of materials as a lubricant to achieve higher densities. The water content in a material may be expressed as the degree of saturation, which tells us how saturated the voids in the material are with water. Three materials were tested using a cyclic load triaxial apparatus to study the response of the materials to the cyclic loading. The materials had some differences in properties like grain shape, mechanical strength, mineralogy and properties of fines, and all three materials were sieved and recomposed into two different grain size distributions, one curve with grading coefficient n= 0.5 and one with grading coefficient n = 0.35. Two of the materials in the study were from the same quarry, one was taken from an early step in the production process, and the other was more refined by adding more steps to the crushing process.

KEY WORDS: Unbound granular aggregates, material properties, grading, triaxial testing, resilient modulus, permanent deformations.

1. INTRODUCTION

Material properties like grain shape, grain size, mineralogy and mechanical strength are important for the behaviour of unbound granular materials when subjected to traffic. All these properties act together, giving different response to loading for different materials. Other factors like stress level, presence of water and also density is known to have a significant effect on the behaviour of unbound granular materials.

Hicks and Monismith [1] concluded that the most important factors influencing the resilient modulus of unbound granular aggregates was the stress level, density, gradation, aggregate type and degree of saturation. Rada and Witczak [2] found when investigating different materials of gravel and crushed rock that the primary variables that influence the resilient response of granular materials were the stress state, degree of saturation and degree of compaction. This has been confirmed in later studies [3,4].

Grain size distribution and fines content is often used in requirements regarding water sensitivity and frost susceptibility. It seems like there is a limit for the amount of fines in a material, dependent on the overall grain size distribution, amount of fines, the grading of the fines and also the quality of the fines. Many researchers have reported a significant effect of the amount of fines on the deformation properties of a material. Barksdale and Itani [5] reported decrease in the resilient modulus of 60 % as the fines content increased from 0 to 10 %. They also observed that as the fines content increased, the amount of plastic strain also increased.

The grain shape is often optimized through the crushing process to make cubical aggregates. Cubical aggregates are believed to form more dense structures than flaky aggregates because of the more equidimensional grain shape. Flaky aggregates also tend to break more easily than the more cubical aggregates, mostly because aggregates that become flaky have a weaker structure in the first place.

2. OBJECTIVE

One objective with this study is to investigate the effect of water in combination with material properties like grain size distribution, mineralogy and fines content on the deformation properties of three unbound granular aggregates.

Another objective of this study is to investigate the deformation properties of two materials from one quarry to see the effect of making more cubical aggregates and compare these to a completely different material with different mineralogy and material strength. By composing the same grain size distributions with all three materials, and having information about the differences in grain shape, material strength and the quality of the fines it is possible to obtain reliable results on the effect of the grain shape.

3. MATERIALS AND MATERIAL PROPERTIES

3.1 Mineralogy
The mineralogy of a material is an important parameter influencing on the mechanical strength of the material, the grain shape and texture and also interaction with water. Uthus et al. [6] found that frost susceptibility and also water sensitivity of a material may be detected by looking at the mineralogy of the fines and the amount of fines when testing three different materials with the same maximum grain size and a grading coefficient of 0.35.

The same three materials were tested in this study, two materials from different steps in the crushing process from a quarry in Askøy in Norway with slightly different properties and one material from a quarry in Sweden. Mineralogical composition was found for the rock type by thin section analysis, and for the fines by x-ray diffraction (XRD) and scanning electron microscope (SEM). The XRD analyses were run on bulk samples by the method described in Mladeck [7], and the SEM analyses were run by the method described in Moen et al. [8].

Askøy cubical gneiss
The main minerals in this rock type are quartz (47 %) and feldspar (44 %) with some amount of the minerals amphibole (5 %) and titanite (2 %). The texture of the rock is fine grained, with a grain size between 0.2 and 1.5 mm.

In the fines the mineralogical distribution is different. Table 1 shows the mineralogy found by XRD analysis in material < 0.063 mm and material <0.020 mm. 14 % mica occurs in the fines < 0.063 mm, even if this mineral was not found in the thin section sample.

Table 1. Mineralogical distribution found by XRD for cubical gneiss from Askøy

Mineral	Mineral content in % of material < 0.063 mm	Mineral content in % of material < 0.020 mm
Quartz	12	27
Plagioclase	46	31
Alkali feldspar	24	31
Mica	14	6
Chlorite	1	2
Pyrite	T	T
Amphibole	3	2

T = Traces of the mineral

Askøy flaky gneiss
The flakier product from Askøy has a slightly different mineralogy, and has a distinct foliation. Here the main minerals found by thin section analysis are quartz (40 %) and feldspar (50 %), with a smaller amount of mica (8 %). The texture of the rock type varies from very fine grained to fine grained, about 0.2 to 1.0 mm.

The mineralogical composition of both the fines < 0.063 mm and < 0.020 mm found by XRD analysis is shown in Table 2, and it is slightly changed in the fines compared to the thin section. Especially the mica is accumulated in the fines, as 36 % of the material < 0.063 mm is mica and 17 % of material < 0.020 mm. Mica is a soft mineral and is easily crushed, so this may be the reason why the mica is accumulated in the fines.

Table 2. Mineralogical distribution found by XRD for flaky gneiss from Askøy

Mineral	Mineral content in material < 0.063 mm	Mineral content in material < 0.020 mm
Quartz	16	21
Plagioclase	23	37
Alkali feldspar	18	16
Mica	36	17
Chlorite	2	4
Pyrite	T	T
Amphibole	5	5

T = traces of the mineral

Swedish gneiss
The gneiss from a quarry outside Gothenberg in Sweden is a fine grained to medium grained gneiss. The main minerals are plagioclase (37 %), mica (33 %), both biotite and muscovite, and also a smaller amount of quartz (19 %) and epidote (9 %).

Table 3 shows the mineralogy of the fines found by both XRD and SEM analyses. Here the mica is slightly increased in material < 0.063 mm, but it is quite low in the material < 0.020 mm found by XRD. Because of this odd result the material was also investigated using a SEM. When analyzing the material < 0.020 mm by SEM the amount of mica is higher than found by the XRD. XRD is a more semi quantitative method for quantifying the mineralogy in the fines, so the result from the SEM is more correct.

Table 3. Mineralogical distribution found by XRD and SEM for gneiss from sweden

Mineral	Mineral content in material < 0.063 mm by XRD	Mineral content in material < 0.020 mm by XRD	Mineral content in material < 0.020 mm by SEM
Quartz	8	21	28
Plagioclase	34	53	27
Alkali feldspar	18	11	8
Mica	35	11	24
Chlorite	2	3	1
Epidote	3	T	3
Other			9

T = traces of the mineral

3.2 Grain size distribution

Fuller and Thompson [9] were the first to describe Equation 1 for concrete design. They found that a curve composed by Equation 1 with a grading coefficient of 0.5 would give maximum density for spherical particles.

$$P = \left(\frac{d}{D_{Max}}\right)^n$$

(Eq. 1)

where;
d = sieve size
P = percent smaller than d
D_{Max} = the maximum particle size
n = the grading coefficient

Crushed rock will of course deviate from the spheres when it comes to maximum density, because of the irregular shape. It is later found that maximum density for crushed rock is achieved at grading coefficients of about 0.45-0.5.
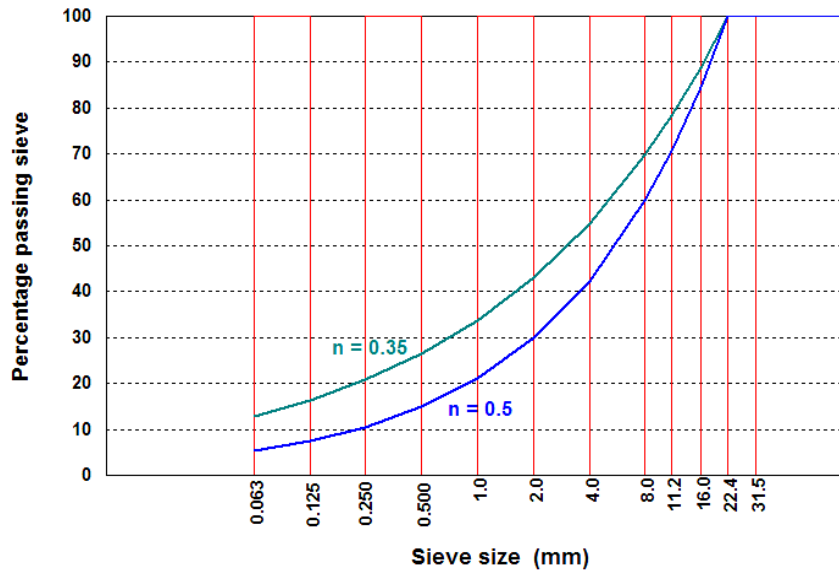
Figure 1. Grain size distribution 0/22 mm, n = 0.35 and n = 0.5

Here two grain size distributions for material 0/22 mm are chosen, where one is a well graded curve with grading coefficient - n of 0.5 (fuller curve) and the other one is a curve with grading coefficient 0.35, as shown in Figure 1. All three materials were sieved in small fractions and recomposed to these two grain size distributions.

Ekblad [10] tested one type of material in his study, with a gradation ranging from 0-90 mm, composed into four different curves with grading coefficients of n=0.8, 0.5, 0.4 and 0.3. Here the resilient modulus decreased with increasing water content from a drained state to a soaked state (close to 100 % saturation) for the grading coefficients of 0.5, 0.4 and 0.3. The largest decrease in modulus was seen for the gradings with n=0.4 and 0.3.

3.3 Grain shape

For characterization of grain shape of base materials the Flakiness Index (FI) (NS-EN 933-3) [11] is the most common test method. This is a simple test based on sieving and it gives an indication of the amount of flaky grains in the sample as a percentage of the total mass of the sample. For the materials in the study the total FI for the cubical material from Askøy was found to be 12, while the flakier product from Askøy had a FI of 28.

Page 4

The material from Sweden was also quite flaky and had a FI of 24. The Norwegian design guide 018 [12] requires a Flakiness Index of less than or equal to 30, which means that all three materials are within the requirements.

The sample is divided into different fractions based on selected sieve sizes and a Flakiness Index is also found for each fraction. In Figure 2 the FI for all fractions is presented.
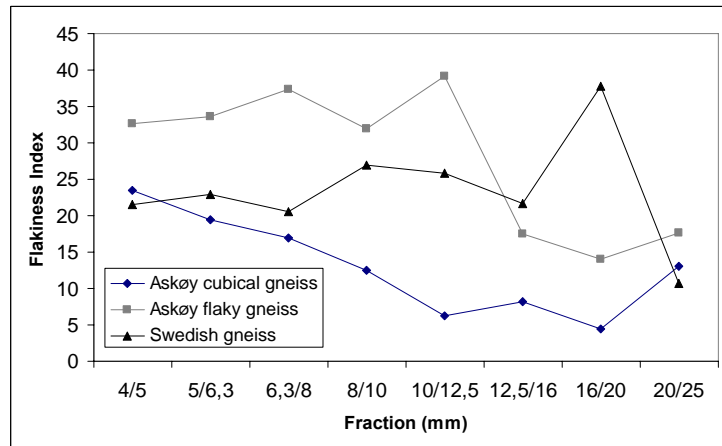
Figure 2. Flakiness Index for all fractions

3.4 Material strength
The cubic material from Askøy has a Los Angeles (LA) value (NS-EN 1097-2) [13] of 17, while the flaky material from Askøy has a LA value of 20. The Swedish material has a LA value of 24. In the Norwegian design guide 018 the requirements regarding the Los Angeles value for base materials are less than or equal to 35. This means that all three materials are within these requirements.

3.5 Properties of the fines
The grading of the fines is one of the most important properties of material < 0.063 mm. The grading of fines is normally found by hydrometer analysis, but in this case the grading is found by a method called Coulter analysis [14], which is a method that uses laser technology to measure grain size of fines. Figure 3 shows the grading of the fines for the three materials in percent by volume.
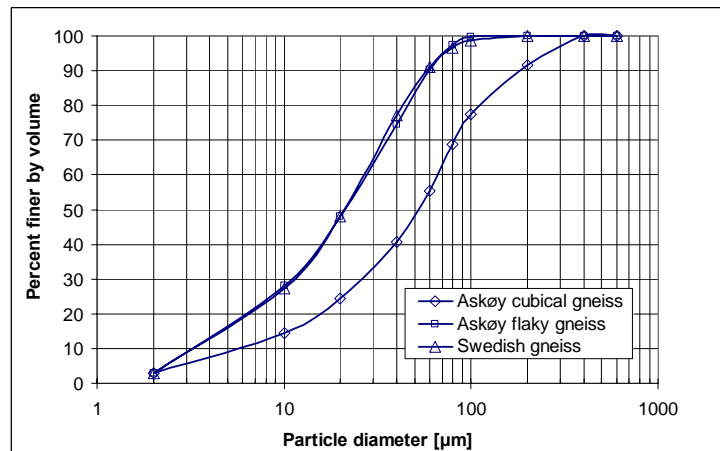
Figure 3. Grading of fines by COULTER LS 230

Page 5

The Coulter analysis is not recognized as a method for characterizing the grading of fines for use in pavements. Here the flaky gneiss from Askøy and the Swedish gneiss show almost equal grading for the fines fraction, while the cubic material from askøy has a slightly coarser grading.

Mineralogical composition of the fines is described earlier and this is strongly connected to the specific surface area, as different minerals have different shape and surface area. In this case the fines of the materials were found by BET analysis [15]. The cubic material from Askøy had a specific surface area of 1.58 m^2/g, while the flaky material from Askøy had a specific surface area of 4.88 m^2/g. This may be due to the higher mica content in the flaky material, as mica has a very high specific surface area. The Swedish gneiss had a specific surface area of 4.73 m^2/g.

4. CYCLIC LOAD TRIAXIAL TESTING

Cylindrical samples of the three materials with a diameter of 150 mm were compacted in 5 layers in a gyratory mould using a Kango vibrating hammer. To reduce the separation in the sample during mixing each of the five layers was composed with the amount of material required for one layer. The height of the samples varied from around 220 to 240 mm, which differs from the recommendations in the European EN-standard [16] where the height is recommended to be twice the diameter of the sample. Dongmo-Engeland [17] performed a study on the influence of sample height on permanent deformation behaviour of unbound aggregates. Here it was concluded that samples with a height/diameter ratio ranging from 1:1 to 1.5:1 showed little difference, with respect to resilient modulus and the resistance against permanent deformations.

The loading was applied according to the European standard EN-13286-7, multi stage loading procedure, high stress level [16]. The objective with this procedure is to determine stress limits to avoid the development of excessive permanent deformations. The procedure consists in applying different stress paths, with constant confining pressure, on the same specimen. Each deviatoric stress is applied for 10 000 load cycles. The loading is disrupted at 0.5 % permanent axial deformation for each load sequence of constant confining stress and increasing deviatoric stress.
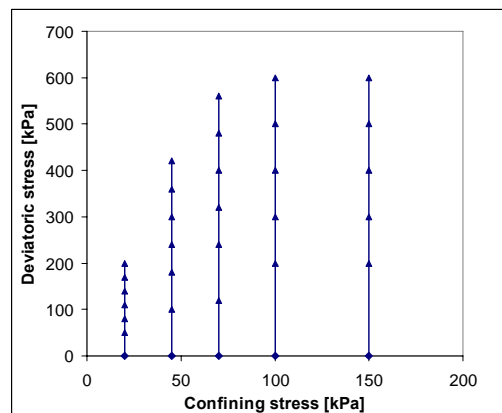
Figure 4. Loading procedure for the EN-13286-7 standard,
multistage loading

Figure 4 shows the procedure with the applied constant confining stresses and the increasing deviatoric stress per confining stress. All deviatoric stresses applied have amplitude that goes from 0 to the maximum value, as shown in the figure above. The sample is drained at the top.

5. RESULTS

5.1 Resilient modulus
The resilient modulus was found by the expression in Equation 2 as a mean value for each combination of confining stress and deviatoric stress.

$$M_R = \frac{\sigma_d^{dyn}}{\varepsilon_a^e}$$
(Eq. 2)

where,

M_R = resilient secant modulus;

σ_d^{dyn} = applied dynamic deviator stress;

ε_a^e = axial resilient strain.

In Figure 5 the resilient modulus as a function of mean stress, defined as $\sigma_m = 1/3(\sigma_d + 3\sigma_3)$, is shown for the cubical material from Askøy, n = 0.5. Here the degree of saturation S_r is presented for each sample. This factor is found as the ratio of the volume of water in the sample to the volume of voids in the sample. In this case the water content is found after compaction of the sample, so some loss of water by handling the sample has to be taken into consideration.

This means that the sample with the highest degree of saturation (~100 %) in reality probably have a slightly lower value. Degrees of saturation close to 100 % may cause problems with excess pore pressure, because the water cannot migrate from the pores fast enough as the sample is loaded with cyclic loading. The sample with $S_r = 31$ % shows slightly lower resilient modulus than the others for higher stress level, while the samples with 65 % and close to 100 % saturation show approximately the same moduli. All samples show very near the same resilient moduli for the lower stress level.

Figure 6 shows the resilient modulus as a function of mean stress for the flaky material from Askøy, n=0.5. Here the differences in strength between the single samples are not as large as for the cubical material, even though the two materials have very near the same variation in degree of saturation. All samples seem to give about the same modulus function. Also here the sample with lowest degree of saturation (37 %) is in the lower part of the envelope.

Figure 7 shows the resilient modulus as a function of mean stress for the Swedish gneiss, n=0.5. The highest degree of saturation is slightly lower for this material than for the other two. For the lowest stress levels the resilient modulus is equal for different degrees of saturation this material, but for higher stress levels the sample with $S_r = 75$ % shows a significantly lower resilient modulus.
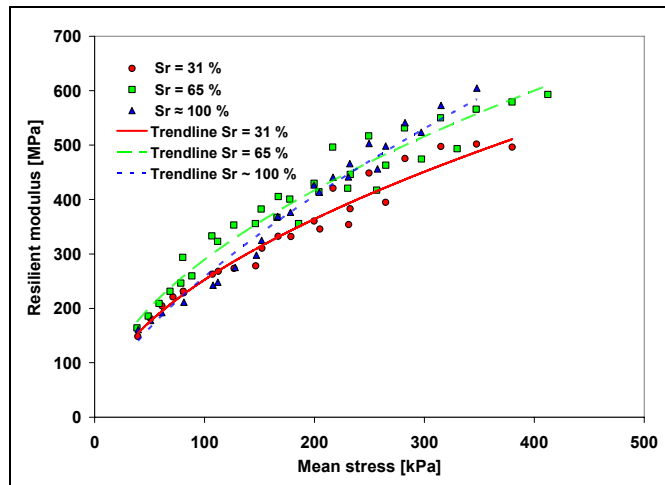
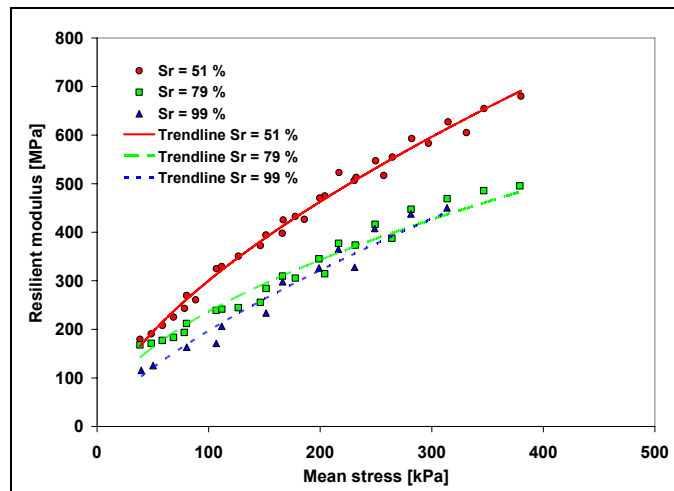Figure 5. Resilient modulus as a function of mean stress for cubical Askøy, n=0.5
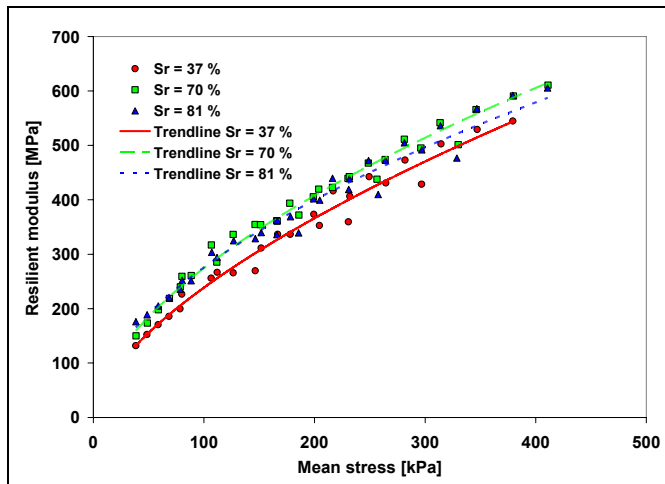
Figure 6. Resilient modulus as a function of mean stress for flaky Askøy, n=0.5
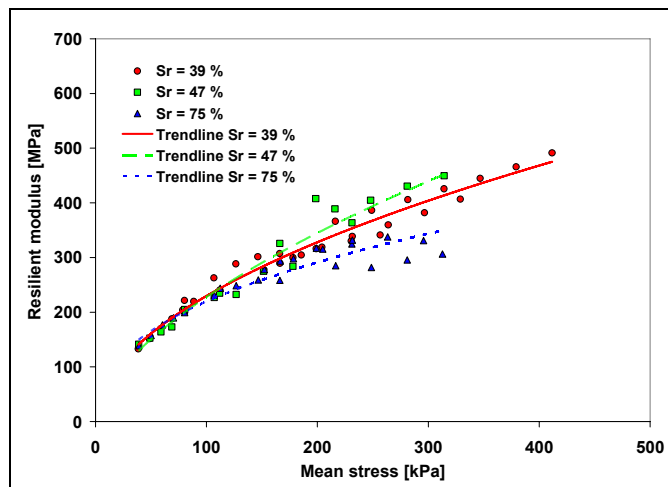
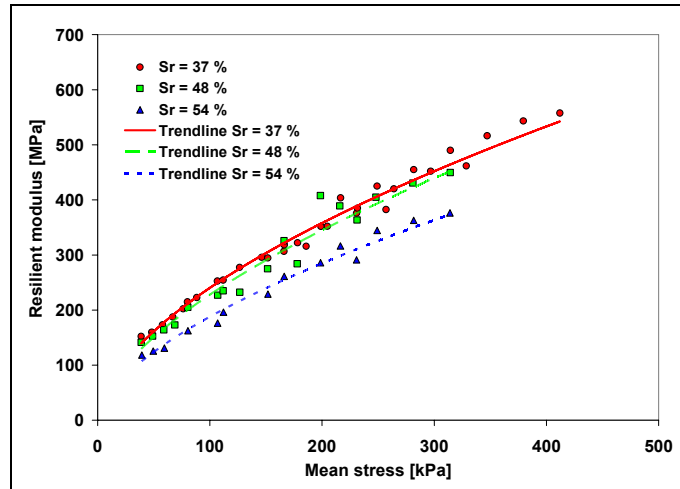Figure 7. Resilient modulus as a function of mean stress for Swedish gneiss, n=0.5

In Figure 8 the resilient modulus for the cubical gneiss from Askøy is presented, n = 0.35. In this case there is a tendency that the sample with the lowest degree of saturation (34 %) has the highest resilient modulus for all stress levels tested. The two samples with 88 % and 89 % saturation, which in reality is the same value, have significantly lower resilient modulus.

Figure 9 shows the resilient modulus as a function of mean stress for the flaky material from Askøy, n= 0.35. Here we see the same tendency; the sample with lowest degree of saturation has the highest resilient modulus. This is even more pronounced for high stress levels.
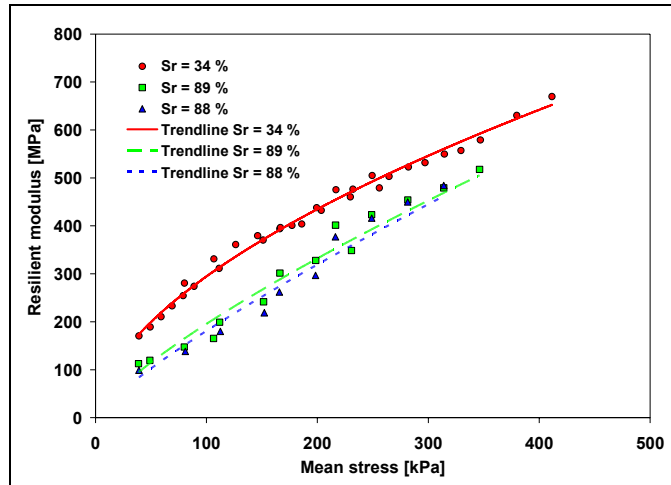
Figure 8. Resilient modulus as a function of mean stress for
cubical gneiss from Askøy, n=0.35

Figure 9. Resilient modulus as a function of mean stress for
flaky gneiss from Askøy, n=0.35

Figure 10. Resilient modulus as a function of mean stress for
gneiss from Sweden, n=0.35

In Figure 10 the results on the resilient modulus for the Swedish gneiss is presented, n = 0.35. Here the variation in degree of saturation is low, only from 37 % to 54 %. The samples with 37 % and 48 % saturation show close nearly coinciding resilient modulus for all stress levels tested, while the sample with S_r = 54 % show a significantly lower resilient modulus.

5.2 Permanent deformation behaviour
Each load step (combination of confining stress and deviatoric stress) may be categorized into three classes from the strain rate. This idea was originally developed by Hoff [18], who used the elastic and a plastic limit to classify the materials by their permanent deformation behaviour. Werkmeister [19] used the average strain rate from cycle 3000 to 5000 to range the deformation behaviour of materials into three ranges. Hoff et al. [20] used average strain rate $\dot{\varepsilon}$ for the last 5000 to 10000 cycles, and the range limits were modified according to the observed total strain / physical "failure" for the material tested. This method has been used in this study to range the behaviour into three different ranges;

Range - A:	$\dot{\varepsilon} < 2.5 \cdot 10^{-8}$	Elastic range
Range - B:	$2.5 \cdot 10^{-8} < \dot{\varepsilon} < 1.0 \cdot 10^{-7}$	Elasto-plastic range
Range - C:	$\dot{\varepsilon} > 1.0 \cdot 10^{-7}$	Plastic/failure range

When evaluating all load steps according to these three classes the steps being in the elastic range are marked by square symbol, the points being in elasto-plastic range are marked by triangles and the points in the failure range are marked by circles.

All load steps shown in a σ_3-σ_d plot and ranged by the three classes above may look like in Figure 11.
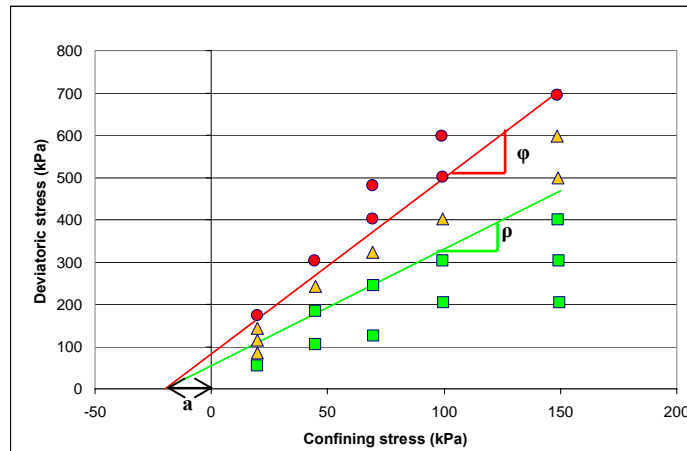
Figure 11. All load steps for one sample categorized into three categories (example)

The Coulomb criterion is used to find the stress envelope for the design stage and the failure stage, shown by the lower and the upper line respectively. The equations of these lines are:

Elastic limit: $\sigma_3 = \sin\rho(\sigma_1 - \sigma_3) + a$ (Eq. 3)

Failure limit: $\sigma_3 = \sin\varphi(\sigma_1 - \sigma_3) + a$ (Eq. 4)

Where σ_1 and σ_3 are principal stresses and ρ and φ are angles of the elastic and plastic limit lines.
The apparent attraction "a" was interpreted to be close to 20 kPa for all the samples. To ease the comparison between the samples a fixed value of a = 20 kPa was used for all samples. The result of this interpretation for each series may be shown by the sin ρ and sin φ values for each sample as an indication of the strength.

In Figure 12 the elastic and the plastic limit for the cubical material from Askøy, n=0.5, is presented in combination with the dry density for the samples. It seems like the sample with a degree of saturation of 65 % has the highest elastic and plastic limit, even though the sample which is close to fully saturated has a higher dry density. The sample with lowest degree of saturation has the lowest resistance to permanent deformations. This is probably caused by a significantly lower density.

In Figure 13 the results from the permanent deformation behaviour of the flaky material from Askøy, n=0.5, is presented. Here the sample with a degree of saturation of 70 % seems to have the highest resistance to permanent deformations, closely followed by the sample with 81 % saturation. The sample with the lowest degree of saturation shows the lowest elastic and plastic limits. It seems like the results are closely connected to the dry density also in this case, as the behaviour follows the dry density curve.

Figure 14 shows the elastic and plastic threshold limits for the gneiss from Sweden, n= 0.5. The sample with lowest saturation shows the highest resistance to permanent deformations in this case followed by the material with S_r = 75 %. In this case the resistance to permanent deformations also follows the dry density.
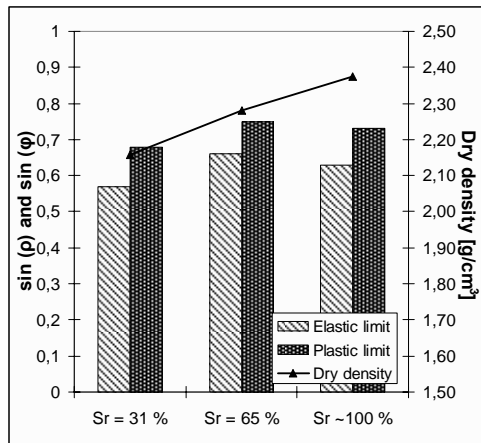
Figure 12. Elastic and plastic ("Failure") limits for Askøy cubic n= 0.5
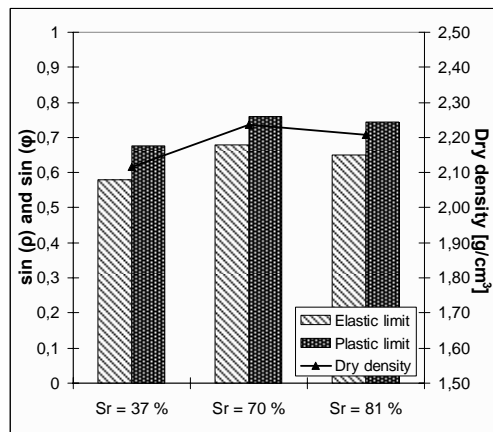
Figure 13. Elastic and plastic ("Failure") limits for Askøy flaky n= 0.5
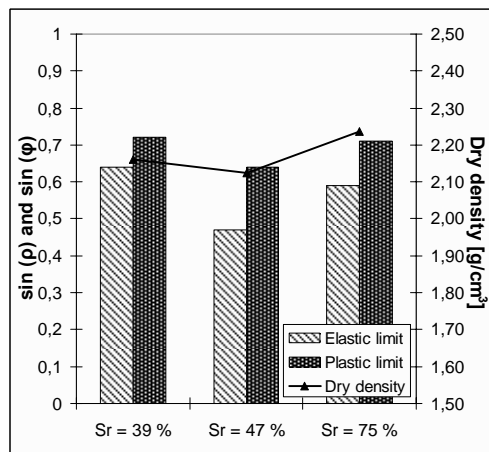
Figure 14. Elastic and plastic ("Failure") limits for Swedish gneiss n= 0.5

In Figure 15 the elastic and plastic limits for the cubical gneiss from Askøy, n= 0.35, is presented. The sample with the lowest degree of saturation shows significantly higher resistance to permanent deformations than the two samples with close to equal saturation of 88 and 89 %. It seems like the degree of saturation overrides the effect of lower dry density for the sample with the lowest saturation (39 %).

In Figure 16 we can see the same tendency for the flaky material, as the samples with lowest degree of saturation has the highest elastic and plastic limit. The elastic and plastic limits seem to decrease with the degree of saturation. Here the dry density is very near the same for all three samples.
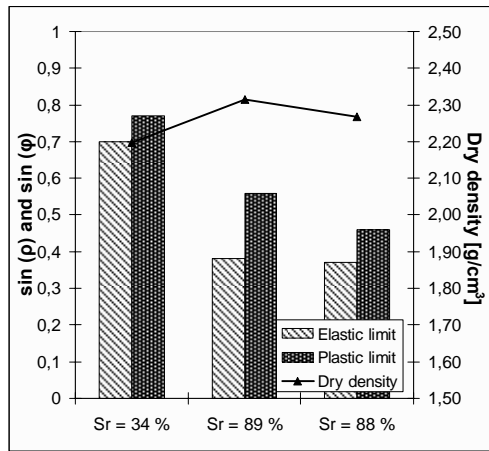
Figure 15. Elastic and plastic ("Failure") limits for cubical gneiss Askøy n= 0.35
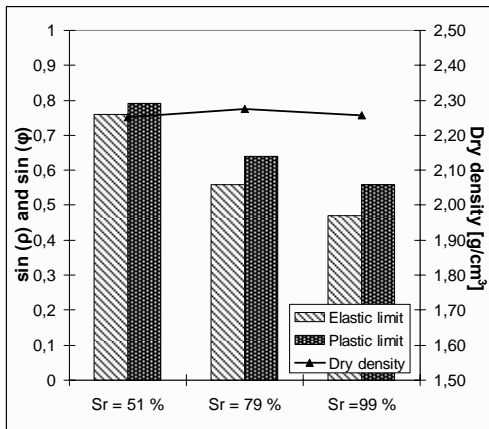
Figure 16. Elastic and plastic ("Failure") limits for flaky gneiss Askøy n= 0.35

Figure 17 shows the results from the Swedish gneiss, n = 0.35. Here the variation in degree of saturation is relatively low, only from 37 % to 54 %, but still we can observe the same effect of water content as for the other two materials. The sample with lowest degree of saturation shows a significantly higher resistance to permanent deformations than the other two samples. There is also a small decrease in elastic and plastic limit for the friction angle (ρ, φ) from S_r=48 to 54 %. The dry density in this case is the same for all three samples.
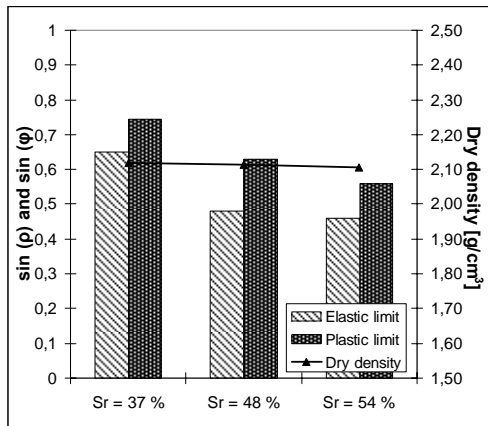
Figure 17. Elastic and plastic ("Failure") limits for Swedish gneiss n= 0.35

5.3 Comparison of samples with similar degree of saturation

To see the effect of the grading and the material we wanted to look at samples from the three materials and the two gradings that had comparable degrees of saturation, both for the resilient and the permanent deformation behaviour.

In Figure 18 the resilient modulus is shown as a function of the mean stress for all three materials with grading coefficient of n= 0.5. Here the saturation has some variation (from 65 to 75 %), but a tendency may be seen between the materials. The resilient modulus for both materials from Askøy show very near the same dependency of mean stress in the whole stress range. The material from Sweden shows a significantly lower resilient modulus for high stress levels. This is most probably caused by the different mineralogy and mechanical strength of the material.
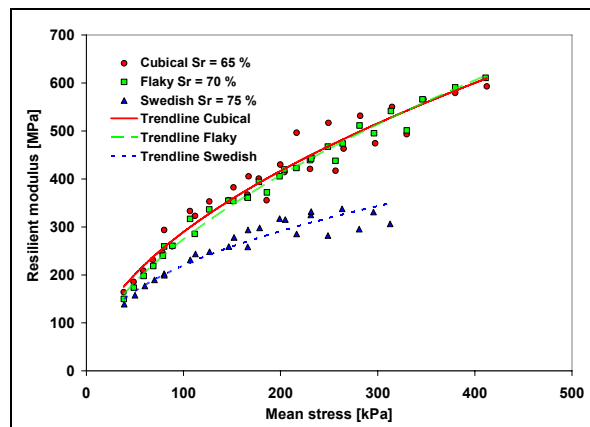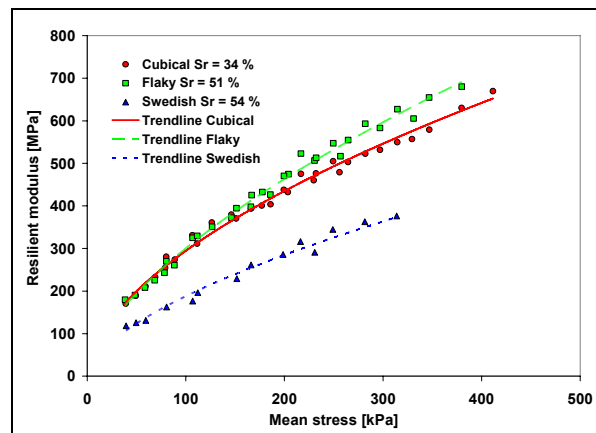

Figure 18. Resilient modulus as a function of mean stress for
all three materials, n=0.5, with comparable degrees of saturation

In Figure 19 the permanent deformation behaviour for the same samples is presented together with the dry density. The samples from Askøy have near the same resistance to permanent deformations. The material from Sweden has the lowest resistance to permanent deformations, even though the material has the same dry density as the samples from Askøy. The slightly higher degree of saturation may contribute to this but the main cause is most probable the mineralogy and mechanical strength of the material.
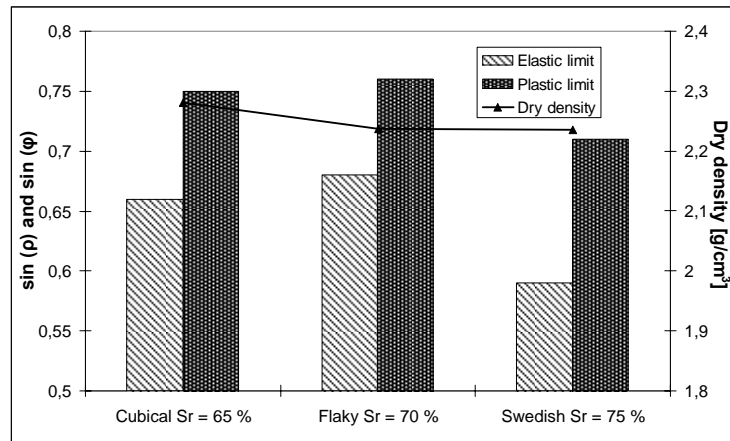
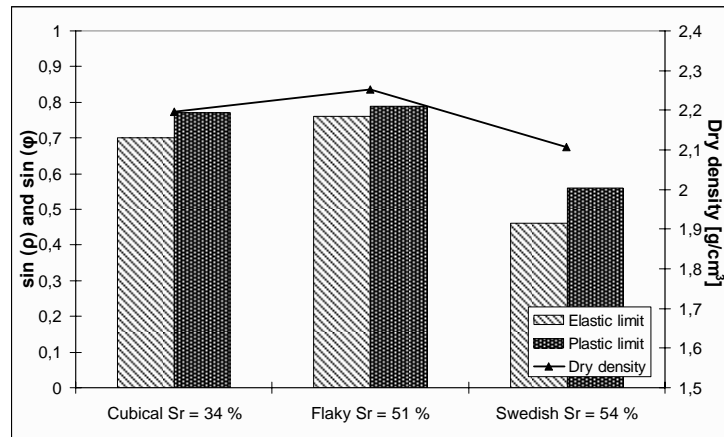Figure 19. Elastic and plastic/"failure" limit for
all three materials, n=0.5, with comparable degrees of saturation

Figure 20 shows the resilient modulus for samples of the three materials with comparable degree of saturation. Here there is some variation in the degree of saturation, but for the material from Askøy the degree of saturation does not have any big impact. The Swedish material seems lo have significantly lower resilient modulus for all stress levels, even if the degree of saturation of this sample is comparable at least with the sample with flaky material from Askøy.

Figure 20. Resilient modulus as a function of mean stress for
all three materials, n=0.35, with comparable degrees of saturation

In Figure 21 the permanent deformation behaviour for the same samples is presented. The defined friction angle, based on the criterion for permanent deformations explained earlier, clearly follows the dry density of the samples. For the flaky and the cubical samples from Askøy the degree of saturation are 51 and 34 % respectively. The flaky sample has a higher degree of saturation and a higher dry density and is stronger than the cubical sample in this case. The dry density seems to have a higher influence on the behaviour than the degree of saturation, it is however hard to tell what the effect of the particle shape is for these samples. The flaky sample and the Swedish sample have close to equal degrees of saturation, but the flaky sample has a higher dry density and a higher friction angle.

Figure 21. Elastic and plastic/"failure" limit for
all three materials, n=0.35, with comparable degrees of saturation

6. DISCUSSION

6.1 Effect of grading
The first factor to discuss is the influence of grain size distribution on the deformation properties. All three materials were composed with the same two gradings. The main difference between the two gradings is the amount of fines. When investigating the different materials and the two different gradings by running cyclic load triaxial testing on samples with different water contents, it seems like the grain size distribution with grading coefficient of 0.5 results in lower sensitivity to water than the grain size distrinution with grading coefficient of 0.35. This behaviour is distinct both for the resilient modulus and the permanent deformation behaviour. This confirms the findings of Ekblad [10], who concluded that the sensitivity to water on resilient behaviour increases with a decreasing grading coefficient from n=0.5 to n= 0.3.

6.2 Effect of properties of the fines
The grain size distribution of the fines is found by Coulter analysis. It seems like the grain shape of the fines has a significant influence on the grading of the fines, as the cubical material seems to be coarser and also has a lower specific surface area than the other two materials. This may be caused by the grain shape and the method of finding the grading of the fines, as all three materials were sieved through the 0.063 mm sieve. The grain shape of the particles in the fines will most likely influence the grading dependent on the method used.

6.3 Effect of density
It seems like the dry density is a key parameter for the materials with grading coefficient of 0.5, as the behaviour of the materials follows the dry density of the samples. The density seem to override the effect of the degree of saturation for the gradation with n=0.35.

6.4 Effect of mineralogy
The mineralogy is also a key parameter as the gneiss from Sweden shows a significantly lower resilient modulus and lower resistance to permanent deformations than the other two materials for similar grading, dry density and degree of saturation. Mica is a very soft and mechanically weak material, known to interact with water. In the Swedish material 33 % mica was found by the thin section analysis, which seems to have an effect on the strength of the material. But as the mineralogy in each grain particle might vary considerably, this is hard to say from just one thin section analysis.

6.5 Effect of grain shape
When looking at the two materials from Askøy it seems like the effect of grain shape is negligible. Actually the flaky material is stronger in some of the cases and not as sensitive to water as the cubical material.

Page 16

7. CONCLUSIONS

The grain size distribution seems to be important for the sensitivity to water, as a grain size distribution with grading coefficient n=0.5 is less sensitive to water than a grain size distribution with n=0.35, this is mainly linked to the associated content of fines.

Density is more important for materials with high content of fines, as the behaviour of the material with n=0.35 is strongly dependent on the density for similar degrees of saturation.

Mineralogy may be the determining factor for the deformation behaviour of a material. Mica is a mineral that may reduce the stiffness and strength of a material, and in this case the material from Sweden is highly influenced by the mica.

Making more cubical grains by for instance refining the crushing process may not improve the deformation properties of a material. In this case, the flaky material shows similar or even higher strength when subjected to the same loading as the cubical material.

REFERENCES:

[1] Hicks, R.G and Monismith, C.L. Factors Influencing the Resilient Response of Granular Materials. *Paper Highway Research Record 345*, Highway Research Board, Washington DC, USA, 1971, pp 15-31.
[2] Rada, G. and Witczak, M. W. Comprehensive Evaluation of Laboratory Resilient Moduli Results for Granular Materials. *Paper Transportation Research Record 810*, Transportation Research Board, Washington DC, USA, 1981, pp 23-33.
[3] Kolisoja, P. Large Scale Dynamic Triaxial Test with Coarse Grained Aggregates. *Paper, Proceedings of the 4th International Conference on the Bearing Capacity of Roads and Airfields*, Minneapolis, Minnesota, USA, 1994, pp 883-898.
[4] Kolisoja, P. Resilient Deformation Characteristics of Granular Materials. *Publication 223.* Thesis, Tampere University of Technology, Tampere, Finland, 1997.
[5] Barksdale, R, and S. Itani. Influence of Aggregate shape on Base Behaviour, *Paper Transportation Research Record 1227,* Transportation Research Board, National Research Council, Washington DC, USA, 1989, pp 173-182.
[6] Uthus, L., Hermansson, Å., Horvli, I. and Hoff, I. A study on the influence of water and fines on the deformation properties and frost heave of unbound aggregates. *Paper, Proceedings of the 13th Intl. Conference on Cold Regions Engineering*, Orono, Maine, 2006. (CD-ROM)
[7] Mladeck, M.H. Mineralidentifikasjon ved røntgenmetoder (In Norwegian). Universitetsforlaget, Oslo, Norway, 1976.
[8] Moen, K., Malvik, T., Breivik, T. and Hjelen, J. Particle Texture Analysis in Process Mineralogy. Paper, Proceedings for the XXIII International Mineral Processing Congress, Istanbul, Turkey, 2006.
[9] Fuller, W and Thompson, S. E. The laws of proportioning concrete. *Paper no 1053, Transactions of the American Society of Civil Engineers,* 1907. pp 67-143.

[10] Ekblad, J. Infuence of Water on Resilient Properties of Coarse Granular Materials. *TRITA-VT FR 04:03*, Licentiate Thesis Kungliga Tekniska Högskolan (KTH), Stockholm, 2004.

[11] Standard Norge. Prøvingsmetoder for geometriske egenskaper for tilslag Del 3: Bestemmelse av kornform Flisighetsindeks (Flakiness Index) (In Norwegian). *NS-EN 933-3*. 1997.

[12] Statens vegvesen. Håndbok 018 Vegbygging (In Norwegian). Oslo, Norway. 2005.

[13] Standard Norge. Prøvingsmetoder for mekaniske og fysiske egenskaper for tilslag Del 2: Metoder for bestemmelse av motstand mot knusing. (Los Angeles method) (In Norwegian). *NS-EN 1097-2*. 1998.

[14] Coulter Corporation. Product Manual for Coulter LS 2300. Miami, Florida, USA, 1994.

[15] DIN - Deutches Institut für Normung. Bestimmung der spezifiscen Oberfläche von Feststoffen durch Gasadsporption nach Brunauer, Emmet und Teller (BET). *DIN 66131,* Germany. 1993.

[16] CEN - European Commite for Standardization. Unbound and hydraulically bound mixtures – part 7: Cyclic load triaxial tests for unbound mixtures. *EN 13286-7*. Brussels, 2000.

[17] Dongmo-Engeland, B. GARAP Influence of sample´s height on the development of permanent deformations. *STF50 A05075*. SINTEF Technology and Society, Road and Railway Engineering, Trondheim, 2005.

[18] Hoff, I. Material Properties of Unbound Aggregates for Pavement Structures. *IVJ-Medd. 28.* Thesis, Norwegian University of Science and Technology (NTNU), Trondheim, Norway, 1999.

[19] Werkmeister, S. Permanent Deformation Behavior of Unbound Granular Materials in Pavement Constructions. *Thesis*, Technischen Universität Dresden, Dresden,2003.

[20] Hoff, I., Bakløkk, L. and Aurstad, J. Influence of Laboratory Compaction Method on Unbound Granular Materials. *Paper, Proceedings for the 6th International Symposium on Pavements Unbound (UNBAR 6)* (CD-ROM), University of Nottingham, UK, 2003.

In Figure 13 the angles of the elastic and the plastic limits are functions of ρ and φ, respectively

The Equations 1 and 2 in the text should be corrected to:

Elastic limit: $\sigma_d = \dfrac{2sin\rho \cdot (\sigma_3 + a)}{(1 - sin\rho)}$ (Equation. 1)

Failure limit: $\sigma_d = \dfrac{2sin\varphi \cdot (\sigma_3 + a)}{(1 - sin\varphi)}$ (Equation. 2)

EFFECT OF GRADING AND MOISTURE ON THE DEFORMATION PROPERTIES OF UNBOUND GRANULAR AGGREGATES

By
Lillian Uthus
Department of Civil and Transportation Engineering,
Norwegian University of Science and Technology (NTNU)
Høgskoleringen 7A, 7491 Trondheim, Norway
+4773595000
Fax: +4773591478

ABSTRACT
It is found that the sensitivity to water of an unbound granular base material is not only dependent on the grading and the fines content, but also on factors like mineralogy, specific surface area of fines, grain shape. These factors may in some cases cancel out the effect of grading. In the design guidelines in many countries the sensitivity to water of unbound materials is indirectly accounted for by requirements regarding gradation and limitations on the amount of material less than 0.063 mm or 0.020 mm. These requirements are based on the assumption that the gradation is the main parameter deciding the pore size distribution in the material, and thereby also the permeability and the ability to keep water inside the material. Many test methods have been developed over the years to test unbound materials for water sensitivity, one of the recent methods is the Tube Suction test. This test uses the dielectric properties to measure the ability of the material to suck water. Cyclic load triaxial testing is used for characterization of the deformation properties of the different gradings. By adding different amount of water to samples with the same grading, the sensitivity to changes in degree of saturation is seen.

Key words: Unbound granular aggregates, grading, water sensitivity, triaxial testing

INTRODUCTION

Water is needed in unbound materials during compaction to achieve high levels of compaction. In this case the water acts as a lubricant between the grains, allowing them to slide into the most effective packing when using proper compaction equipment.

During springtime the materials in the road are often subjected to extreme environmental conditions, and water may be trapped in the base course and sub base layer. The melting starts mainly at the surface but also from the subgrade, leaving a frozen layer that acts as an almost impermeable layer somewhere in the structure. Water from the melting and even water from the sides and through the asphalt may thus be trapped in the unbound material, dependent on the permeability of the material and the drainage conditions of the road structure. The effective stresses in the structure are reduced and an excess pore water pressure may occur.

In many countries the sensitivity to water is indirectly accounted for in the design guidelines by requirements regarding gradation and limitations on the amount of material smaller than 0.063 mm or 0.020 mm. These requirements are based on the assumption that the

gradation is the main parameter deciding the pore size distribution in the material, and thereby also the permeability and the ability to keep water inside the material.

The objective of this study is to test one material composed into four different grain size distributions to study the effect of the grading on the water sensitivity of a material both by the Tube Suction test and by cyclic load triaxial testing of the material at different degrees of saturation.

WATER SENSITIVITY IN UNBOUND GRANULAR AGGREGATES

It is found that the sensitivity to water is dependent on more than gradation and fines content. Parameters as mineralogy, specific surface area of fines, grain shape may in some cases cancel out the effect of gradation or amount of fines *(1)*.

Christine Hauck *(2)* studied the water sensitivity of gravel in her Cand. Scient thesis at the University in Oslo by studying parameters like grading, fines content, mineralogy, plasticity and grain shape and by using CBR as a measure of the strength of the material.

The conclusions from this work was that the water sensitivity of a material should better be classified by the amount of material passing the 0.075 mm sieve, and the study showed that the amount of material < 0.020 could vary in the range 50-90 % of the total material smaller than 0.075 mm without affecting the stability dependent on the material type. It was also concluded that aggregate from schist and limestone and fines with high plasticity index should be avoided. This is because of possibly reduced internal friction and thereby an increasing possibility of pore pressure development. This study was the basis of the requirements in the Norwegian specifications today, which requires 8 % or less material passing the 0.063 mm sieve of material smaller than 20 mm *(3)*.

The ability of a material to suck water may be a measure of the water sensitivity. The Tube Suction test was developed by the Finnish National Road Administration and the Texas Transportation Institute *(4)* to determine the moisture susceptibility of an unbound material. This is a relatively new test that classifies the materials by the measured dielectric value after 10 days of water suction.

The dielectric value of a sample with three phases of materials; aggregates, water and air, depends on the volumetric distribution of these three different phases and the dielectric constant of each of them. Saarenketo and Scullion *(3)* listed typical dielectric value for several materials, where air has a dielectric value of 1, dry aggregates has a value of 4 to 6, and free water has a dielectric value of 81. The dielectric value of tightly bound water is about 3 or 4 *(4)*. As the free water has a very high dielectric value compared to the other constituents of an aggregate sample, the total dielectric value measured on the top of a cylindrical sample is very sensitive to free water, which is measured in the mix after 10 days of suction.

MATERIAL PROPERTIES

One material was used in this study, and only the grain size distribution was varied. The material was gneiss from a quarry in Askøy outside Bergen in Norway. This is a fine-grained rock where the main minerals determined by thin section analysis are quartz (47 %) and feldspar (44 %) with some amount of the minerals amphibole (5 %) and titanite (2 %). In the fines > 0.020 mm the main minerals found by X-ray diffraction (XRD) are plagioclase (31 %), alkali feldspar (31 %) and quartz (27 %) with some amount of mica (8 %) chlorite (2 %) and amphibole (2 %).

The gradation curves were determined from the following relationship.

$$P = \left(\frac{d}{D_{Max}} \right)^n$$

(Eq. 1)

where;
d = sieve size
P = percent smaller than d
D_{Max} = the maximum particle size
n = the grading coefficient

Equation 1 was originally presented by Fuller and Thompson (6) for design of dense concrete mixes.

In Figure 1 the three main grain size distributions are presented together with a fourth grading only used in the Tube Suction test, as a more extreme grading. The curves marked with n= 0.35 and n=0.5 are both 0/22 mm material with two different grading coefficients normally used as unbound road materials. The grading coefficient n=0.25 represents a material with far too high fines content according to the Norwegian specifications. The grain size distribution denoted PPP is the upper limit curve of a grading used in a Public Private Partnership project (PPP) in the southern part in Norway, 0/32 mm.
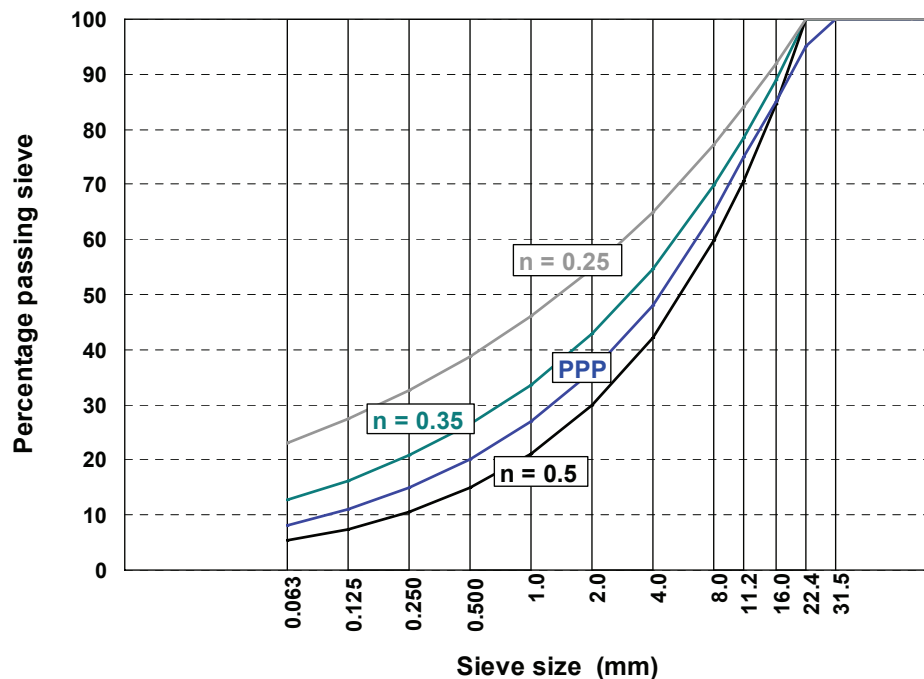
FIGURE 1. Grain size distributions of the material used in the study

In the Norwegian guidelines the requirements for non-water susceptible soils are defined by the amount of material smaller than 0.063 mm for unbound base materials. For crushed rock the maximum amount of fines ≤ 0.063 mm is 8 % within the material smaller than 20 mm. This means that the two lower curves are within the limits, while the two upper curves are above the limit given in the Norwegian requirements.

TEST METHODS

Tube Suction test

The procedure has been under constant development, and there is still no standard method. In this study the procedure described by Guthrie et al. *(5)* was used, with some modifications.

A cylinder with an inner diameter of 149 mm and a height of 304.8 mm was used; in Guthrie et al. *(5)* the diameter of the cylinder was 152.4 mm. About 6 mm from the bottom of the cylinder holes with diameter 3 mm were drilled around the circumference for water intake. The spacing between the holes was 12.7 mm and 4 additional holes were drilled in the bottom of the cylinder. Guthrie et al. *(5)* described holes with 1.6 mm diameter, but these would probably easily clog. The samples were compacted in the cylinder in four layers to a final height of 200 mm by using a Modified Proctor hammer with 50 strokes per layer with a weight of 4.5 kg dropped from a height of 457 mm. The compacted samples were dried in an oven for four days in 40°C (45°C until constant mass). Then they were placed in water bath with distilled water reaching 12.7 mm over the bottom of the sample for 10 days. This setup is shown in Figure 2.

FIGURE 2. Sample setup during ten days of water absorption

FIGURE 3. Adek Percometer^{TM} and the surface probe used in this study

The measurements in the Tube Suction test are based on measuring the dielectric properties of the material. This value is defined as the ratio of the materials dielectric permittivity to the dielectric permittivity of free space. This gives a measure of the amount of free water in the sample. Measurements of the dielectric value and electrical conductivity were done during 10

days on the top surface of the samples. The equipment used is a Percometer^{TM} with a surface measurement probe as shown in Figure 3. This equipment measures 25 mm into the material according to the instrument specifications. 18 measurements were done for each sample each time, where the three lowest and the three highest readings were discarded to reduce the variability caused by surface imperfections.

Three different gradings were used throughout this study, but none of them were extreme gradings, therefore another grading was added as a control to represent a more extreme grading, expected to be water susceptible. This was a grading with n=0.25, giving about 23 % material smaller than 0.063 mm. Only one sample was made for each grading.

The maximum aggregate size should not exceed 25 mm, because of the size of the cylinder. One of the gradings in this study is a 0/32 mm, the PPP curve. Saarenketo and Scullion *(4)* suggested removing the larger aggregate grains, but in this case this was not done. To make a smoother surface of the compacted samples some finer material (1/2 mm) of the same material was added on the top of each sample as shown in Figure 4.
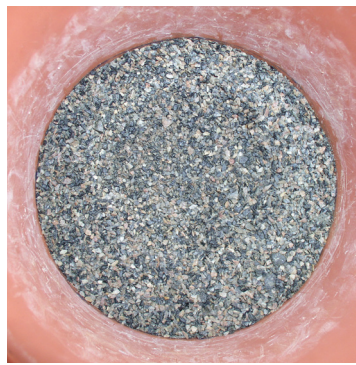
FIGURE 4. The top of a sample with material 1-2 mm on the surface

Guthrie et al. *(8)* suggested a classification for water sensitivity of materials by their mean dielectric value after 10 days of water absorption. This is presented in Table 1.

TABLE 1. Classification of materials by dielectric value

Dielectric Value	Classification
<10	Good
10-16	Marginal
>16	Poor

Cyclic load triaxial testing
The deformation properties of the materials were found by cyclic load triaxial testing of cylindrical samples. The European standard EN-13286-7 *(8)* for triaxial testing of unbound mixtures offers a procedure called multistage loading for investigation of permanent deformations. In this procedure loading is run in five sequences of constant confining stresses (20, 45, 70, 100 and 150 kPa) with increasing deviatoric stress within each confining stress level. The principles of the loading procedure are shown by the stress paths in Figure 5 for "high stress levels". Loading is applied at a frequency of 10 hertz with 10 000 cycles per deviatoric stress level and interrupted when the permanent axial strain reaches 0.5 %. By interrupting the axial loading at this permanent strain level, the sample is still relatively far from its ultimate stress level/failure limit. Thus the next load sequence may be applied to the

material while still being within a design stress level. The triaxial chamber is filled with water as a confining medium.

The samples were saturated by adding water from the bottom and letting the sample drain at the top. Water was added to the sample at a pressure of 20-25 kPa, under a confining stress of 20 kPa. Air was used as a confining medium in the triaxial chamber during saturation. The saturation process was stopped when the amount of water out from the top of the specimen was equal to the water added from the bottom. The sample was then left to equalize for about 12 hours under drained conditions. The setup for the triaxial sample is shown in principle in Figure 6. Strain was measured with three radial and three axial LVDTs (Linear Variable Displacement Transducers).
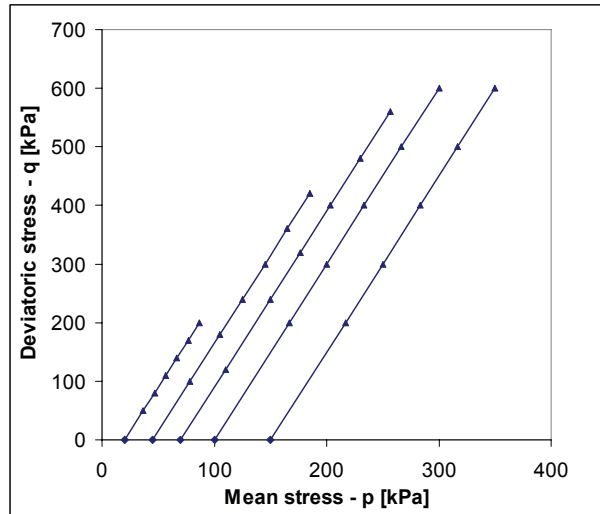
FIGURE 5. Loading procedure from the CEN procedure *(9)*
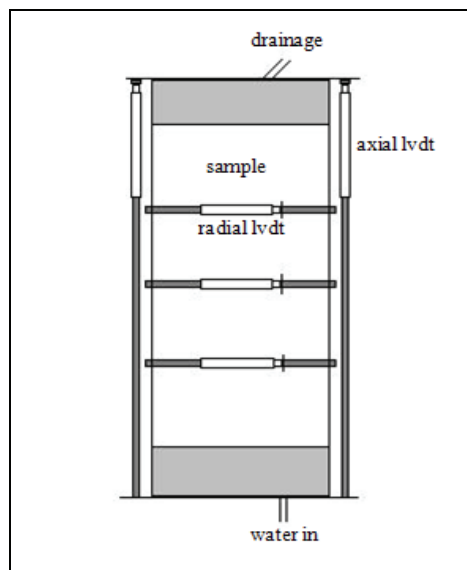
FIGURE 6. Principles of the triaxial setup

RESULTS

Tube Suction test

The results from the measurements of dielectric values on the surface of the sample over a period of 10 days are presented in Figure 7. Here the results seem to be lowest for the grading with the lowest fines content, n=0.5, and highest for the grading with highest fines content, n=0.25. The PPP grading and the grading with n=0.35 both show very stable and low dielectric value for the last measurements. The grading with n=0.35 also have quite stable values, but for the last measurement it seems to decrease slightly. This is probably random, as the dielectric value seems to fluctuate slightly. The curve with grading coefficient of n=0.25 show higher values than the other gradings. The last three readings show an increasing trend, and the last reading is 9.91. This sample should probably have been measured for a few more days to see at what point the dielectric value stabilizes. The last reading for this grading is very near the threshold value of 10 defined for moisture susceptible materials.
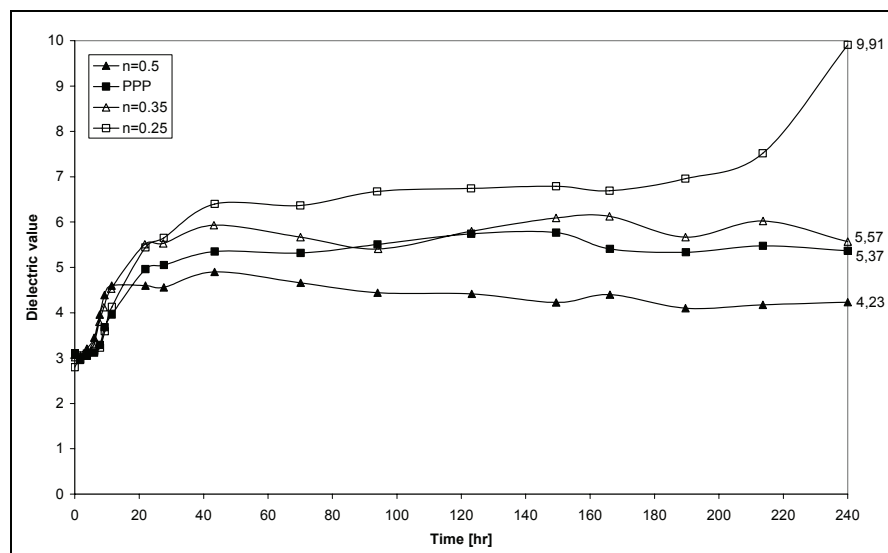
FIGURE 7. Dielectric value as a function of time for the samples

Figure 8 presents the water uptake as a function of time for the samples tested. This shows a distinct difference between the four gradings, showing that the ability of a material to suck water is dependent on the grading and the content of fines. In Table 2 several properties for the samples tested are presented. As can be observed the degree of saturation increases with decreasing grading coefficient. The PPP grading seems to give a slightly lower degree of saturation compared to the grading with n=0.5. When it comes to the dry density of the samples this seems to increase with increasing fines content except for the grading with n=0.25, which shows a small decrease in dry density compared to the grading with n=0.35. However, the increase in water uptake is less than indicated from the last reading of the dielectric value in Figure 7. It is hard to give a good explanation of this.
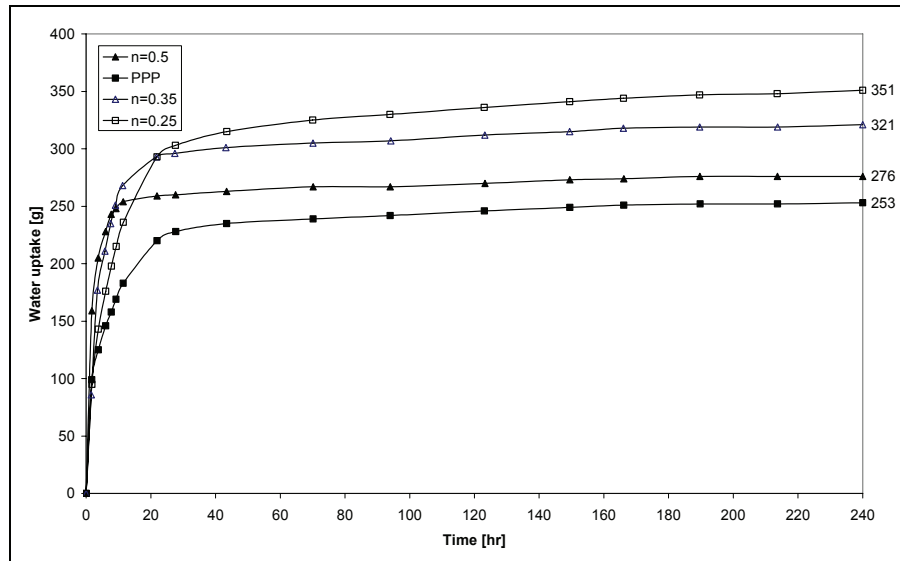
FIGURE 8. Water uptake as a function of time

TABLE 2. Properties of the samples tested

Gradation	n = 0.5	PPP	n = 0.35	n = 0.25
Dielectric mean value	4.23	5.37	5.57	9.91
Standard deviation	0.82	0.16	0.42	0.64
Absorbed water (g)	253	276	321	351
Dry density (g/cm^3)	2.19	2.25	2.28	2.27
Degree of saturation (%)	40.1	39.9	58.6	59.9

Table 2 presents the properties of the different samples found after 10 days of water suction. The standard deviation for the dielectric measurements for the PPP sample is significantly lower than for the other series. The sample with the highest amount of fines (n=0.25) achieved the highest degree of saturation as expected.

In Figure 9 the water contents measured in four levels of the samples are shown; layer number 1 is the bottom of the sample and layer number 4 is the top of the sample. The highest water content, in general, is found in the samples with n=0.25 and n=0.35. All samples have relatively small changes in water content from the bottom to the top, except for the sample with n=0.5, indicating that this material has significantly less ability to suck water than the other specimens even if the PPP-grading show the same average water content.
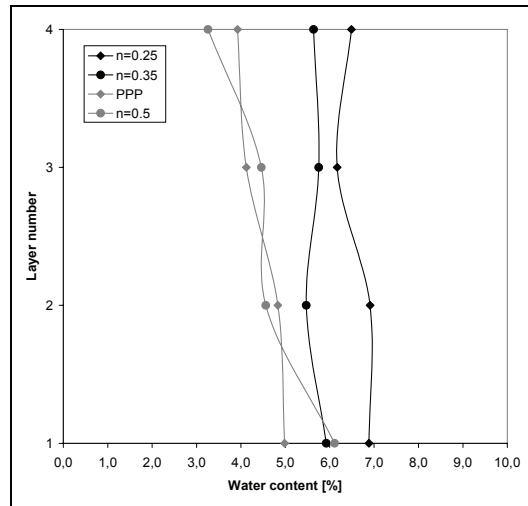
FIGURE 9. Water content in four layers of the samples,
(Layer 1 = top layer, Layer 4=bottom layer)

Cyclic load triaxial testing

Resilient modulus
The resilient modulus M_R is defined as the ratio of applied dynamic deviatoric stress to the axial resilient strain for one load cycle. The average resilient modulus for the 10 000 load cycles in one load step is presented in Figures 10-12. A load step is defined as the combination of a confining stress and a cyclic deviatoric stress.

Figure 10 shows the resilient modulus as a function of the mean stress ($\sigma_m=1/3(\sigma_d+3\sigma_3)$) for the material with the well-graded curve, n=0.5. In this case the highest obtained degree of saturation was 85 %. The sample with the lowest degree of saturation (49 %) shows the highest resilient modulus. All specimens have about the same resilient modulus for low stress levels. For the higher stress levels however, the specimen with S_r=81 % have a lower resilient modulus than the other two; S_r=67 % and S_r=49 % respectively.

In Figure 11 the resilient modulus for the samples with curve n=0.35 is presented. Also here the degree of saturation is maximum 85 %. Here the sample with the lowest degree of saturation (34 %) has a significantly higher resilient modulus for all stress levels tested. The two other samples presented have close to equal resilient response, being lower than for S_r=34 %. This shows that the material with n=0.35 is more affected by smaller changes in water content, thus being more water susceptible than the more open graded material with n=0.5 shown in Figure 9. It is also worth to remark that for n=0.5 the significant reduction of the resilient modulus occurred at S_r=81 % while the drop in the modulus for n=0.35 occurred at a lower degree of saturation; S_r=66 %.

In Figure 12 the data from the samples with the PPP-curve is presented. Here we observe the same tendency as for the n=0.35 grading, but not as pronounced. The sample with the lowest degree of saturation has the highest resilient modulus for all stress levels, while the samples with 58 and 68 % saturation respectively, have almost identical behaviour. For this grain size distribution we did not achieve as high degree of saturation as for the other two, only 68 % at the highest, giving some limitations in the interpretations.
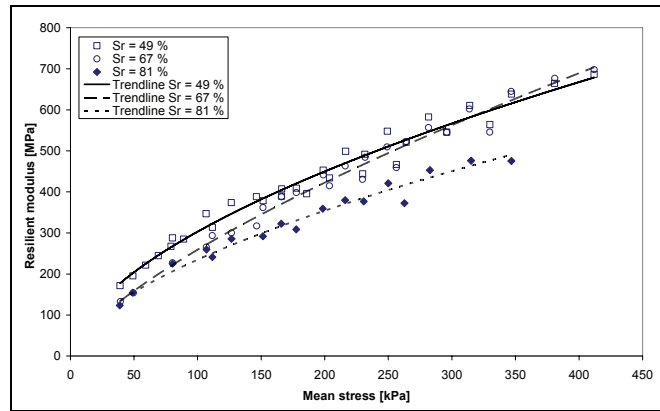
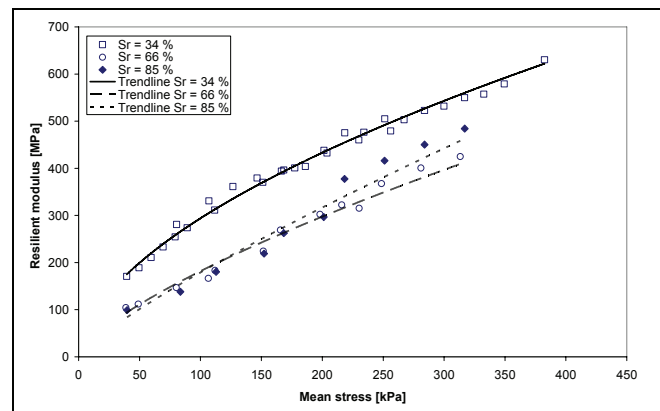**FIGURE 10. Resilient modulus as a function of mean stress for grading n = 0.5**

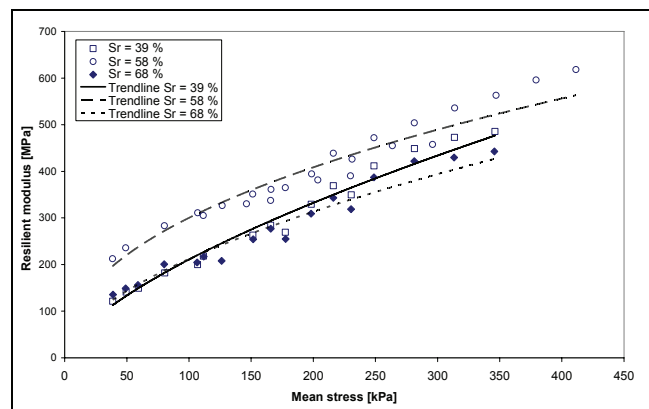**FIGURE 11. Resilient modulus as a function of mean stress for grading n = 0.35**

FIGURE 12. Resilient modulus as a function of mean stress for grading PPP

Permanent deformation behaviour
The main principles of the method for interpretation of the permanent deformation behaviour
are described in Hoff et al. *(9)*, who classified the permanent deformation behaviour of
unbound materials into three different classes ranging from purely elastic response to failure
by the observed strain rate of the last 5000 to 10000 cycles.

Range - A: $\dot{\varepsilon} < 2.5 \cdot 10^{-8}$ Elastic range
Range - B: $2.5 \cdot 10^{-8} < \dot{\varepsilon} < 1.0 \cdot 10^{-7}$ Elasto-plastic range
Range - C: $\dot{\varepsilon} > 1.0 \cdot 10^{-7}$ Plastic/failure range

In Figure 13 the elastic stress stage steps according to this interpretation is marked by square plots, the steps in elasto-plastic range is marked by triangles and the steps giving deformation rates in the failure range is marked by circles. Figure 13 shows a σ_3-σ_d plot of the stress situation for each load step ranged into the three classes above.
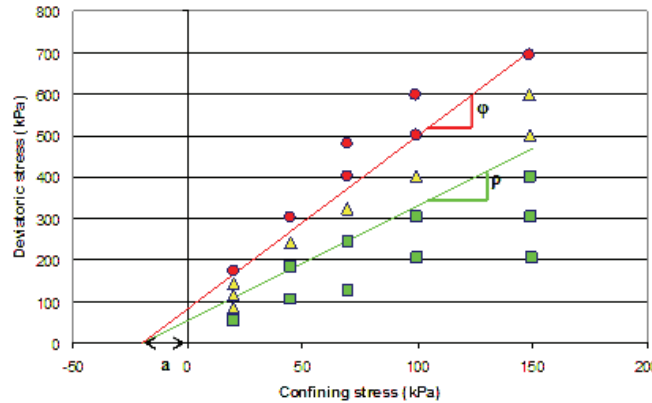
FIGURE 13. All load steps for one sample categorized into three categories (example)

The Coulomb criterion is used to find the stress envelope for the design stage and the failure stage, shown by the lower and the upper line respectively. The equations of these lines are:

Elastic limit: $\sigma_3 = \sin\rho(\sigma_1 - \sigma_3) + a$ (Eq. 1)

Failure limit: $\sigma_3 = \sin\varphi(\sigma_1 - \sigma_3) + a$ (Eq. 2)

Here σ_1 and σ_3 are principal stresses and ρ and φ are angles of the elastic and plastic limit lines. The apparent attraction "a" was interpreted to be close to 20 kPa for all the samples. The result of this interpretation for each series may be shown by the $\sin\rho$ and $\sin\varphi$ values for each sample as an indication of the strength.

In Figure 14 the elastic and the plastic limit for the grading of n=0.5, is presented in combination with the dry density for each sample. The resistance to permanent deformations seems to be reduced as the degree of saturation increases. In addition the dry density also seem to have an effect on the permanent deformation behaviour as the two samples with the lowest degree of saturation seem to follow the dry density. The highest degree of saturation achieved here was 81 %, which is still quite far from full saturation. However, there is a trend towards pronounced reduction in strength for the highest degree of saturation.

In Figure 15 the permanent deformation behaviour for the grading with n=0.35 is shown. For this grading the reduction in strength with increasing degree of saturation is more pronounced than for n=0.5. The degree of saturation seems in this case to override the effect of dry density, which in fact is increasing. The highest degree of saturation also here is 85 %, and the strength would probably continue to decrease for higher degrees of saturation. We observe a significant drop in $\sin\rho$ even at S_r=66 %. Compared to the samples with n=0.5 the samples with n=0.35 have a lower strength for low degrees of saturation and drops dramatically for increasing saturation.

Figure 16 shows the elastic and plastic limit for the PPP grading. The trend is not as clear as for the other two grain size distributions, as it seems like the sample with a low degree of saturation has a lower resistance to permanent deformation even if the dry density for this sample is slightly higher than the sample with 58 % saturation. The strength decreases from 58 % saturation to 68 %, which follows the decrease in dry density. For this grading only 68 % saturation is achieved, this is low compared to the other two grain size distributions.
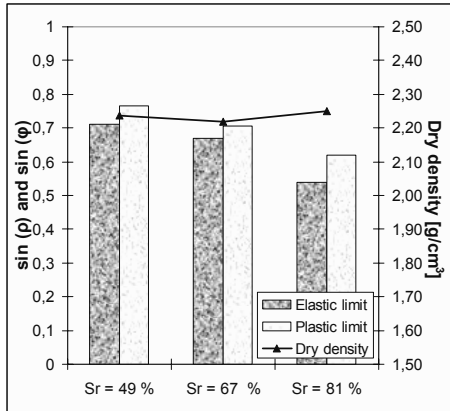
FIGURE 14. Elastic and plastic limits for grading n= 0.5
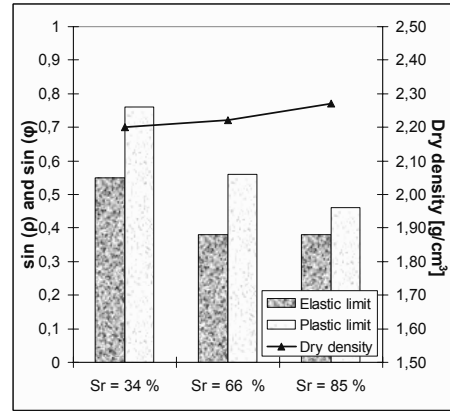
FIGURE 15. Elastic and plastic limits for grading n= 0.35
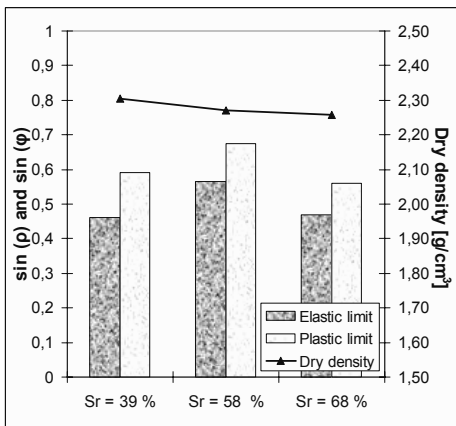
FIGURE 16. Elastic and plastic limits for grading PPP

Comparison samples with close to equal degree of saturation
If comparing samples with the three grain size distributions with near the same degree of saturation, the effect of the gradation becomes more evident. Figure 17 presents the resilient modulus as a function of mean stress for the three gradings tested. The sample with grading coefficient of 0.5 has the highest resilient modulus for this level of saturation. The sample with grading n=0.35 and the PPP grading have near the same resilient modulus for low stress levels. For high stress levels these two gradings give pronounced lower resilient moduli than the same material with grading n=0.5.

In Figure 18 the elastic and plastic limits for the three gradings with near the same degree of saturation are presented. The trend shows that the strength is significantly reduced

with higher fines content (n=0.35 and PPP). The densities for the samples are about identical, so this should not influence the results significantly. A second observation is that the material seems to have a larger area of elasto-plastic behaviour before "failure" for the gradings with more fines, as the difference between the elastic and plastic threshold limits is larger.
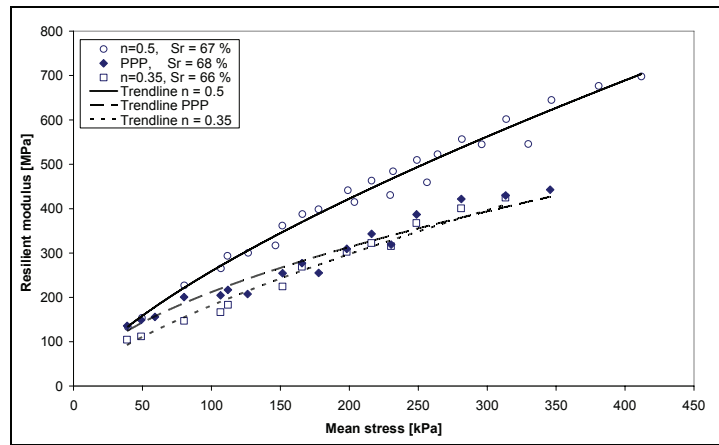

**FIGURE 17. Resilient modulus as a function of mean stress
for all three gradings with near the same degree of saturation**
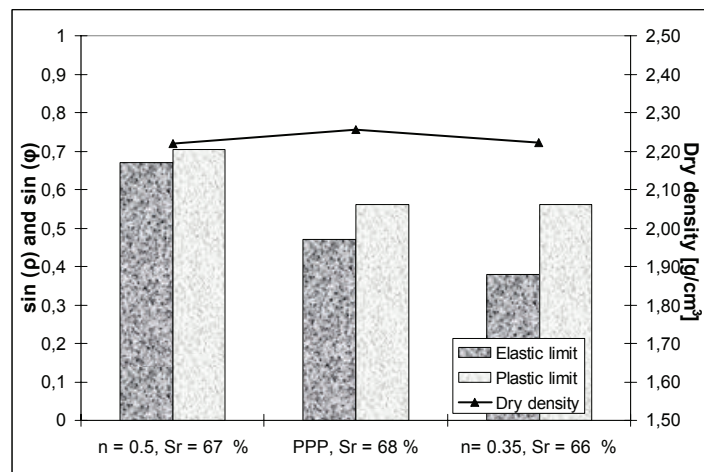
**FIGURE 18. Elastic and plastic ("Failure") limits
for all three gradings with near the same degree of saturation**

DISCUSSION

When studying the dielectric measurements from the Tube Suction test, the results seem reasonable from the information we have about grading, fines content and mineralogy of the material used. The most extreme grading with respect to fines content is the most water sensitive grading found by the Tube Suction test. However, only one sample from each grading was tested, and according to Guthrie et al. *(5)* the method has some variability. From the single samples we observe that the three main gradings, n=0.5 and n=0.35 and the PPP grading, are classified as non-moisture and non-frost susceptible by the suggested classification table presented in Guthrie et al. *(7)*. The more extreme curve with grading

coefficient of n=0.25 may be characterized as moisture susceptible by this table, as the dielectric value is about 10 and seems to be increasing even to a higher value at the end of the test period.

In this test series we did not succeed in achieving 100 % saturation. We did not use de-aired water, but this would probably have a marginal effect. It seems like the PPP curve was the hardest to saturate, as the highest degree of saturation achieved was 68 %.

The cyclic load triaxial testing shows a marked difference in the sensitivity to changes in the degree of saturation on the resilient modulus, showing the material with n=0.35 to be the weakest. For the other two gradings the resilient modulus seems to be highest for a possible optimum degree of saturation. All three gradings show the lowest resilient modulus for the highest degree of saturation, even though the samples were not fully saturated. This shows that when the degree of saturation exceeds a certain level, the resilient modulus decreases. As this effect is more pronounced for the two gradings with the highest fines content, it seems like the fines content affect the sensitivity to changes in water content with respect to the obtained resilient modulus.

When it comes to the permanent deformation behaviour, the samples with n=0.5 are mainly affected by the dry density for the two lowest water contents. For the highest degree of saturation the resistance to permanent deformations decreases even if the dry density is slightly increasing. For the material with n=0.35 the degree of saturation seems to be the key factor controlling the permanent deformation behaviour. In this case the resistance to permanent deformations decreases dramatically with increasing degree of saturation from 34 % to 85 %. This is true even when the dry density increases.

The samples with the PPP grading are obviously influenced by both the degree of saturation and the density. For the lowest degree of saturation (39 %) the resistance to permanent deformations is lower, even if the dry density is higher for this sample compared to the other samples. The sample with the highest degree of saturation is influenced by both the dry density and the degree of saturation as the elastic and plastic limit decreases with decreasing dry density and increasing saturation.

By comparing samples with equal degree of saturation of about 68 %, the effect of the different gradings and changes in dry density may be more evident. Regarding the resilient deformation behaviour, the material with n=0.5 show a significantly higher resilient modulus that the other two gradings. The material corresponding to the PPP grading and the material with n=0.35 show similar behaviour for all stress levels even if the PPP sample have a higher dry density. This means that the resilient modulus decreases with increasing fines content for this degree of saturation.

The permanent deformation behaviour shows the same trend, as the material with grading coefficient n=0.5 has the highest elastic and plastic limit. The material with the PPP grading have almost identical plastic limit as the material composed with n=0.35 and a higher elastic limit for a higher dry density. This means that for this degree of saturation the resistance to permanent deformation decreases with increasing fines content.

CONCLUSIONS

The Tube Suction test seems to be a good method to detect water and frost susceptibility. For the four different grain size distributions in this study, the dielectric constant seems to increase with increasing fines content.

It seems like a high degree of saturation affect the resilient modulus of the different grain size distributions tested, as the resilient modulus decreases when the degree of saturation reaches a certain level. Increasing fines content makes the resilient modulus decrease also at a lower degree of saturation.

Both the resilient modulus and the permanent deformation seem to decrease for increasing fines content under constant dry density. Low fines content therefore assure for a good performance of unbound materials even under fluctuating water contents.

ACKNOWLEDGEMENTS

REFERENCES

1. Uthus, L., Hermansson, Å., Horvli, I. and Hoff, I. A study on the influence of water and fines on the deformation properties and frost heave of unbound aggregates. *Proceedings for the 13th International Conference on Cold Regions Engineering* (CD ROM), Orono, Maine, 2006.
2. Hauck, C. Water sensitivity of gravel materials (In Norwegian). *Cand. Scient thesis*, University of Oslo, Norway, 1989.
3. Vegdirektoratet. Håndbok 018 Vegbygging (In Norwegian), Oslo, Norway, 2005.
4. Saarenketo, T. and Scullion, T. Using Suction and Dielectric Measurements as Performance Indicators for Aggregate Base Materials. *Transportation Research Record 1577*, Transportation Research Board, Washington DC, USA, 1997.
5. Guthrie, W.S., Ellis, P.M. and Scullion, T. Repeatability and Reliability of the Tube Suction Test. *Paper no 01-2486 Transportation Research Record 1772*, Transportation Research Board, Washington DC, USA, 2001.
6. Fuller, W and Thompson, S. E. The laws of proportioning concrete. *Transactions of the American Society of Civil Engineers. Paper no 1053*, 1907. pp 67-143.
7. Guthrie, W.S., Hermansson, Å. and Scullion, T. Determining Aggregate Frost Susceptibility with the Tube Suction Test. *Proceedings for the 11th International Conference on Cold Regions Engineering,* Anchorage, Alaska, 2002. pp 663-674.
8. CEN - European Commite for Standardization. Unbound and hydraulically bound mixtures – part 7: Cyclic load triaxial tests for unbound mixtures *EN 13286-7*. Brussels, 2000.
9. Hoff, I., Bakløkk, L. and Aurstad, J. Influence of Laboratory Compaction Method on Unbound Granular Materials. *Proceedings for the 6th International Symposium on Pavements Unbound (UNBAR 6)* (CD-ROM), University of Nottingham, Great Britain, 2003.

PAPER VI

Discrete Element Modelling of the Resilient Behaviour of Unbound Granular Aggregates

L. UTHUS*†, M. A. HOPKINS ‡; and I. HORVLI§

†Research Fellow, Norwegian University of Science and Technology, Lillian.Uthus@ntnu.no
‡Researcher, Ice Engineering Branch, Cold Regions Research and Engineering Laboratory, Hanover NH, USA.
§Professor, Norwegian University of Science and Technology, Norway.

The scope of this study is to use a three dimensional discrete element model to simulate the resilient response of an unbound granular material subjected to sinusoidal loading in a triaxial sample and to compare the simulated results to experimental results. Uniform spherical grains were used in both the DEM simulations and in the triaxial tests. A three-dimensional discrete element model allows a micromechanical approach to modeling, where each grain interacts with its neighbor grains. By doing a sensitivity analysis on the input parameters the model can be evaluated and insight gained about the factors that affect the resilient behaviour. Two contact models, linear viscous-elastic and Hertzian, and two types of confinement, a rigid cylinder and a flexible membrane, are tested. Comparison of the simulation results with the results of similar laboratory experiments shows that the discrete element approach is suitable to model idealized aggregate grains.

Key words: Unbound granular aggregates; cyclic load triaxial testing; resilient modulus discrete elements; contact models.

Introduction

Road pavement performance is still not yet fully understood because it has been necessary to simplify the material behaviour, particularly for the unbound granular materials used to support the roadbed. These materials are typically modeled as continuous, but in reality they exhibit discontinuous behaviour as the individual grains only interact at the contact points where sliding is common. Observations from the testing of aggregate materials show that they do not always fit even the advanced continuum models based on non-linear behaviour very well. Discrete element modeling (DEM) allows discontinuity in a material and is therefore more suitable for simulation of the behaviour of unbound materials. Discrete element modeling of granular assemblies of two-dimensional discs was described by the pioneers *Cundall and Strack* (1979). The scope of this study is to use a three dimensional discrete element model to simulate the resilient response of an unbound granular material subjected to sinusoidal loading in a triaxial sample and to compare the simulated results to experimental results. Uniform spherical grains were used in both the DEM simulations and in the triaxial tests. In the DEM model it is possible to do a parameter study in a more effective way than in the laboratory by changing the interparticle friction, the grain shape or the elastic stiffness of the grains.

Experimental Description

Cyclic load triaxial testing of granular aggregates was developed to simulate the traffic loading on a road structure. Elastic response to traffic loading is a non-linear process that can be quantified by the resilient modulus M_R. By running a cyclic load triaxial test at constant confining pressures, one can compute the resilient modulus using the equation

$$M_R = \frac{\sigma_d}{\varepsilon_a} \tag{1}$$

where σ_d is the applied deviatoric stress, and ε_a is the axial strain. The axial strain is the peak-to-peak measurement.

In the triaxial apparatus at NTNU 150 mm diameter cylindrical samples of unbound granular material are tested. The height of the samples varies from 220 to 300 mm. A snapshot of the laboratory triaxial test sample is shown in Figure 2. Nearly uniform aggregate spheres were made from rock material to have a grain shape that would be easy to simulate in the DEM system. The rock material is gneiss collected in a quarry in Askøy outside Bergen, Norway. It is a common material used for road construction in Norway and is quite hard. Figure 1 shows several aggregate spheres used in the laboratory experiments.

Figure 1. Aggregate spheres used in the laboratory experiments.

In a random selection of 10 spheres the radius varied from 7.22 to 7.87 mm. The material properties of the Askøy gneiss, a mixture of quartz and feldspar, were measured by testing five cored samples in a uniaxial apparatus with static loading. The Young's modulus was found to be 80 GPa and the Poisson ratio was 0.3. Subsequently, *Cole et al.* (in prep) performed micromechanical contact experiments on pairs of aggregate spheres using both monotonic and cyclic loading in both the normal and sliding modes. The normal contact behaviour was found to be Hertzian at the force levels in these experiments. The observed elastic modulus ranged from 53 to 80 GPa. *Cole et al.* (in prep) found the coefficient of static friction to be approximately 0.28. A sample of the latex material used for the sample membrane in the laboratory experiments was tested and found to have an elastic modulus of approximately 4 MPa at a strain of about 10%.

The cylindrical samples used in laboratory testing contained approximately 1500 spheres. The samples are constructed using light vibration for compaction. Some water is added to the sample, so the aggregates spheres are moist. The aggregate spheres are placed in a gyratory mold and a vacuum is used to keep the grains in position while a rubber membrane is applied to confine the aggregate. The sample is mounted in a triaxial apparatus and water is used as

the surrounding medium for application of the confining stress. The axial strain is measured over the entire length of the sample, both in the model and the laboratory tests.

Figure 2. Experimental triaxial sample.

In the experiments we apply a modified version of the EN standard for cyclic load triaxial testing of unbound mixtures, EN 13286-7 (CEN, 2000). To obtain as much information as possible from each sample, without getting large permanent deformations, a multistage loading procedure is used in which the confining stress is increased sequentially. Within each load sequence performed at a constant confining stress the deviatoric stress is increased in steps. Each sample is subjected to five sequences with five confining stresses. Each confining and deviatoric stress combination is subjected to 10000 load cycles. A sequence is interrupted prematurely when the axial permanent deformation reaches 0.5% measured during the current loading state. In the laboratory experiments with spherical particles the deviatoric stress had to be reduced from the level in the EN-standard due to the relative weakness of the spherical aggregate. The sinusoidal deviatoric stress is applied with a frequency of 10 Hz. The confining stresses and deviatoric stresses used in the experiments are listed in Table 1.

Table 1. Load sequence stress values.

	Confining Stress σ_3 (kPa)			
	45	70	100	150
Deviatoric Stress σ_d (kPa)	50	75	110	100
	55	80	120	150
	60	85	140	200

Description of the Discrete Element Model

We use a discrete element approach developed by *Hopkins* (2004). It is applicable for granular materials with varying properties and ellipsoidal grain shapes. Each particle is defined by its shape, position, velocity and orientation. The calculations in the model are done in the following order:

1) Find neighbouring particles
2) Find and define contacts between neighbours
3) Calculate forces
4) Move particles

The first step in the calculations is to identify the neighbouring particles. The search for neighbours is performed by superimposing a 3D grid on the system of particles. The search is limited to the cells immediately surrounding each particle in the grid. This way the search for contacts is reduced from an order n^2 problem to an order n problem, where n is the number of particles.

Contact detection using dilated particles is described in *Hopkins* (2004). Each particle has an extra layer outside the basic ellipsoidal shape that is obtained by dilating the original particle by a sphere with radius R that is small relative to the particle size. Thus, in effect, each particle is covered by an infinite set of spheres and contact detection is reduced to the process of finding the pair of spheres, one in each set, that are closest. The basic ellipsoidal shape is called the constraint surface of the particle. Contact detection is performed by stretching a rubber band between the two particles. Each end of the rubber band is constrained to remain within its respective constraint surface. The elasticity in the rubber band pulls the ends of the vector along the respective constraint surface as long as there is a nonzero tangential component of the elastic force. The process is iterative and continues until the motion of the elastic band vector from one iteration to the next falls below a preset tolerance. The overlap δ between a pair of particles is defined as

$$\delta = \bar{d}\,g\hat{n} - R_1 - R_2 < 0 \tag{2}$$

where $\bar{d}\,g\hat{n}$ is the magnitude of the elastic vector that defines the shortest distance between the two particles, and R_1 and R_2 are the dilating radii of particle 1 and 2, respectively.

We began the simulations using a linear viscous-elastic contact force model that is common in discrete element modeling. In the linear model particle contact forces are described in the normal direction by a normal contact stiffness, represented by a spring with a spring constant k_n and a viscous damping parameter η as

$$F_n = k_n\delta - \eta\bar{V}_{1/2}\cdot\hat{n} \tag{3}$$

where F_n is the force component normal to the surfaces at the point of contact and $\bar{V}_{1/2}$ is the relative velocity of particle 1 with respect to particle 2 at the point of contact given by

$$\bar{V}_{1/2} = \bar{V}_1 - \bar{V}_2 + (\bar{r}_1 \times \bar{\omega}_1) - (\bar{r}_2 \times \bar{\omega}_2) \tag{4}$$

where $\bar{r}_1$ and $\bar{r}_2$ are the vectors from the center of particles 1 and 2 to the contact point and $\bar{\omega}_1$ and $\bar{\omega}_2$ are the rotational velocities of particles 1 and 2.

Coulombic frictional forces act between each grain pair. For the loading part the frictional contact force F_t at time m is calculated from the force at the previous time step (m-1), as shown in Equation 4.

$$\bar{F}_t^{m} = \bar{F}_t^{m-1} - \left[k_t \cdot \Delta t\, (\bar{V}_{1/2} - \bar{V}_{1/2} \cdot \hat{\bar{n}}) \right] \tag{5}$$

where k_t is the tangential contact stiffness and Δt is the time step. The tangential force is also damped. Once the frictional force reaches the Coulomb limit sliding begins. For the sliding part of the friction model the following limit is applied to F_t

$$\text{If} \quad \left| \bar{F}_t^{m+1} \right| > \mu F_n^{m+1}, \text{ then } \left| \bar{F}_t^{m+1} \right| = \mu F_n^{m+1} \tag{6}$$

where μ is the coefficient of friction.

When it became apparent that the linear contact model had significant shortcomings in the cyclic loading simulations performed in this study, we implemented a Hertzian contact force model similar to the one used by *Lin and Ng* (1997) that was in turn based on the work of *Johnson* (1987). The Hertzian model is based on a non-linear force-displacement relationship as a consequence of the fact that the contact area between particles increases with the normal load. The equation for the normal contact force F_n as a function of the particle overlap δ is

$$F_n = \frac{2\sqrt{2}\,G}{3(1-v)}\, R_e^{1/2}\, \delta^{3/2} \tag{7}$$

where G and v are the shear modulus and Poisson ratio of the spheres and R_e is the equivalent radius of curvature, which in this case is the radius of the spheres. The tangential stiffness depends on the normal force. The dependence (*Lin and Ng*, 1997) is

$$k_t = \frac{2\left[3G^2(1-v)F_n R_e \right]^{1/3}}{2-v} \tag{8}$$

The tangential contact force (5) is calculated incrementally to account for the effect of the changing normal contact force on the tangential stiffness. Following *Lin and Ng* (1997) we adjust the direction of the tangential force $\bar{F}_t$ to reflect the changing orientation of the contact normal. This is expressed as

$$\bar{F}_t = \left| \bar{F}_t \right| \frac{\bar{F}_t' - (\bar{F}_t' \cdot \bar{n})\bar{n}}{\left| \bar{F}_t' - (\bar{F}_t' \cdot \bar{n})\bar{n} \right|} \tag{9}$$

where $\bar{n}$ is the updated contact unit normal vector. As with the linear model the Coulomb friction limit (6) is imposed on the frictional force.

Simulation of Cyclic Load Triaxial Testing

We used two types of confinement in the simulations. The first is a rigid cylinder wall to contain the particles while the second is a flexible membrane. In the rigid cylinder walled sample particle interactions with the cylinder wall used a friction coefficient of zero. The diameter of the rigid cylinder changed at each time step in response to the balance of the forces exerted by the particles on the inside wall and the confining pressure applied uniformly to the exterior surface. The cylindrical wall has a specified mass that includes some added mass due to the surrounding fluid.

In the membrane triaxial sample the membrane is implemented using a triangular mesh. A picture of the sample and a part of the mesh is shown in Figure 3.
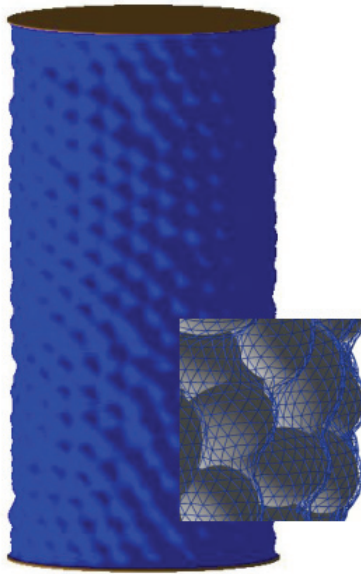
Figure 3. DEM membrane covered triaxial sample. The inset shows the triangular mesh conforming to the spherical particles.

At each node of the mesh there are small spherical particles that have mass and interact with the much larger aggregate spheres. The node spacing is about an order of magnitude smaller than the diameter of the aggregate spheres. Springs and dashpots connect the mesh node particles to simulate the effect of the viscous-elastic membrane. The spring and dashpot forces are calculated from the relative displacement between adjacent nodes using (3) with appropriate values for the elastic stiffness and viscosity. The 4 MPa Elastic modulus of the membrane material used in the experiments is equivalent to an elastic stiffness for the elements between nodes of about 5 kN/m. The node connections do not support moments. The mass of the nodal mesh particles also includes some added mass due to the surrounding fluid. The confining pressure force, proportional to the area of each triangular mesh element, is applied at the centroid of each element in the direction normal to the plane of the triangle. The force is divided among the three nodes at the triangle vertices using a distance weighting formula. A small velocity dependent viscous drag force is applied to each node. At the end of each time step the resultant of the particle, membrane, pressure, and drag forces on each node is calculated and used to solve the motion equations for the node.

Both the membrane and rigid walled samples have rigid disk-shaped plates at the top and bottom. In the rigid cylinder the movement of the top and bottom disks and cylindrical wall are effectively uncoupled while in the membrane cylinder the nodes at the upper and lower edges of the membrane are attached to the disks and the mesh particles can interact with the disk surfaces. In both models the top and bottom disks have the same friction coefficient as the aggregate spheres. In both cases a sinusoidal axial driving force is applied to the bottom disk in the same way that it is applied to the triaxial sample in the laboratory. The stress exerted on the top plate by the aggregate spheres is calculated to monitor stress transmission through the granular aggregate. Gravity acts on the individual particles.

In general the size and shape of the particles is defined by choosing the lengths of the three ellipsoidal axes. The three axes can be varied independently to make various poly-ellipsoidal grain shapes (*Peters, et al.*, in prep.). However, in this work we restrict our particles to nearly uniform sized spheres for comparison with the experimental results. Sample size is dictated by the size and number of particles. Initially the particles were placed in a dilated configuration at the nodes of a grid and kinematically compressed, with gravity turned off, until the stress within the aggregate reached 20 kPa while retaining an approximate 2:1 ratio of height to diameter. Following kinematic compression, gravity was turned on and the samples were dynamically equilibrated in a rigid cylinder configuration by running each sample for several hundred oscillations at each confining stress. The solid fraction of the final samples was approximately 60%. The membrane samples require an additional equilibration step wherein the rigid cylinder is transformed to a flexible membrane. The aggregate particles are frozen during the membrane equilibration. Once equilibration is complete a simulation is run with the desired confining and deviatoric stress levels and duration. Logging of output data is done at 500 hz.

Parameter values used in the simulations are listed in Table 2. The parameter values were chosen to agree as closely as possible with the experimental values. The overall radii of the aggregate spheres varied uniformly between 7.25 and 7.75 mm to reproduce the distribution measured in the real samples. The dilating radius was 1 mm. The triaxial sample height and diameter were nominally the same as in the experiments. The samples contained 1700 aggregate spheres.

While computer capability is improving, it is still not possible to do real-time simulation of laboratory scale samples on a desktop system. The rigid walled and membrane simulation run times were about 35 and 300 min/s, respectively, on a single Xeon processor. The time step Δt used in the simulations is calculated from the period of oscillation of the spring used to calculate the normal contact force in (3) and (7)

$$\Delta t = \frac{\pi}{10}\sqrt{\frac{M}{k_n}} \tag{10}$$

where M is the nominal particle mass and k_n is the normal contact stiffness. The effective stiffness for the Hertzian contact model is estimated from (7) using the observed maximum force levels of approximately 200 N.

We applied the same confining and deviatoric stress levels, sinusoidal cyclic loading, and oscillation frequency of 10 Hz to the simulations as in the laboratory experiments. However, the simulations used a different loading procedure. Separate equilibrated samples were constructed for each level of confining stress. All load steps for each confining stress were run

from the same equilibrated sample. The simulations were run for just 100-200 cycles at each load. A modest, progressive increase (order 10%) in the resilient modulus was observed as the number of cycles increased.

Table 2. Parameters used in the simulations.

Parameter	Symbol	Quantity
Number of particles		1700
Overall particle radius		7.25 – 7.75mm (Spheres)
Dilating radius	R	1 mm
Specific density	ρ_s	2.7 g/cm^3
Linear normal contact stiffness	k_n	31.5 MN/m
Linear tangential contact stiffness	k_t	18.9 MN/m
Shear modulus	G	24 and 30 GPa
Poisson ratio	ν	0.3
Approx. time step	Δt	$2.5 *10^{-6}$ sec
Oscillation frequency		10 hz
Particle surface friction	μ	0.2-0.8
Approx. cylinder radius		74.6 mm
Approx. cylinder height		297.0 mm
Cylinder lid mass		1 kg
Rigid cylinder mass		50 kg
# mesh nodes (circumferential)		200
# mesh nodes (vertical)		150
Mesh node mass		1 mg
Membrane elastic coefficient (lab)		5 kN m^{-1}
Gravity constant	g	9.81 m s^{-2}

Comparison of Results of the Simulations and Experiments

We began by studying the sensitivity of the resilient modulus to variations in the membrane elastic stiffness, the lid mass, and the friction coefficient. We tested lid masses of 0.5, 1.0, and 1.5 kg. The variation produced no discernible effect on the modulus. We used the middle value of 1 kg for subsequent simulations. We tested membrane elastic stiffness coefficients of 5, 10, 15, 20, 25, and 30 kN/m. The variation produced no discernible effect on the resilient modulus. The stiffness of the 1 mm thick latex membrane used in the experiments was about 5 kN/m. We used that value for subsequent simulations.

The analysis of the sensitivity to variation of the friction coefficient was performed using a confining stress of 70 kPa and a deviatoric stress of 80 kPa. The coefficient of friction was varied from 0.2 to 0.8. The results are shown in Figure 4. The average of the experimental results is plotted as a horizontal line. The results for the linear contact force model and the Hertzian model show very different response to increases in the friction coefficient. The explanation probably lies in the fact that the tangential stiffness in the linear model is a constant, independent of the normal contact force, while in the Hertzian model the tangential stiffness (8) is a function of the normal force. While the Hertzian stiffness is almost the same magnitude as the linear stiffness at peak contact forces it is much lower in lightly loaded contacts. As the tangential stiffness determines how quickly the tangential force (5) reaches the Coulomb limit (6) this implies that the frictional forces at lightly loaded contacts are higher with the linear model contributing to higher sample strength. Furthermore, in a cyclic loading environment the more rapid loading of the frictional forces to the Coulomb limit

8

probably causes the aggregate to stiffen increasing the resilient modulus. The sensitivity to friction in the linear model was even more extreme at the 100 and 150 kPa confining stresses. We used a friction coefficient of 0.3 for subsequent simulations at the various stress levels.
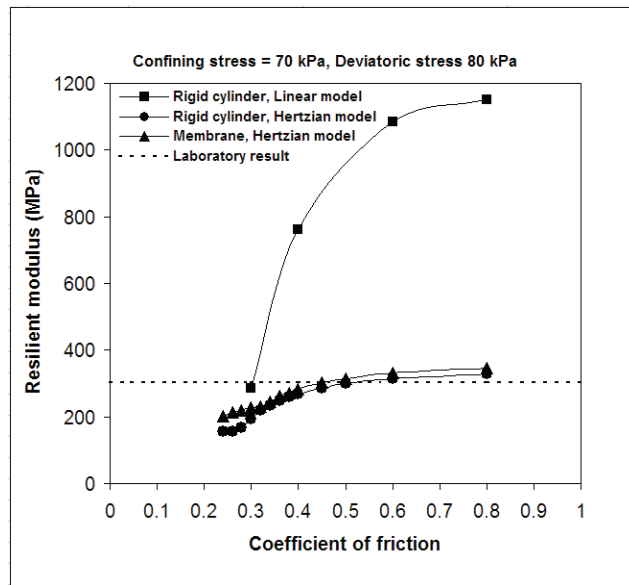

Figure 4. Showing the resilient modulus as a function of the friction coefficient for a confining stress of 70 kPa and deviatoric stress of 80 kPa.

Figures 5-8 show the resilient modulus as a function of the mean stress for confining stresses of 45, 70, 100, and 150 kPa respectively. The laboratory results are shown for 3 different experiments designated spheres 1-3. Mean stress is the mean value of the principal stresses defined as $1/3(\sigma_d+3\sigma_3)$. For each confining stress the Hertzian membrane simulations show the best agreement with the results of the laboratory tests.
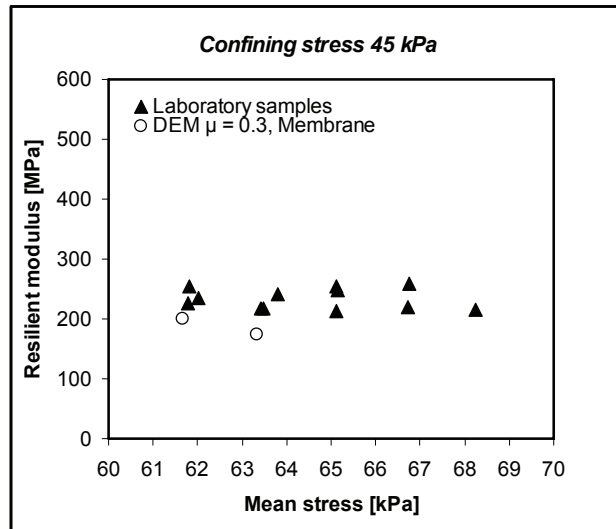
Figure 5. Showing the resilient modulus as a function of the mean stress for a confining stress of 45 kPa and a friction coefficient of 0.3.

9
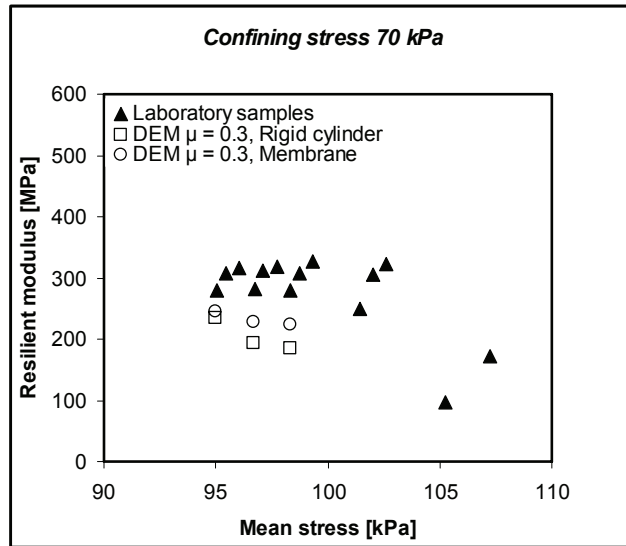
Figure 6. Showing the resilient modulus as a function of the mean stress for a confining stress of 70 kPa and a friction coefficient of 0.3.
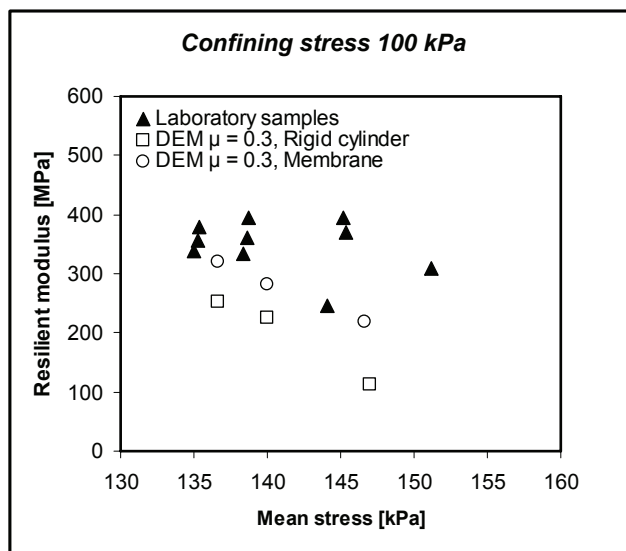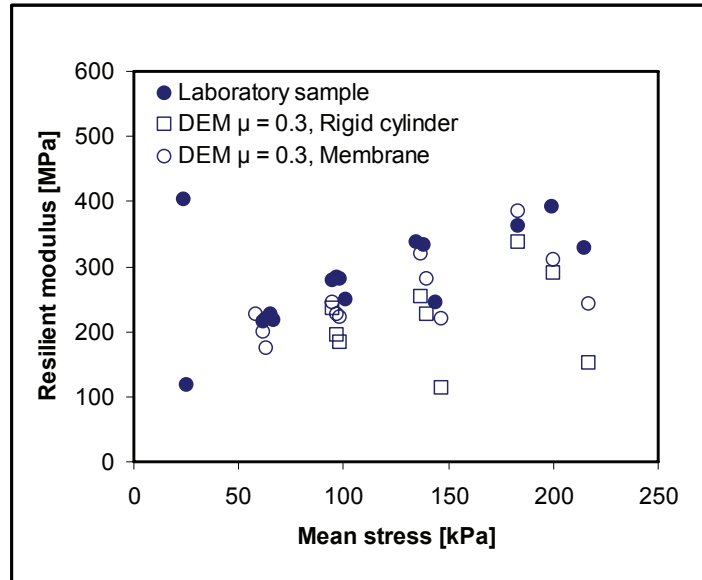

Figure 7. Showing the resilient modulus as a function of the mean stress for a confining stress of 100 kPa and a friction coefficient of 0.3.

Confining stress 150 kPa
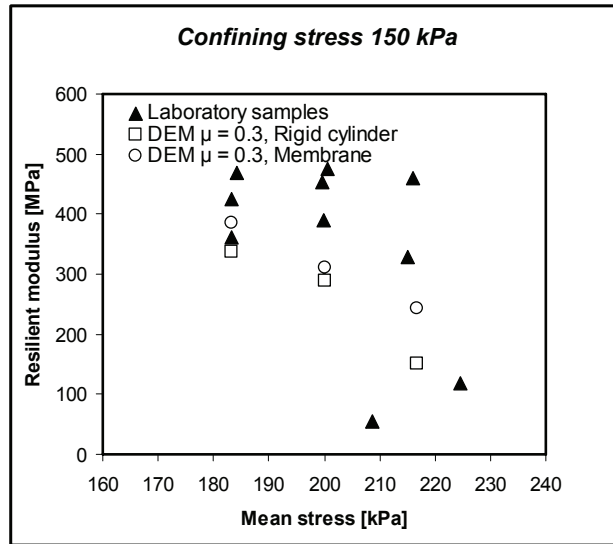
Figure 8. Showing the resilient modulus as a function of the mean stress
for a confining stress of 150 kPa and a friction coefficient of 0.3.

It is well known that the resilient modulus is highly dependent on the stress level (*Hicks and Monismith*, 1974). From results at several confining stresses the laboratory samples show a tendency for the resilient modulus to remain constant as deviatoric stress increases before rolling off at higher stress levels. The Hertzian rigid cylinder model shows greater decrease in the resilient modulus with increasing deviatoric stress than the experimental and Hertzian/membrane model results. In fact both the linear and Hertzian rigid cylinder models typically became unstable and collapsed during the third increment of the deviatoric stress. Work done with DEM by *Zeghal* (2004) showed that the resilient modulus increases with increasing confining stress. He also found that the effect of the deviatoric stress is important at low confining stresses, but become negligible at high values (140 kPa).

Figure 9 shows the resilient modulus as a function of mean stress for all confining stresses for the laboratory samples and the simulations with μ=0.3. The results from the laboratory sample and the simulations both show quite a bit of scatter. However, both sets of simulation results seem to fall within the scatter of the laboratory samples. Figure 9 shows a general tendency for the resilient modulus across the entire test series to increase with increasing mean stress even though the resilient modulus for each confining stress decreases slightly with increasing deviatoric stress.

Figure 9. Showing the resilient modulus as a function of the mean stress for all confining stresses and a friction coefficient of 0.3. Both simulations used Hertzian contact force models.

Conclusions

While the DEM simulations and laboratory experiments are just about as similar as it is possible to make them be there are still significant differences between the two systems. For example it is difficult to capture all of the variations in the real materials. Parameters such as mineralogy, anisotropy, and microscopic roughness of the aggregate particles may affect the results. Also it was not practical with our existing computational capabilities to run each of the simulations for more than approximately 100-200 oscillations. Results from the experiments show further increases of 5-10% in the resilient modulus after 100 oscillations.

Although the simulations do not exactly reproduce the experimental results they do come quite close. Two different contact force models were used in the simulations, a linear model and a Hertzian model. It is often assumed that the details of the normal contact law are not important. However, the Hertzian model produced better agreement with the experimental results at all stress levels. The coefficient of friction between particles is a key parameter in determining the resilient modulus of the aggregate.

The linear contact model shows a much greater and probably unrealistic sensitivity to the friction coefficient than the Hertzian model. This sensitivity is probably exacerbated by the cyclic loading imposed on the triaxial sample. The simulations also compared a rigid cylinder triaxial sample and a flexible membrane triaxial sample. The flexible membrane generated resilient modulii that were significantly closer to the experimental values than the rigid walled cylinder. The flexible membrane also contributed to greater stability of the aggregate at higher deviatoric stresses. The instability exhibited by the rigid cylinder with increasing deviatoric stress is probably due to the fact that the rigid cylinder responds to average forces. If a few particles impose a large force on the cylinder it expands removing support from particles in lighter contact. Both models show that increasing the confining stress produces an increase in the resilient modulus, as does an increase in the mean stress. Both models show that the resilient modulus varies inversely with the deviatoric stress.

We did not find much evidence of a dependence of the average coordination number on the confining stress or the mean stress state. We did note a decrease in the coordination number with increasing deviatoric stress, but this seemed more indicative of failure of the aggregate. We found the resilient modulus to depend more strongly on the confining stress than the deviatoric stress, at least prior to the onset of failure. From the findings in this study it may be concluded that the DEM simulations using the Hertzian contact force model are suitable for simulation of the behaviour of idealized aggregate grains under cyclic loading. The use of a flexible confining membrane in the simulations gives some increased realism and accuracy with a significant penalty in computation time.

Acknowledgments

References

Cole, D.M, Uthus, L. and M.A. Hopkins (in prep.). Normal and sliding contact experiments on smooth, spherical grains of gneiss.

CEN - European Committee for Standardization, (2000). EN 13286-7 Unbound and hydraulically bound mixtures – part 7: Cyclic load triaxial tests for unbound mixtures, Brussels, 2000.

Cundall, P.A. and Strack, O.D.L (1979). A discrete numerical model for granular assemblies, *Geotechnique,* Vol. 29, No. 1, 47-65.

Hicks, R.G and C.L. Monismith, (1974). Factors influencing the resilient response of granular materials. Highway Research Record Number 345, Highway Research Board, National Research Council, Washington DC, 15-31.

Hopkins, M. A. (2004). Discrete element modeling with dilated particles. *Journal of Computations*, Vol. 21, No. 2/3/4, 422-430.

Johnson, K.L. (1987). *Contact Mechanics*, Cambridge University Press, 452 p.

Lin, X. and NG, T.-T. (1997). A three-dimensional discrete element model using arrays of spheres. *Géotechnique*, Vol. 47, No. 2, 319-329.

Peters, J.F., M. A. Hopkins, R. E. Wahl, and R. Kala (in prep.), A Poly-Ellipsoid Particle for Non-Spherical DEM, to appear in the *proceedings of the 4th International Conference on Discrete Element Methods*, August 27-29, 2007, Brisbane, AU.

Suiker, A.S. J and N. A. Fleck (2004). Frictional Collapse of Granular Assemblies, *Journal of Applied Mechanics*, Vol. 71.

Zeghal, M. (2004). Discrete Element Method Investigation of the Resilient Behaviour of Granular Materials, *Journal of Transportation Engineering*, vol. 130, No 4.

APPENDIX

EXTRACT FROM DRAFT PAPER

Extraxt from draft paper

NORMAL AND SLIDING CONTACT EXPERIMENTS ON SMOOTH, SPHERICAL GRAINS OF GNEISS

David M. Cole[1], L. Uthus[2] and M. A. Hopkins[1]

[1]U.S. Army Engineer Research and Development Center- Cold Regions Research and Engineering Laboratory, Hanover, NH 03755. David.M.Cole@erdc.usace.army.mil
[2] Department of Civil and Transport Engineering, Norwegian University of Science and Technology, NTNU, Høyskoleringen 7A 7491 Trondheim, Norway

Abstract
The development of reliable discrete element models to simulate the mechanics of granular media requires knowledge of the laws that govern the behavior of the grain-to-grain contacts of the material. As part of an effort to develop a discrete element simulation of the triaxial response of specimens of uniform-sized spheres of gneiss, we have conducted a series of experiments on the spheres to provide the contact laws needed to support the DEM analysis.

The contact experiments employed segments of 14.72 mm-diameter spherical grains that had been used in laboratory triaxial experiments. The grains were formed by a process that resulted in uniform-sized spheres with a very smooth surface finish. The contact experiments employed monotonic and cyclic loading in both the normal and sliding modes. In the normal contact experiments, deformation and frictional loss was measured for forces ranging up to approximately 100 N. In general, the normal contact behavior was Hertzian, with stiffness increasing from $\approx$ 2 to 15 MN m^{-1} over the range of normal force examined. The sliding experiments employed dead loads up to approximately 20 N, and produced a value of the coefficient of static friction of 0.28. The stiffness of the sliding contact was $\approx$ 0.2 MN m^{-1}. Small but measurable frictional losses were observed in both the normal and sliding modes. The frictional loss in the sliding mode decreased with increasing normal load, and pre-sliding tangential deformation was observed.

Introduction
The discrete element method (DEM) is being applied to a wide variety of problems involving the mechanical properties of granular media. The input for this class of models includes laws that describe the stiffness and friction associated with the contact points in the granular media, and the validity of such models depends critically on how well the contact laws reflect true material behavior. Consequently, the reliability of DEM simulations of a specific granular medium can be greatly improved if the grain-scale contact laws for that medium are available. With this in mind, we have conducted grain-scale contact experiments on a geologic material (a Norwegian gneiss) that has been employed in a series of laboratory triaxial experiments, and is the subject of a DEM modeling effort (Uthus et al., 2005, 2007).

The normal and sliding contact experiments were conducted on segments of the 14.6 mm-diameter grains of gneiss. Since the micromechanical component of the project was of limited scope, the experiments were all conducted on one pair of grains. The spheres

were very consistent with regard to size and surface finish, however, and the results are believed to be representative of general behavior. Two test systems were employed for the normal contact experiments, with peak loading capacities of 10 and 100 N. The 10 N-system provided better control over its range than the higher-capacity system and was employed in an initial series of experiments. The 100 N-capacity-system allowed us to examine behavior at the force levels that occurred in laboratory triaxial experiments. The 10 N-capacity system was modified to conduct the sliding friction experiments as described.

Conclusions

Based on the results presented for normal and sliding contact experiments on smooth, spherical grains of Norwegian gneiss, the following conclusions may be drawn:

1. Normal contact stiffness depended on the force level, and typically ranged from 1-2 MN m^{-1} for forces below $\approx$ 30 N, and exceeded 10 MN m^{-1} for forces greater than 100 N.
2. Virgin loading curves for normal contact exhibited Hertzian behavior (force $\propto$ deformation$^{3/2}$), but a fall-off to a lower order dependence was observed (for forces < 6 N) after repeated loadings to $\approx$ 100 N.
3. Frictional losses were generally observed during cyclic loading experiments in both the normal and sliding modes. Apparent internal friction values observed under normal loading decreased monotonically from 0.025 to 0.01 with increasing normal force. For the sliding contact case, the apparent internal friction varied from 0.01 to 0.1, and was a function of the magnitude of both the shear and normal forces.
4. Sliding contact experiments with variable normal loads produced a coefficient of static friction of 0.28.
5. Pre-sliding tangential deflection (PSTD) was observed in the sliding contact experiments.
6. An average stiffness of 0.196 MN m^{-1} was observed in the sliding contact experiments.

References

Buzio, R., K. Malyska, Z. Rymuza, C. Boragno, F. Biscarini, F. B. De Mongeot and U. Valbusa (2004) Experimental investigation of the contact mMechanics of rough fractal surfaces. IEEE Transactions on Nanobioscience, Vol. 3, No. 1, March, pp. 27-31.

Cole, D.M., J.F. Peters (2006) A physically based approach to granular media mechanics: Grain-scale experiments, initial results and implications to numerical modeling. Granular Matter, In press.

Dvorkin, J., M. Prasad, A. Sakai and D. Lavoie (1999) Elasticity of marine sediments: Rock physics modeling. Geophysical Research Letters, Vol. 26, Issue 12, pp. 1781-1784.

Jumikis, A.R. (1983) Rock Mechanics. 2nd Ed., Trans Tech Publication, 411p.

Mindlin, R.D. and H. Deresiewicz (1953) Elastic spheres in contact under varying oblique forces. ASME J. Appl. Mech., Vol. 20, pp. 327-344.

Starr, M.J., E.D. Reedy, A.D. Corwin, R.W. Carpick and Flater, E.E. (2005) Contact Mechanics Description of Inelastic Displacement Response of a Nano-Positioning Device. Proceedings of the 2005 International Conference on MEMS, NANO and Smart Systems, pp. 421-422.

Luck, D.L., M.P. de Boer, W.R. Ashurst, and M.S. Baker (2003) Evidence for pre-sliding tangential deflections in MEMS friction. 12th Intl. Conf. on Solid State Sensors, Actuators and Microsystems, Boston, June 8-12, pp. 404-407.

Uthus, L., I. Hoff, and I. Horvli (2005) Evaluation of grain shape characterization methods for unbound aggregates. Paper Proceedings. 7th International Conference on the Bearing Capacity of Roads, Railways and Airfields, Trondheim Norway.

Uthus, L., Å. Hermansson, I. Horvli, and I. Hoff (2006) A study on the influence of water and fines on the deformation properties and frost heave of unbound aggregates. Proceedings of the 13th Intl. Conference on Cold Regions Engineering, Orono, Maine.

Uthus, L., E. Tutumluer, I. Horvli, and Hoff, I. (2007) Influence of grain shape and surface texture on the deformation properties of unbound aggregates in pavements. International Journal of Pavements. Submitted.
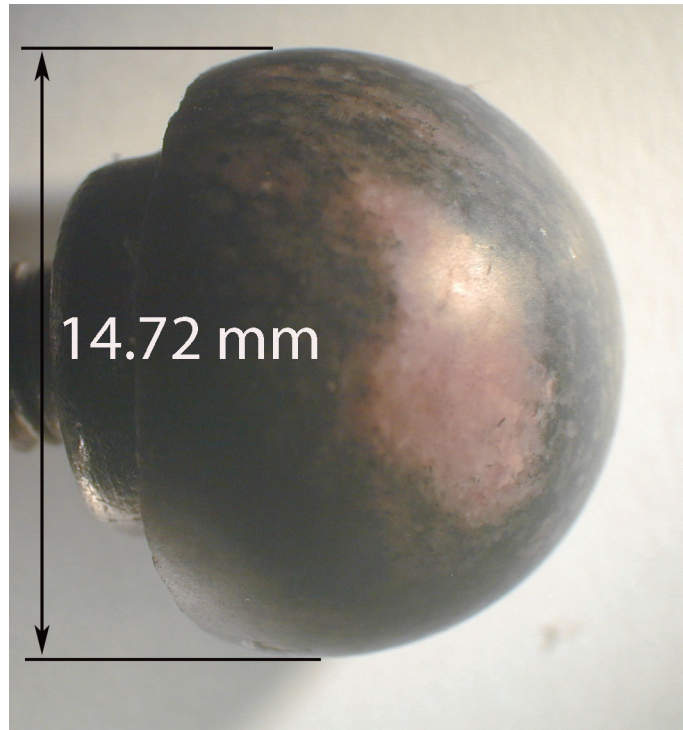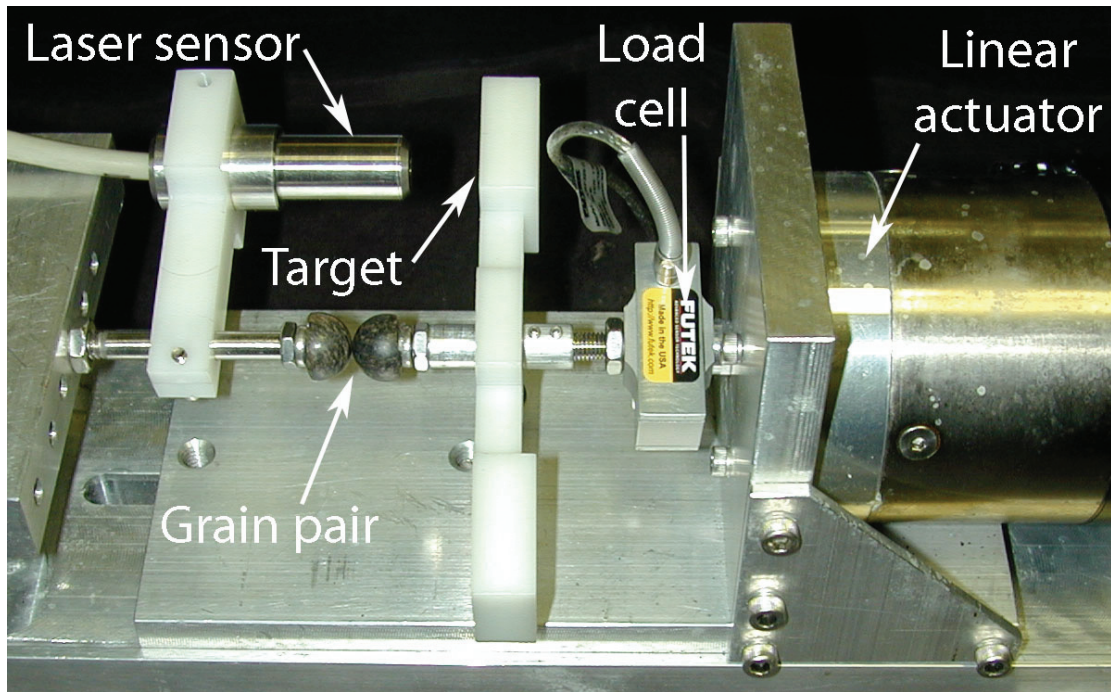
Figure 1. Photograph of one of the grains used in the experiments. The grains were approximately hemispherical and their flat sides were fixed to stainless steel mounts as shown here. The composition of the gneiss was primarily quartz (light regions) and feldspar (dark regions) in approximately equal proportion.
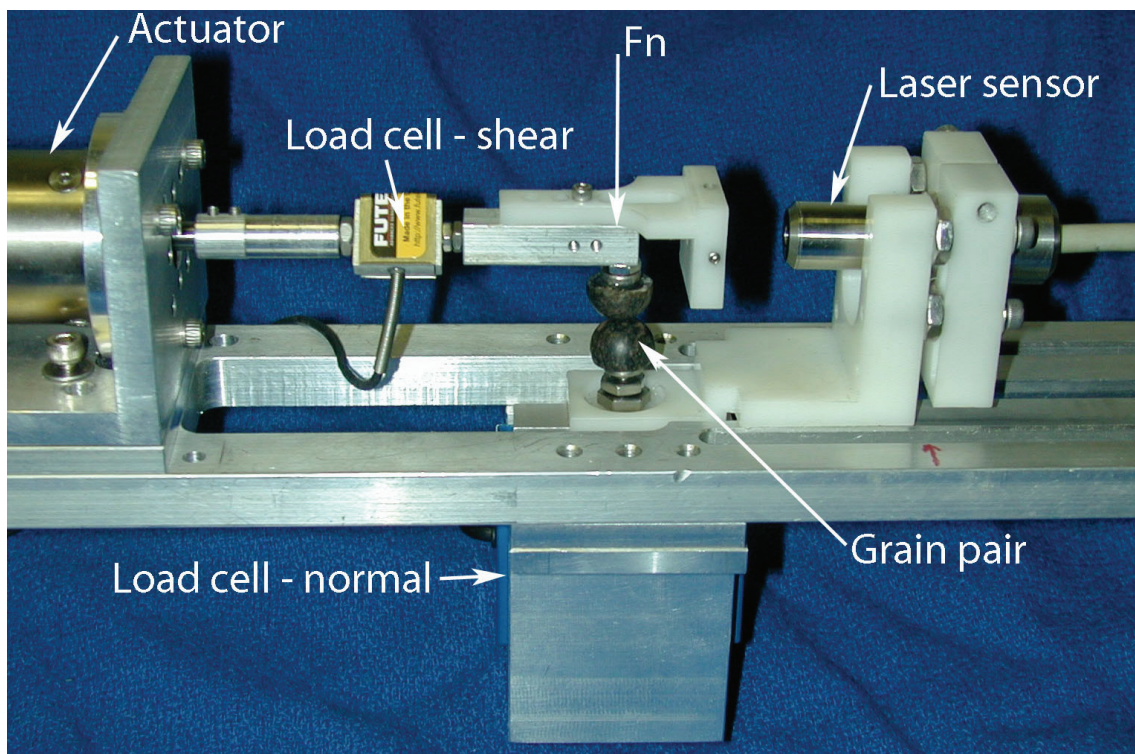
a)

Laser sensor

Target

Grain pair

Load cell

Linear actuator

b)

Actuator

Load cell - shear

Fn

Laser sensor

Load cell - normal

Grain pair

Figure 2. Photographs of the fixtures employed in the present study. a) Fixture used for the high force, normal contact experiments. b) Fixture used for the sliding friction experiments. Both systems employed a high-resolution laser sensor for deformation measurement and the specimens were mounted on the load cells to provide a direct measure of the applied force.
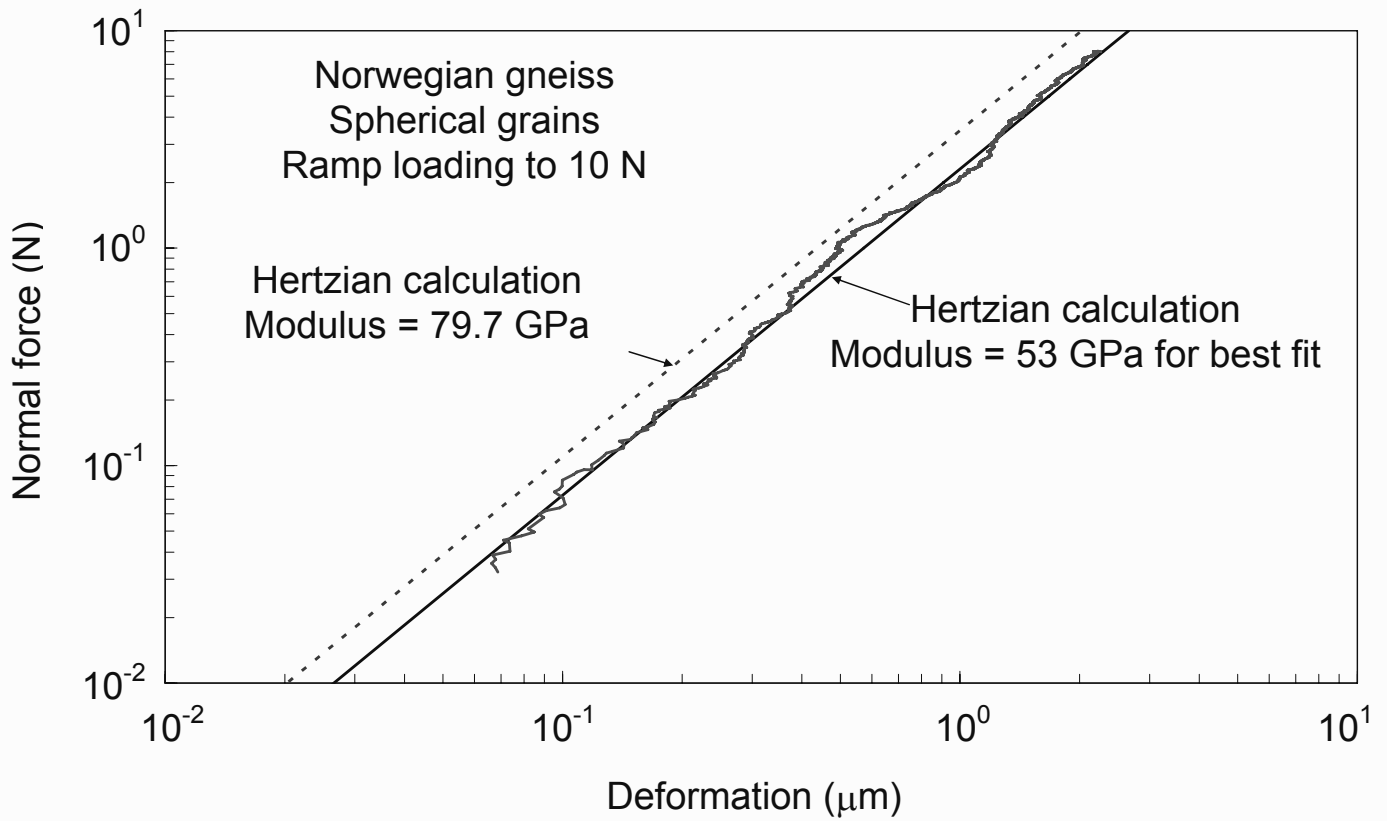
Figure 3. Normal force vs. contact displacement for the smooth spherical segments of gneiss (irregular curve). The straight lines are the Hertzian calculations with a modulus of 79.7 and 53 GPa as indicated. The latter value was obtained from a best fit analysis of the experimental results.
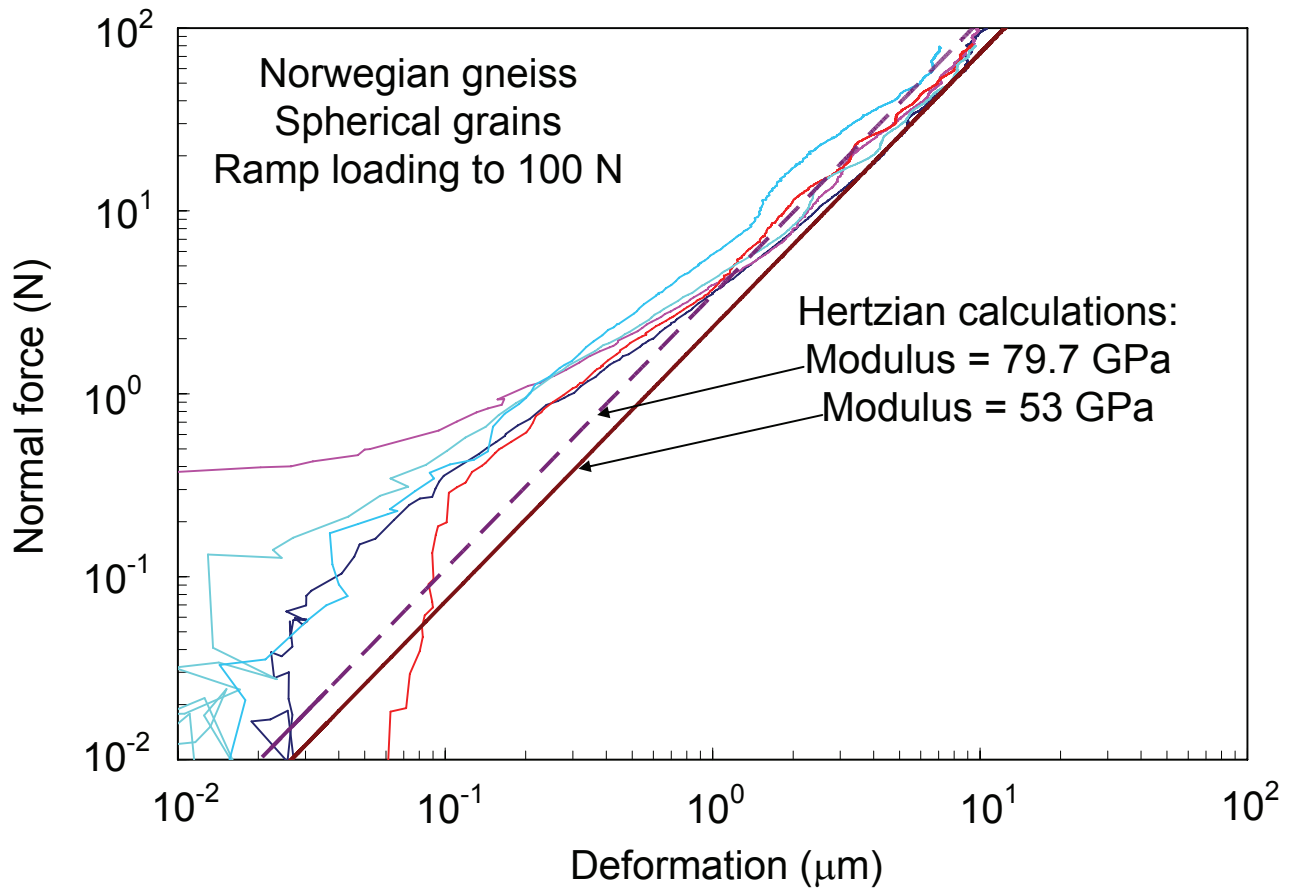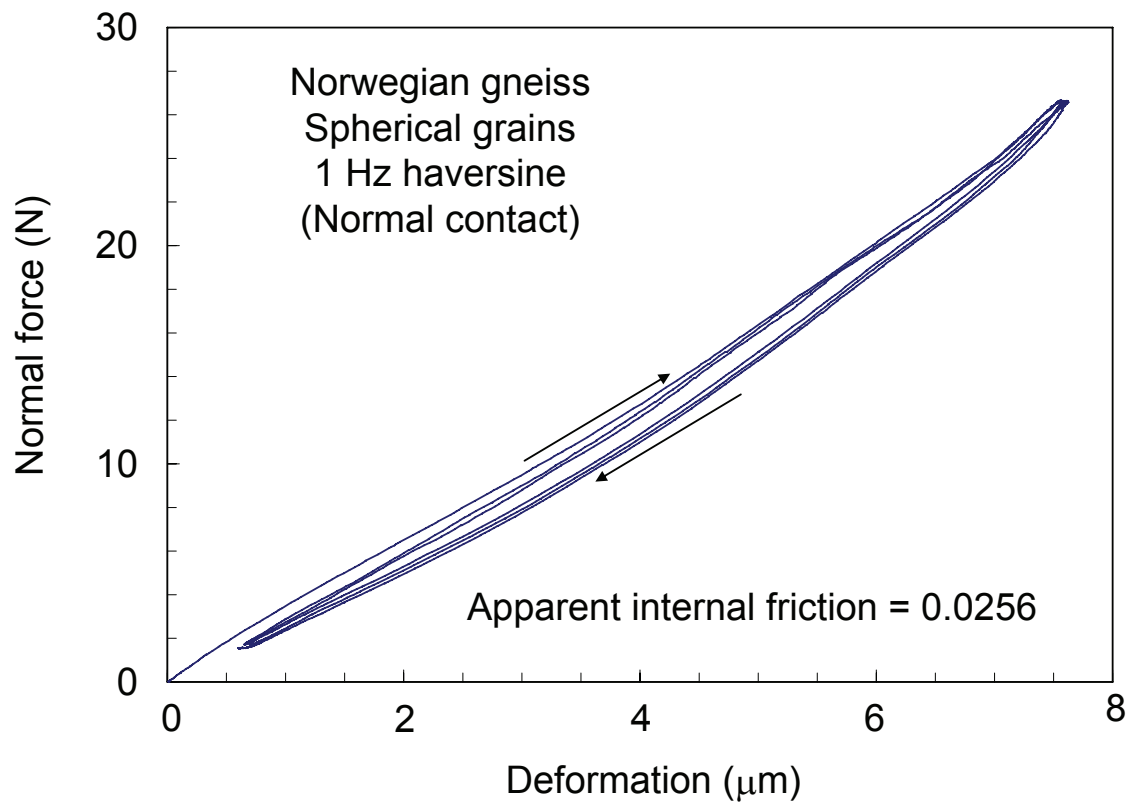
Figure 5. Normal force vs. contact displacement for the spherical grains subjected to ramp loading with the 100 N system. The straight lines indicate Hertzian behavior using the bulk modulus of 79.7 GPa and a modulus of 53 GPa that was obtained from a best-fit analysis of the 10 N ramp as discussed in the text. Note that the behavior at low force levels is somewhat irregular.

Figure 6. Normal force vs. contact displacement for the spherical grains subjected to cyclic loading with the 100-N system. The apparent internal friction value was calculated from the area of the hysteresis loop as discussed in the text. The arrows indicate the direction of loading.
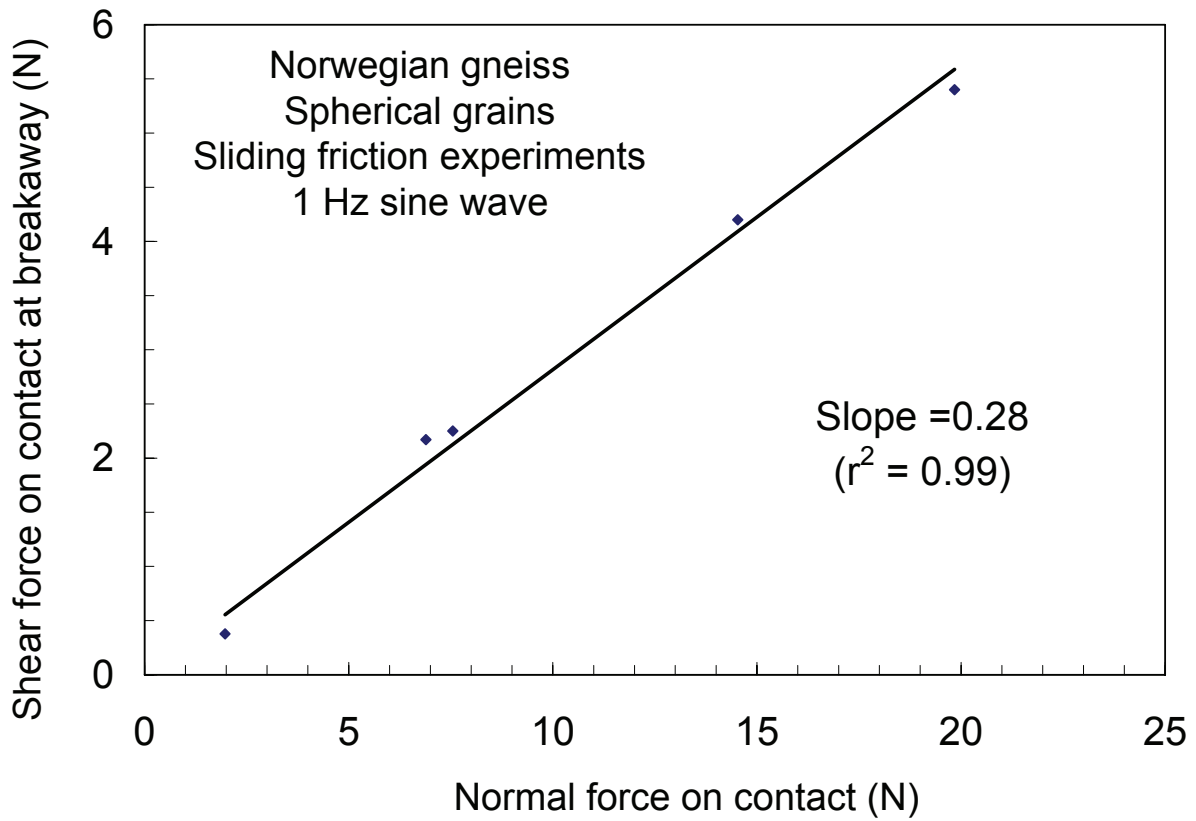
Figure 8. Shear vs. normal force from the sliding friction experiments. These experiments employed a dead load method for applying the normal force and test system actuator was used to apply a cyclic (sinusoidal) shear force to the contact.
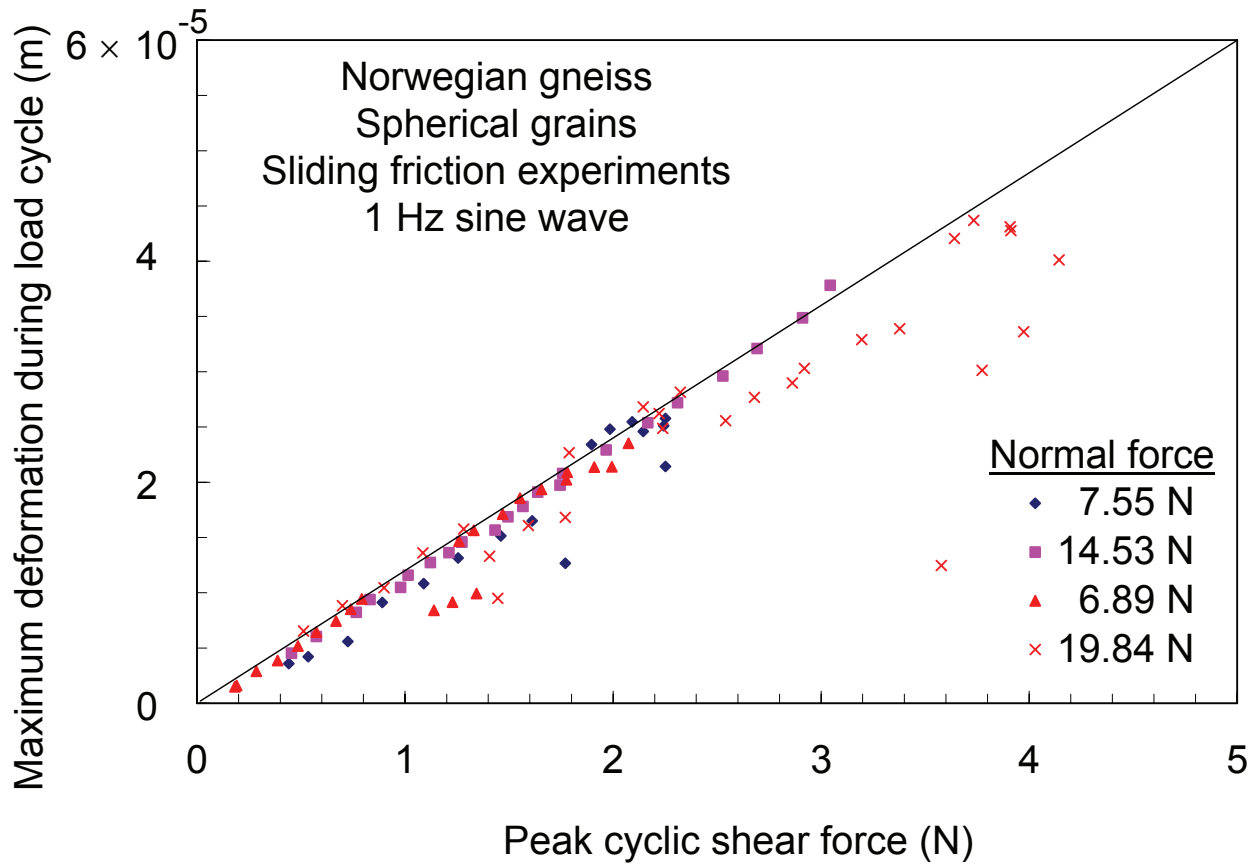
Figure 10. Maximum cyclic shear deformation vs. peak cyclic shear force for the spherical grains subjected to the indicated normal forces.
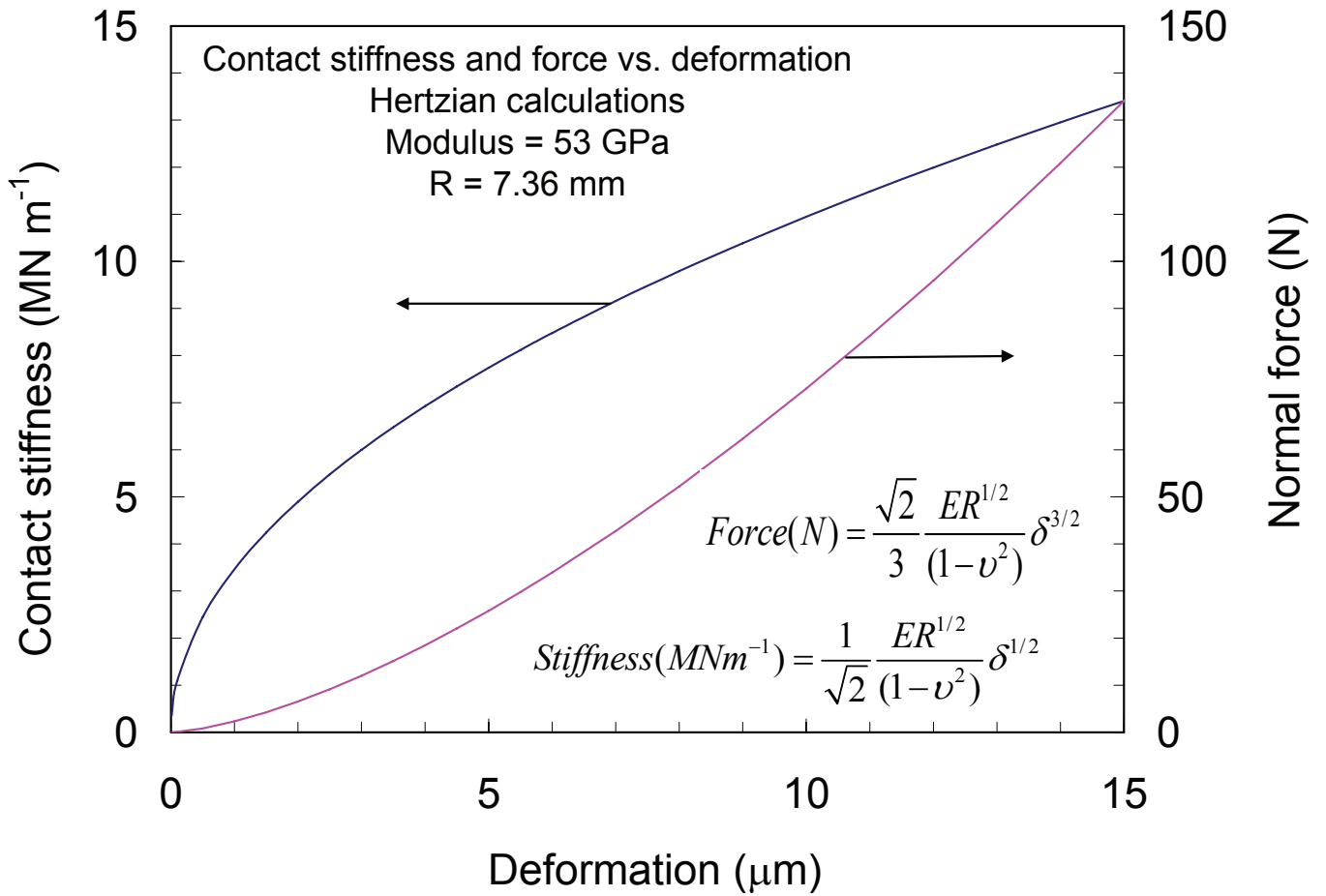
Figure 12. Calculated values of normal contact stiffness and normal force vs. deformation employing the equations that appear in the Figure.
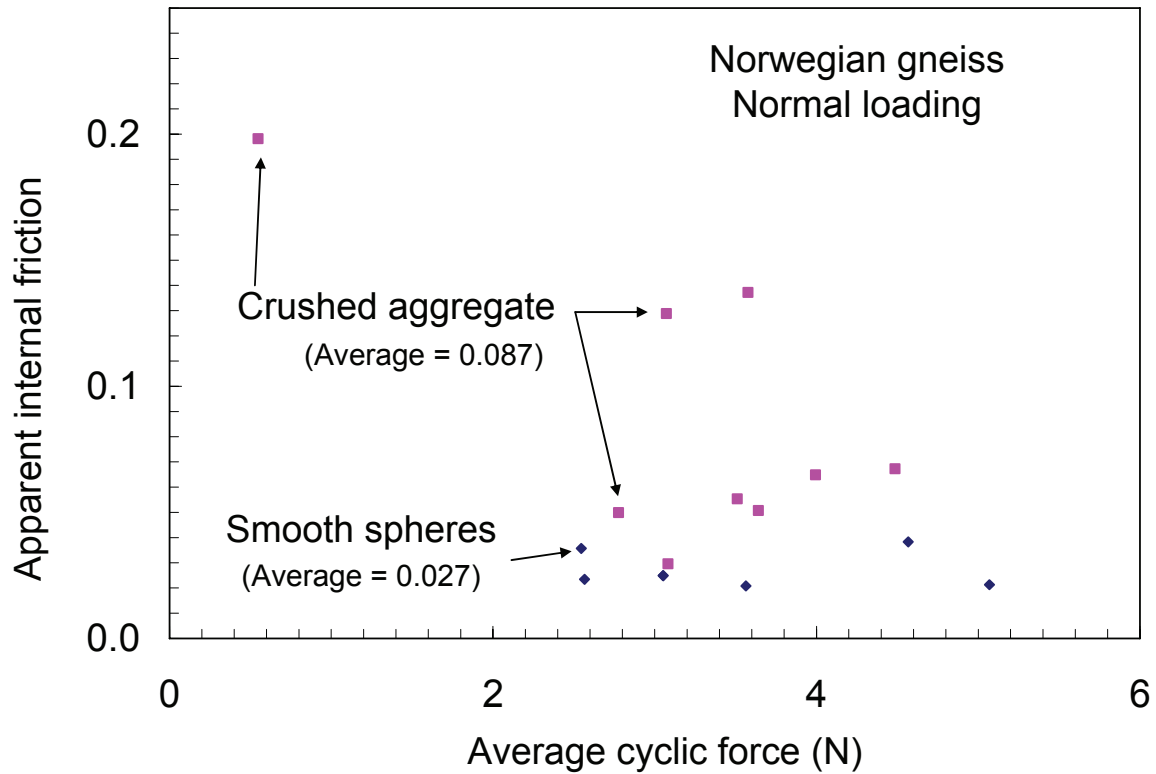
Figure 13. Typical values of the apparent internal friction vs. the average cyclic force for the normal experiment illustrating the effects of surface roughness. Relatively rough surfaces of the grain pairs of crushed gneiss aggregate produced significantly higher frictional losses in the normal contact experiments than observed for the smooth, spherical grains of the same material.